Geophysical Surveys in the Lead Queen Mine Area, Patagonia Mountains, Arizona

Geophysics Field Camp 2018

Laboratory for Advanced Subsurface Imaging

LASI-18-1

June 16, 2018

Paulo E. Moreira Coutinho, Grant J. Gordon, Alan C. Gregorski, Blase LaSala, Tim Moore, Brittany A. Morse, Ethan Moulton, Ben K. Sternberg, Stephanie N. Zech

Table of Contents

Abstract

In late 2015, after abnormally heavy monsoon rains in the Coronado National Forest south of Patagonia Arizona, an orange discharge was observed in the creek bed below the entrance to the abandoned Lead Queen Mine. This caused the U.S. Forest Service and United States Geological Survey (USGS) to mobilize to determine the cause and investigate actions to prevent future occurrences. Our studies included T ransient Electromagnetics (NanoTEM), DC resistivity, EM-31 and Ground Penetrating Radar (GPR) surveys around the Lead Queen Mine for the United States Geological Survey. Data collected around Lead Queen Mine show a large highly conductive layer within the immediate area of the mine. Data from the NanoTEM and DC resistivity surveys show an anomaly with resistivities less than 6 ohm-m at depths varying from 20 to 60 meters. This anomaly is present in all TEM transects and the DC resistivity line. The DC resistivity line also shows a high-resistivity area near where the adit has been predicted to be. Further west, near another adit, a low-resistivity layer does not appear until beyond 60 meters depth. Data collected using the EM-31 shows no change in resistivity or conductivity along the stream-bed near Lead Queen Mine. GPR data did not effectively show a response to the adit, even with extensive manipulation using the RADAN software.

1. Introduction

1.1 History

The Lead Queen Mine resides in the Wieland-Buffalo group, and is underlain by Cretaceous-age porphyrytic andesite and rhyolite. Fractures show zoned, siliceous, metallized veins, the most extensive of which are the pair of veins worked at the Lead Queen Mine. Down dip, the Lead Queen was mined to 50 meters on one of the veins; they are 182 meters apart. The veins are difficult to trace on the surface. They contain lead-silver minerals in the upper 12 meter to 15 meter region and below contain sulfides of lead, silver, and copper (Lead Queen Mine, 2015).

The Mineralized vein system was discovered in 1897, and mining occurred from 1898 to early 1902. It was reopened in 1910 and worked until 1940 (mindat.org, 2015). It was developed to a depth of 166 feet, with about 1,200 feet of workings, including shaft drifts, crosscuts, and stopes at two levels (Schrader, 1915).

1.2 Project Background

The U. S. Geological Survey, in cooperation with the U.S. Forest Service is undertaking an environmental study of the effects of historical mining on water and sediment quality, as well as aquatic and riparian habitat in the Harshaw Creek watershed upstream from Patagonia, Arizona, in the vicinity of the Lead Queen Mine in the Patagonia Mts. The Lead Queen is an abandoned mine located on Forest Service land.

The study was initiated from the recent observation of bright orange sludge discharges from intense monsoon-related precipitation in late September 2014. At the Lead Queen Mine, flushing of adits and shafts by rapid inflow of rainwater apparently led to the mobilization of iron- and aluminum-rich acid waters, which were then deposited as orange precipitate or sludge (Figure 1.1). This precipitate mostly settled in the upper canyons along an approximately 1-mile stretch from the mine site's lower tunnel. Results from this study are being used by Federal and State agencies and by local watershed stakeholder groups to implement remediation and cleanup activities.

Figure 1.1. Pictures of the orange precipitate discharge from the Lead Queen Mine after the late September 2014 heavy monsoon season rains. (Photos courtesy of Glen E. Goodwin).

As of part of a cooperative effort with Federal land-management agencies, the U.S. Environmental Protection Agency, University of Arizona, and concerned local citizens, the U.S. Geological Survey implemented the Abandoned Mine Lands Initiative in 1997. USGS scientists have undertaken comprehensive studies to understand processes and to assess sites in the watershed for remediation. The primary objective of this particular study is to compile data for the identification of faults and associated fracture networks that might transmit groundwater from the naturally occurring pyrite rock wall of the deposit, or leaking discharges from the mine's tailings impoundment. Results from this study will contribute to an understanding of the subsurface area related to the mine and provide data for potential remediation actions to reduce the risk of the discharge reoccurrence.

The University of Arizona in conjunction with the USGS conducted a study during the periods of February 10th to 11th and March 3rd to 4th 2018 of the area directly over the main adit to the Lead Queen Mine, along the stream bed at its entrance, and over another adit 260-meters southwest of the Lead Queen adit, which is referred to as the Other Adit (OA). During these periods, subsurface measurements were performed using various geophysical methods, including Ground Penetrating Radar (GPR) methods, Transient Electromagnetic Methods (TEM), DC Resistivity methods, and a ground conductivity (EM) measurements. Data were compiled from these measurements to provide an assessment of the substructure to identify possible fracture networks that may transmit groundwater and areas of high conductivity that may show water collection areas.

1.3 References:

Mineral Appraisal of Coronado National Forest, Part 7, Patagonia Mountains-Canelo Hills Unit Cochise and Santa Cruz Counties, Arizona, Mineral Land Assessment Open File Report/1994 MLA 22-94, U.S. Department of the Interior Bureau of Mines

Lead Queen Mine (Golden Rose; Mono Mine), Buffalo Mine group (Jefferson group), Wieland group (Wieland group claims), Harshaw, Harshaw District, Patagonia Mts, Santa Cruz Co., Arizona, USA. (2015, January 11). Retrieved April 13, 2018, from https://www.mindat.org/loc-33878.html

Schrader, F. C.and Hill, J. M., 1915, Mineral Deposits of the Santa Rita and Patagonia Mountains, Arizona, U.S. Government Printing Office, 373p.

2. Location Maps

2.1 Background Information

The geophysical data stations along each profile were recorded using handheld Garmin GPSMAP 64ST GPS units. To maintain our various lines, we used the GPS compasses and location markers to maintain our proper headings. The GPS coordinates were added into ArcMap using ArcGIS NAD 1983 HARN State Plane Arizona Central FIPS 0202 Feet Intl coordinate system (converted to meters for this study), Transverse Mercator projection, D North American 1983 HARN Datum, and Central Meridian of – 111.9 and into Google Earth Pro, last map update 2015.

2.2 Geographic Location

The survey area is located in the Wieland-Buffalo Group Mine Area in the Coronado National Forest south of Patagonia, Arizona on the south side of Red Mountain in the Harshaw Creek Watershed (Figure 2.1). Multiple profiles were performed in the area, trending northwest-southeast, located in a square bounded by UTM coordinates 12R 526332 to 526609 eastings and 3983278 to 3483226 northings. The northern set of profiles, referred to as Lead Queen, runs perpendicular to the main Lead Queen Mine adit on a line heading of 120 (-300) degrees and is centered on the adit entrance. A southern profile, referred to as the Other Adit (OA), runs perpendicular to this adit with a line heading of 100 (-280) degrees with the center of the adit on the 18 meters point of the profile. The Other Adit is located 225 meters, 263 degrees southwest of the Lead Queen adit. Figure 2.2 illustrates the access roads to the mine site from Patagonia, Arizona. Locations for all four geophysical methods (GPR, DC Resistivity, TEM, and FEM) were recorded and displayed in Figure 2.3 & Figure 2.4.

2.3 TEM Survey Location

The Transient Electromagnetic (TEM) surveys included small loops for data collection. The transmitter loop size used for all profiles was 20m x 20m. A total of 27 loops were recorded for the Lead Queen Mine profile, four lines of 5 loops (100 meter by 80 meters total), one line of

four loops (20 by 80 meters) and one of three loops (20 by 60 meters) for a total area of 10,800 square meters covered. Additionally, three loops in a single east-west line were recorded at the Other Adit (20 by 60 meters) for an area of 1,200 square meters. Effort was made to avoid excessively steep terrain and to minimize disruption of the ground vegetation, leading to the shifting of the last two lines of TEM centers on the Lead Queen Mine profiles. The TEM receivers and wire loops are displayed in Figure 2.3 for both profiles.

2.4 FEM Survey Location

An EM31 instrument was used for the Frequency Electromagnetic (FEM) collection, with measurements every 5 meters for a line distance of 400 meters in length. The path followed a wash that extended from 100 meters upstream from the Lead Queen adit to 300 meters below the adit. The FEM survey line is displayed on Figure 2.4.

2.5 DC Resistivity Survey Location

An Advanced Geosciences Inc. (AGI) Sting-Swift system was used for the DC Resistivity survey. This was connected to an 84-meter-long array line that followed the same line as the centers of the first TEM survey line on the Lead Queen Mine (line LQ1). The array was laid out perpendicular to the adit with the 42-meter electrode of the array centered on the adit as displayed on Figure 2.5.

2.6 Ground Penetrating Radar (GPR) Survey Location

The ground Penetrating Radar survey took place right on top of the Lead Queen Adit trending southeast-northwest. The data acquisition consisted of an 18-meter-long section where the adit was roughly located at the 10m mark. Difficulties related to the steep terrain made it complicated for the crew to carefully manage the equipment. It was crucial for the students to build a trail among the trees to gather these data. Effort was made to diminish any environmental damages when making the trail. After the survey, a small remediation reconstruction was made to make the GPR trail look just like it used to be before the survey. The GPR line is displayed in Figure 2.6.

2.7 Location Errors

According to U.S. Government tests of GPS accuracy, the Garmin GPSMAP 64ST has an average accuracy of 3.09 meters over a 60-second average (US Forest Service, 2017). When the GPS positions were collected in the field, the GPS unit was left in place until the measured GPS error was less than 3-meters. Based on the 3-meter average horizontal error in the Garmin GPS units, the GPS points were plotted, and a best fit line was used to portray line and grid plots (Figure 2.8). Additionally, there was a high variation in the elevations recorded by the GPS units, so a high-resolution digital elevation model (DEM) was used in ArcGIS and the elevation data from Google Earth Pro were used to constrain elevations. Figures 2.9 to 2.18 are a comparison of GPS, ArcGIS, and Google Earth Pro elevation data. The maps used in ArcGIS had a resolution of 2 meters per 2 meters in the cell size. Considering that the maps are 277 pixels wide, there is a potential position error of 0.7%.

2.8 Geologic Map

Before interpreting the geophysical data, it is important to know the geology of the site prior to the data acquisition. A geological map combined with a topographic map was prepared to illustrate the layout of the geological formations over the field of study. The Lead Queen mine is located over trachyandesite (Ka) lithology from the upper cretaceous. Its description consists of gray, greenish-gray, or grayish-red, porphyritic to fine-grained, thin to very thick flows of trachyandesite. Its maximum thickness is roughly 914 meters (USGS Map). Figure 2.19 illustrates a wide view of the geological setting.

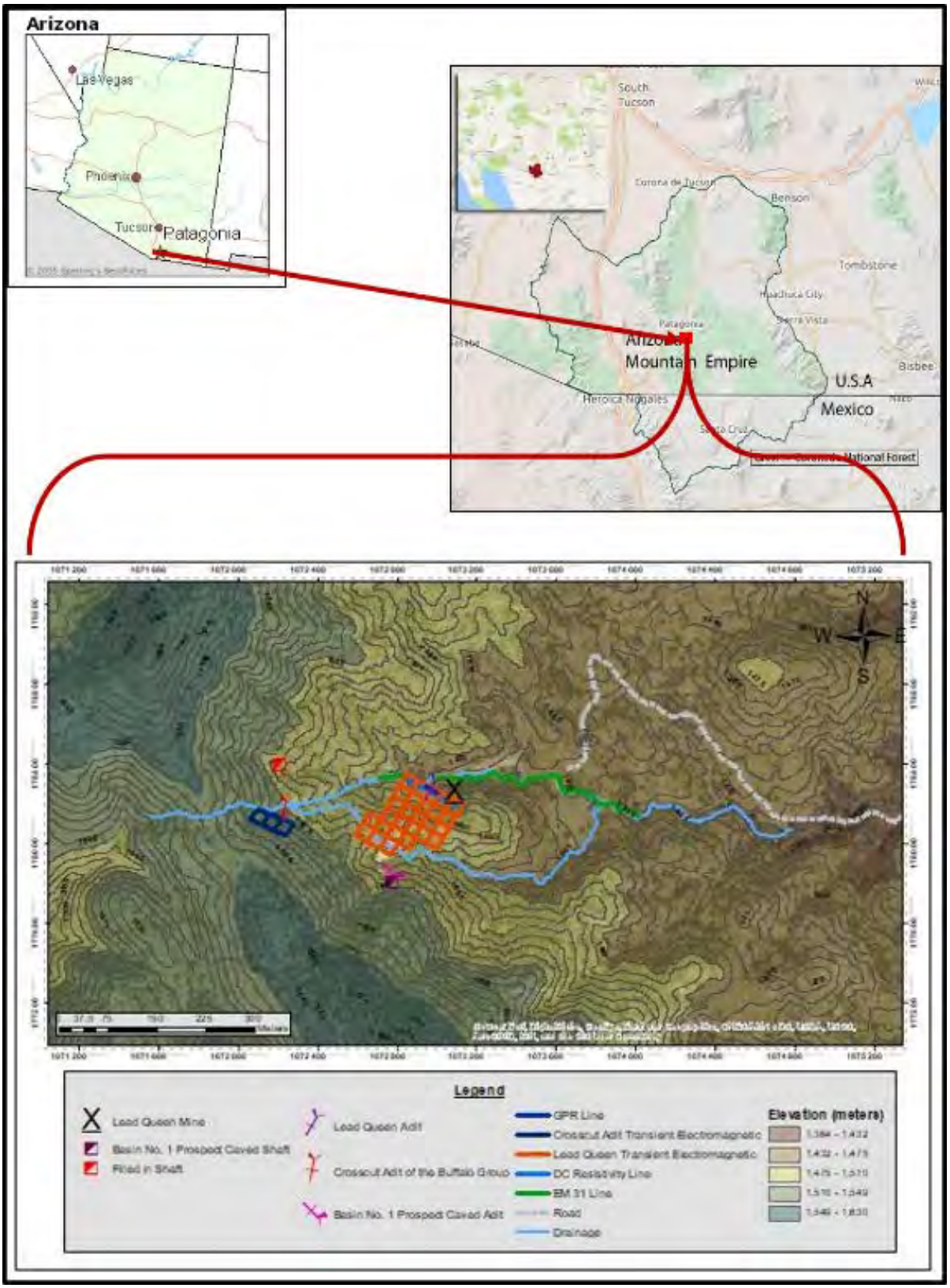

Figure 2.1. Overview map of the location. The Lead Queen site was located south of Patagonia Arizona on the southwest side of Red Mountain.

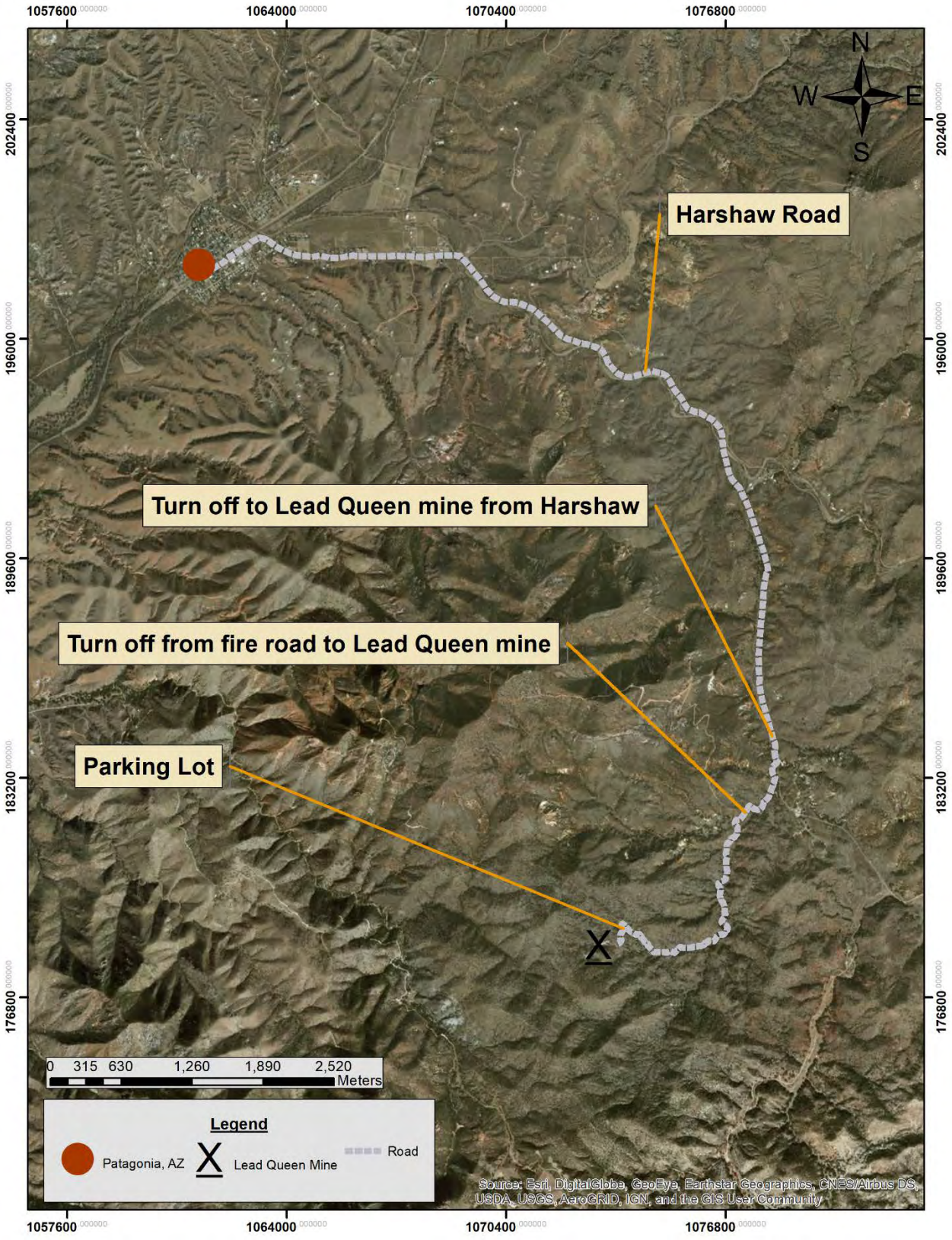

Figure 2.2. Road map to the Lead Queen Mine site from Patagonia, Arizona.

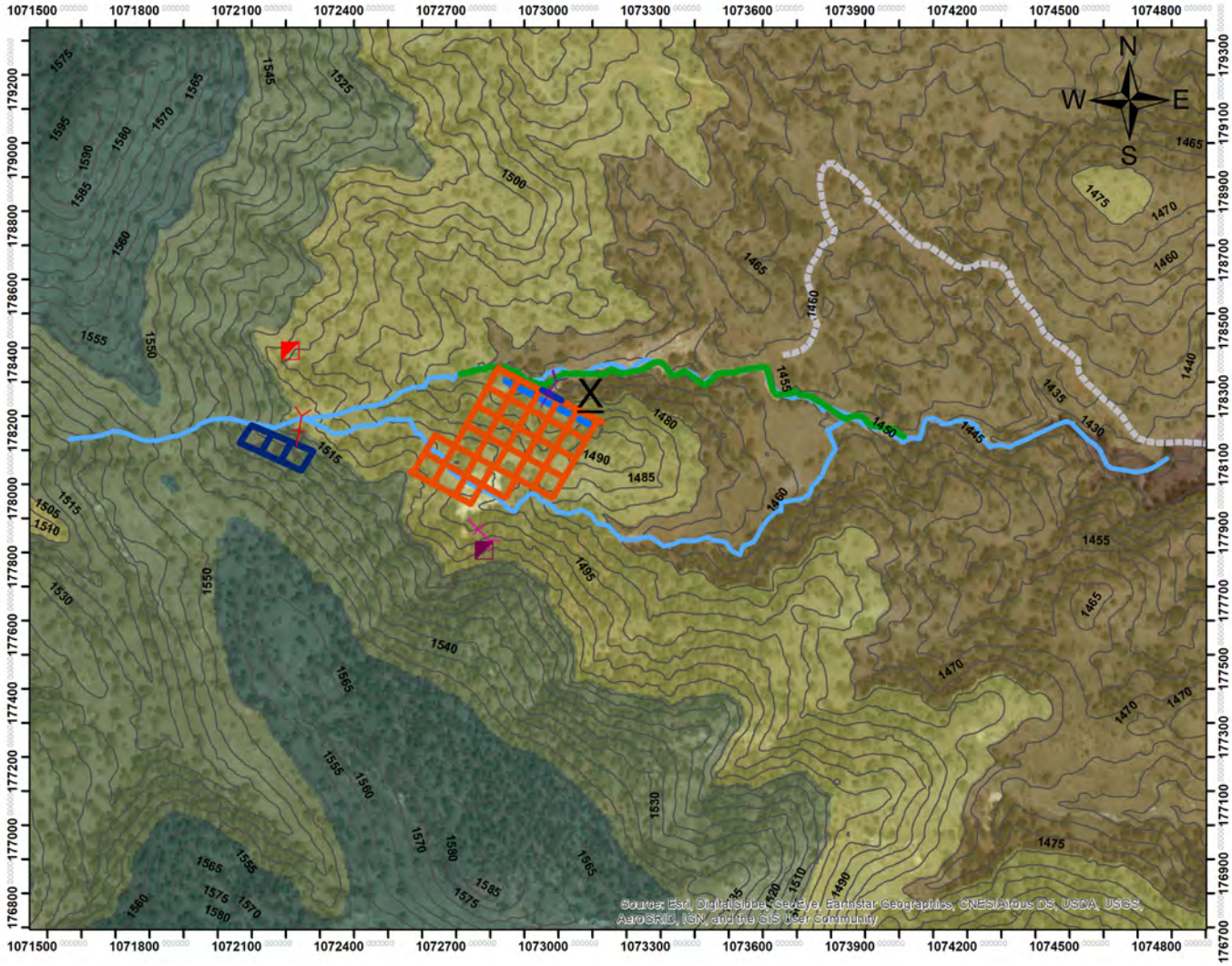

Figure 2.3. Site plan for Lead Queen Mine subsurface measurement. Measurement methods include TEM, DC Resistivity, GPR, and EM-31.

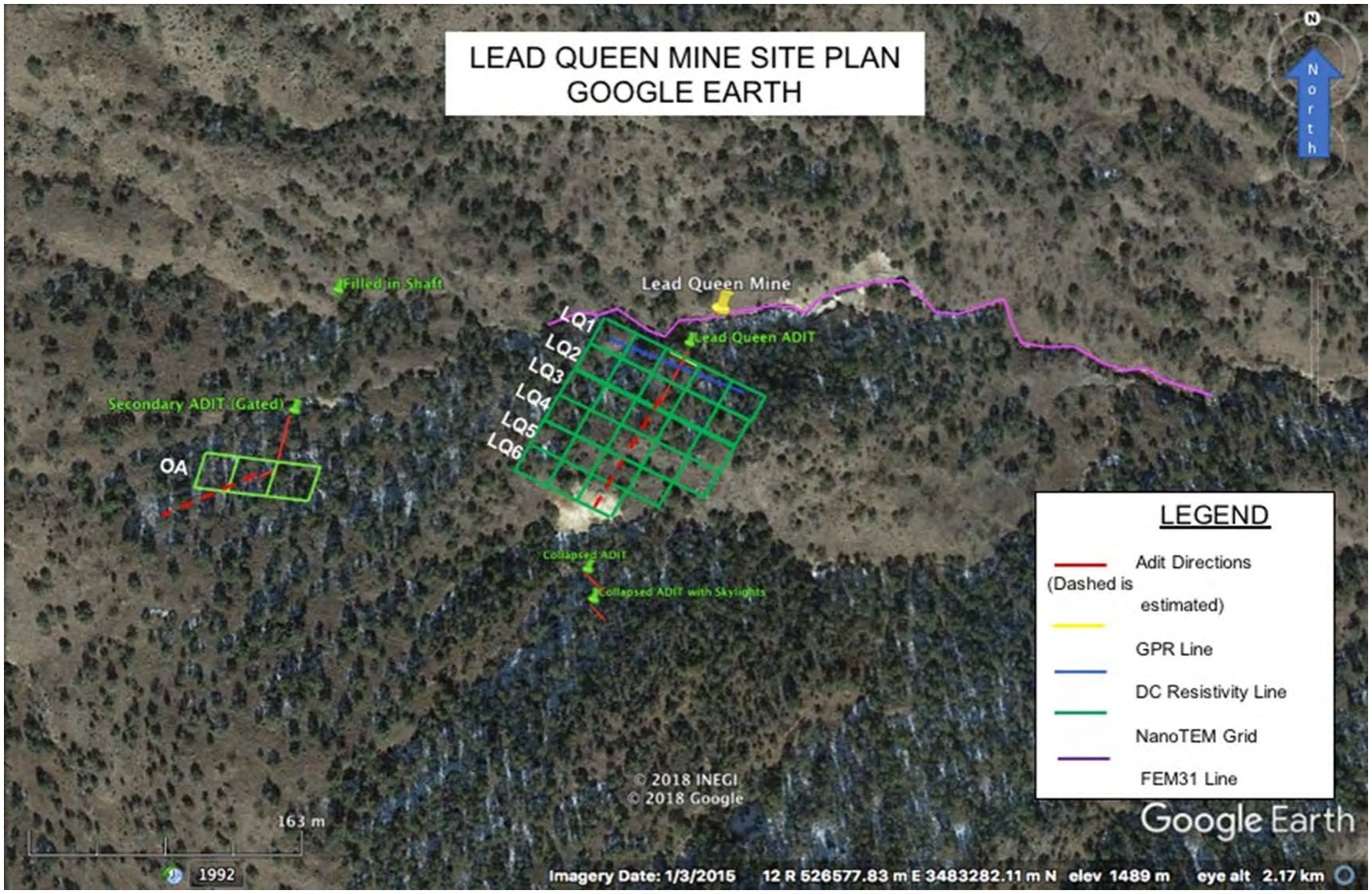

Figure 2.4. Site plan for Lead Queen Mine subsurface measurement map showing terrain and vegetation. Measurement methods include TEM, DC Resistivity, GPR, and EM-31.

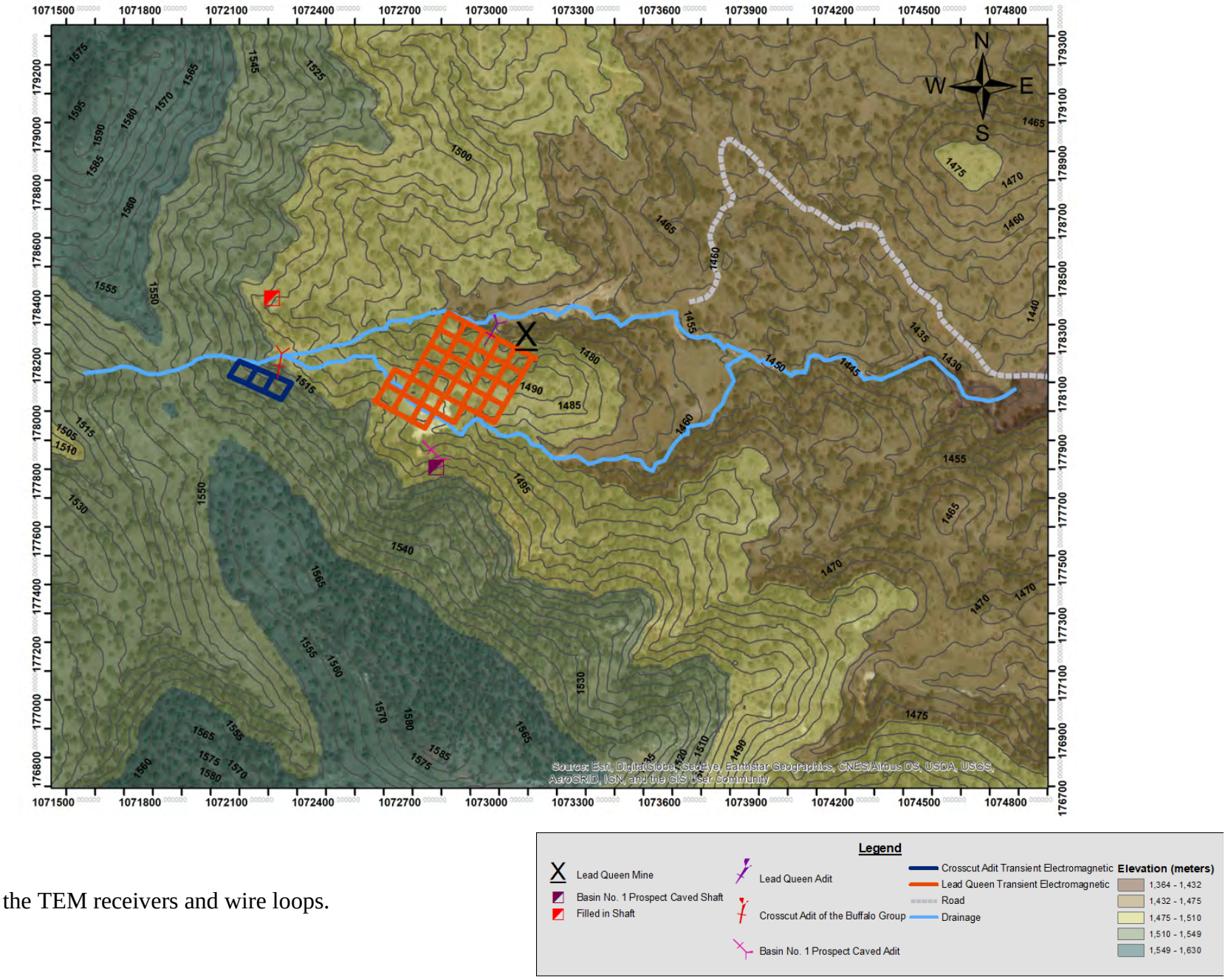

Figure 2.5. Map of the TEM receivers and wire loops.

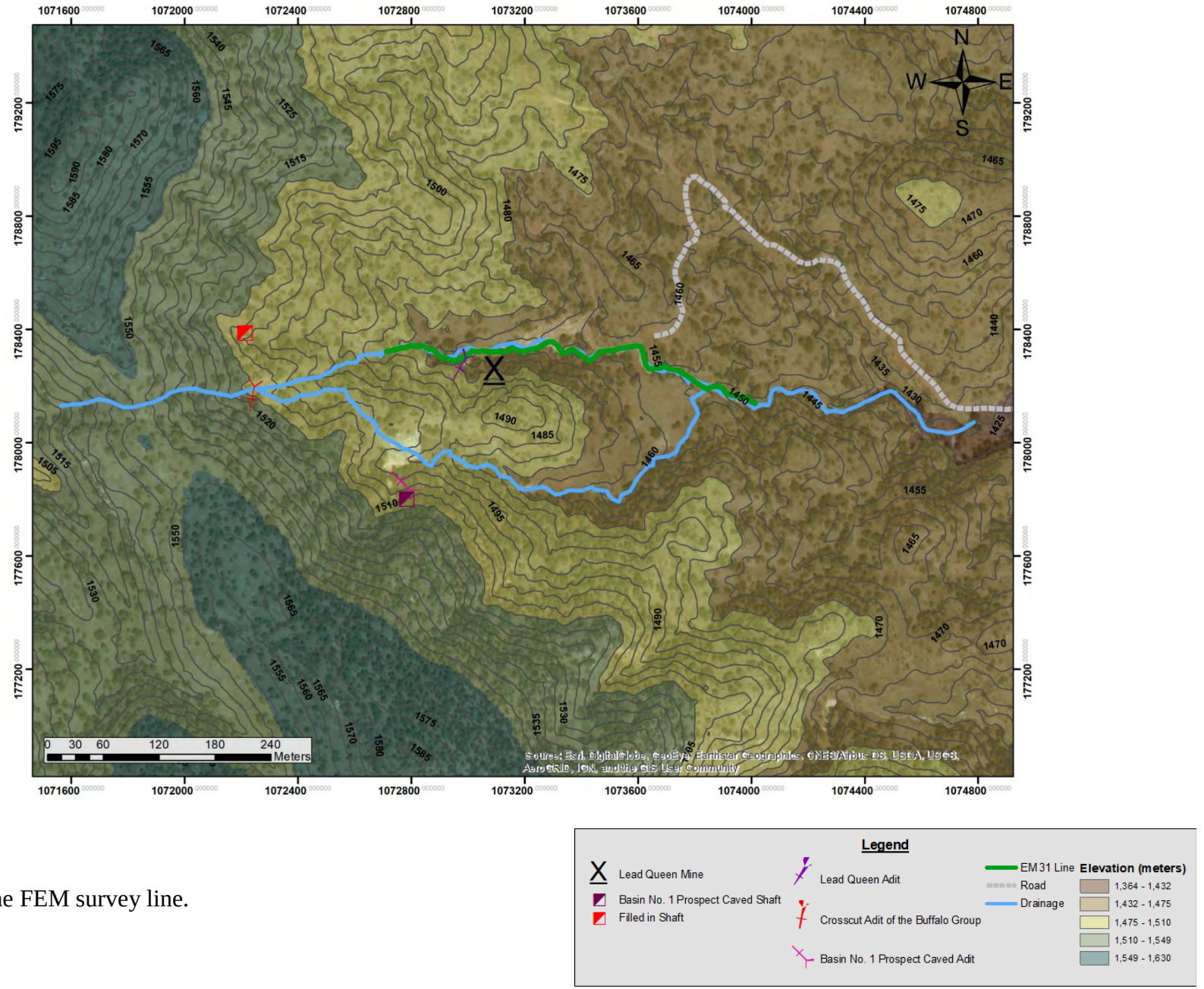

Figure 2.6. Map of the FEM survey line.

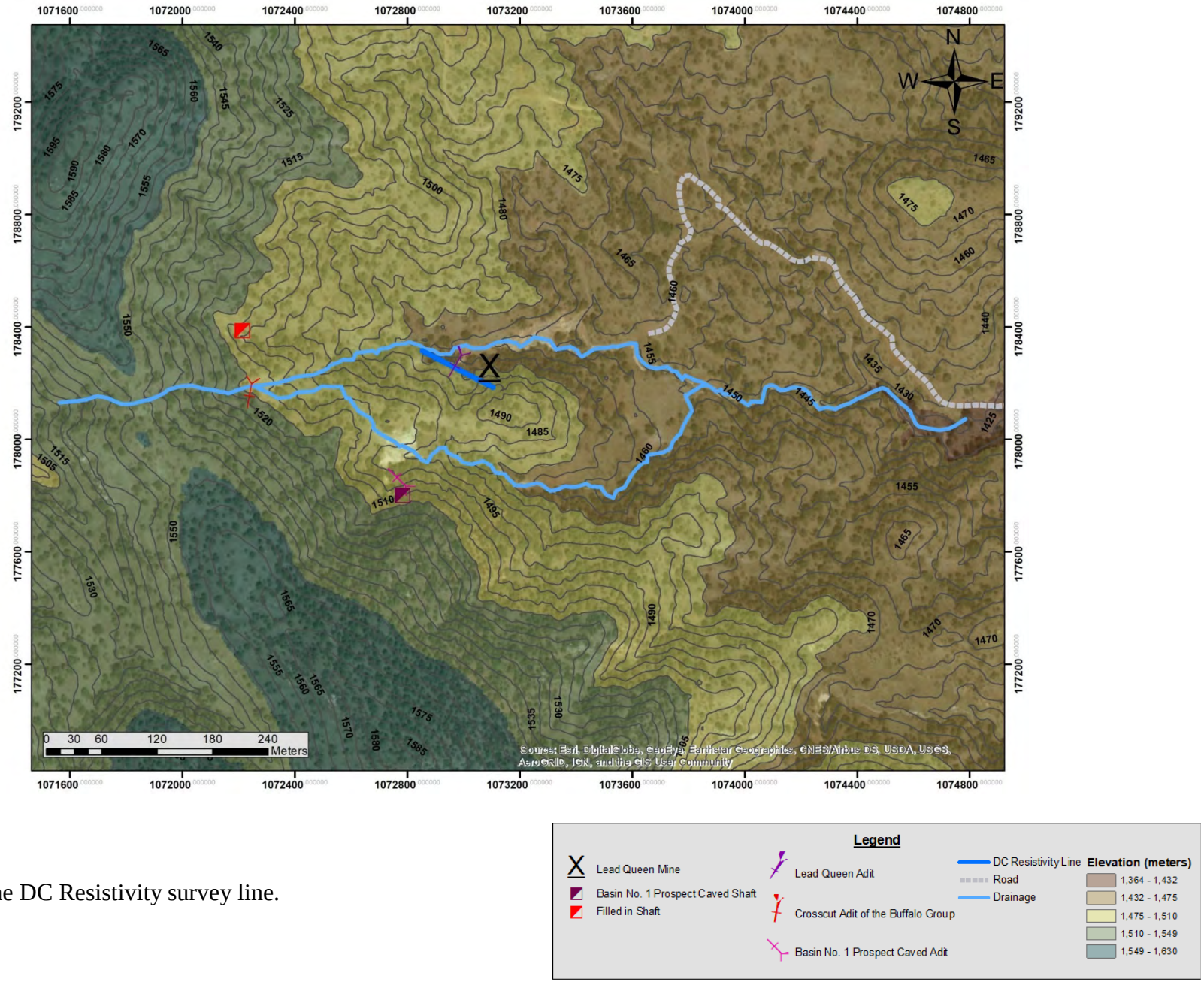

Figure 2.7. Map of the DC Resistivity survey line.

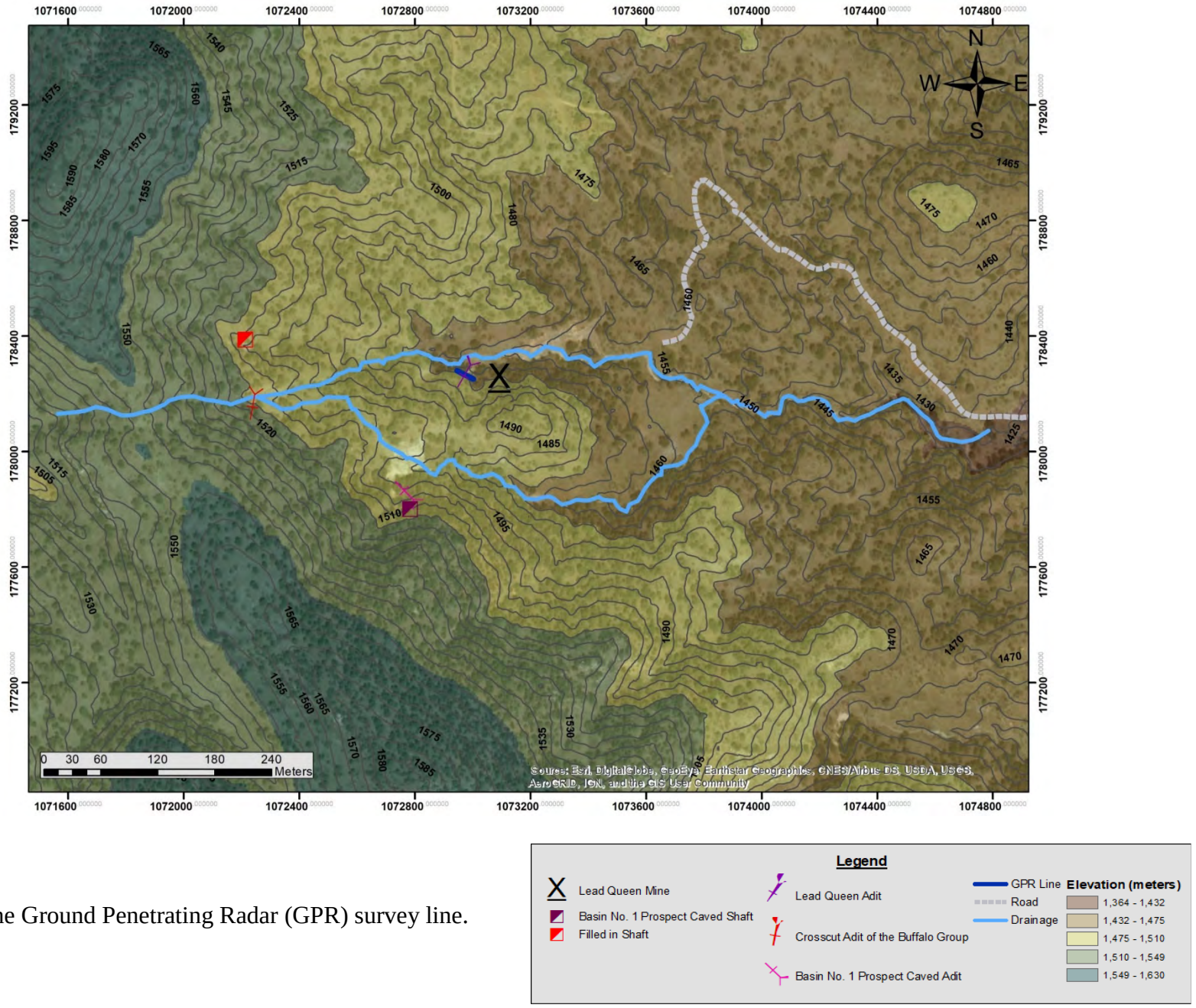

Figure 2.8. Map of the Ground Penetrating Radar (GPR) survey line.

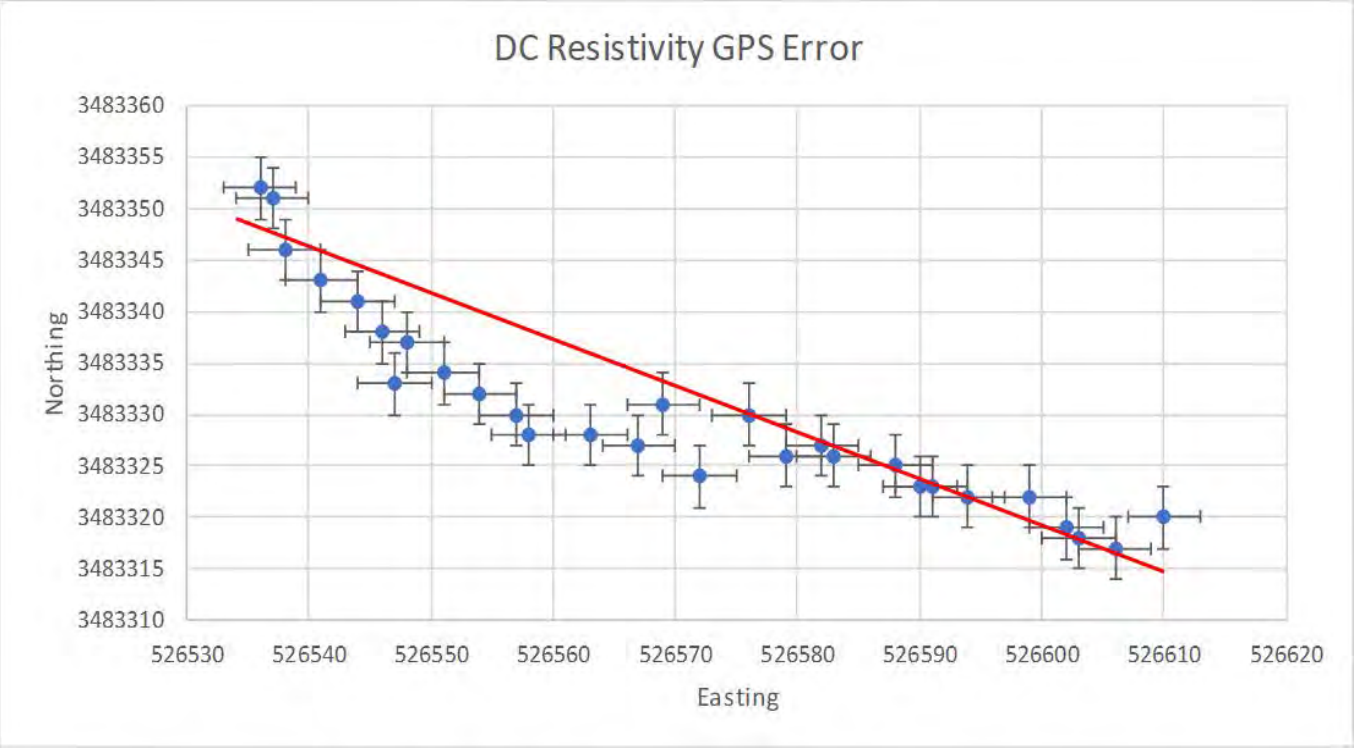

Figure 2.9. Plot of DC Resistivity GPS positions with 3 meter error bars. The red line indicates the averaging used for calculation of the array line position.

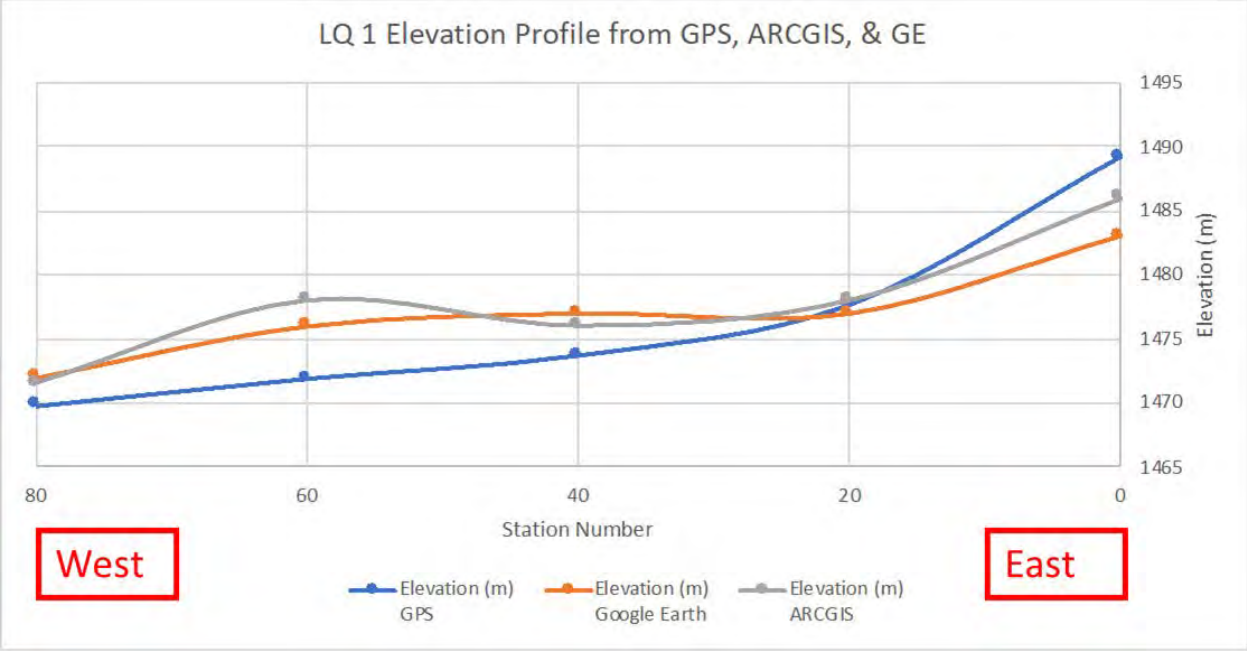

Figure 2.10. Comparison of GPS, ArcGIS and Google Earth Pro elevation profiles from west to east across TEM line LQ1.

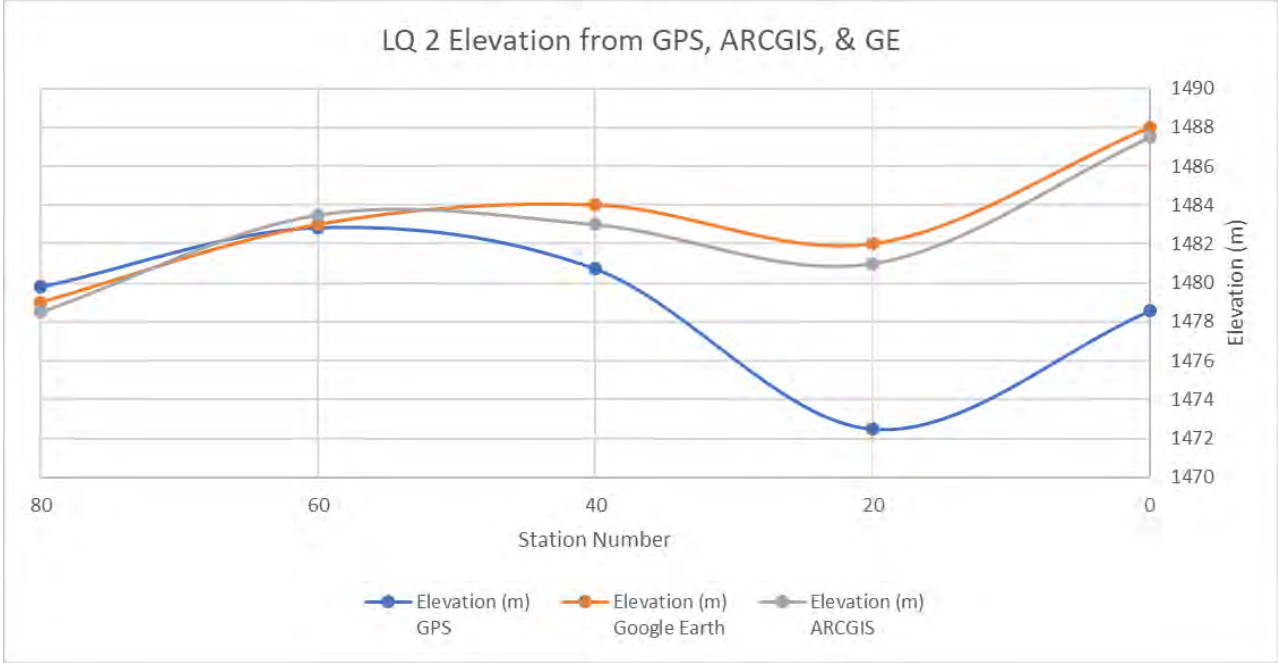

Figure 2.11. Comparison of GPS, ArcGIS and Google Earth Pro elevation profiles from west to east across TEM line LQ2.

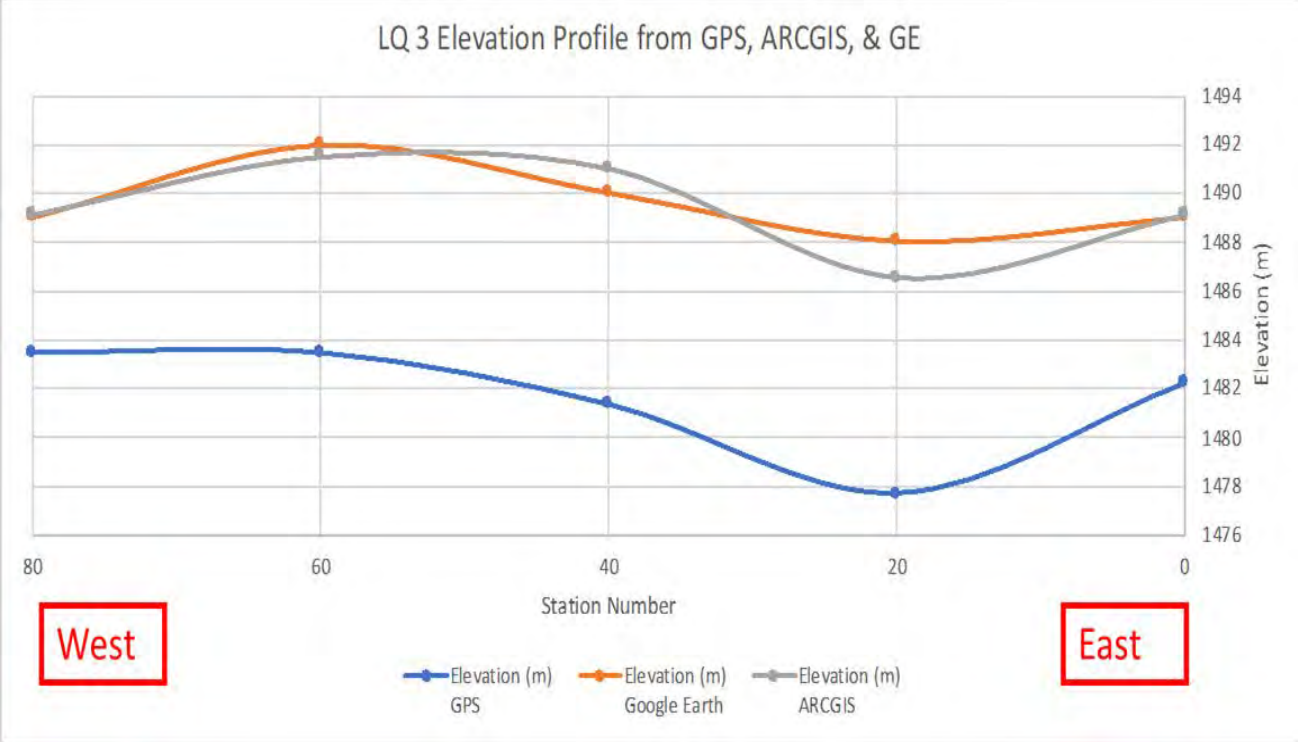

Figure 2.12. Comparison of GPS, ArcGIS and Google Earth Pro elevation profiles from west to east across TEM line LQ3.

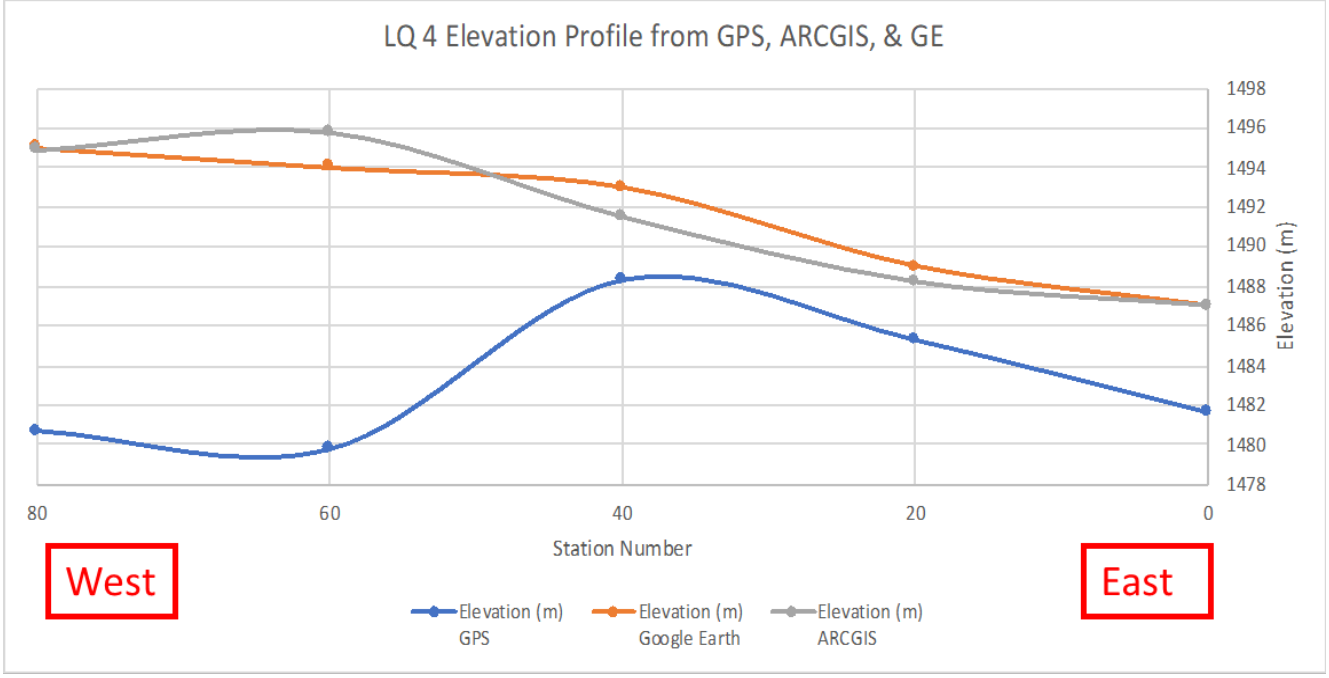

Figure 2.13. Comparison of GPS, ArcGIS and Google Earth Pro elevation profiles from west to east across TEM line LQ4.

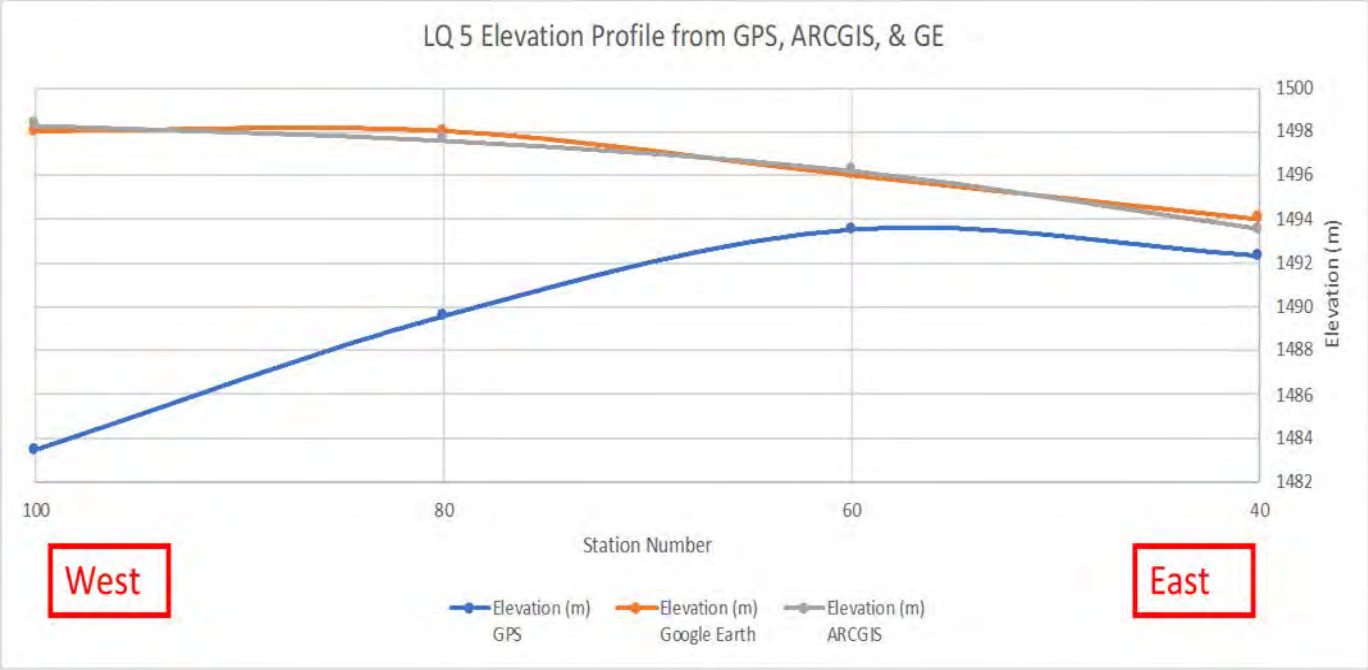

Figure 2.14. Comparison of GPS, ArcGIS and Google Earth Pro elevation profiles from west to east across TEM line LQ5.

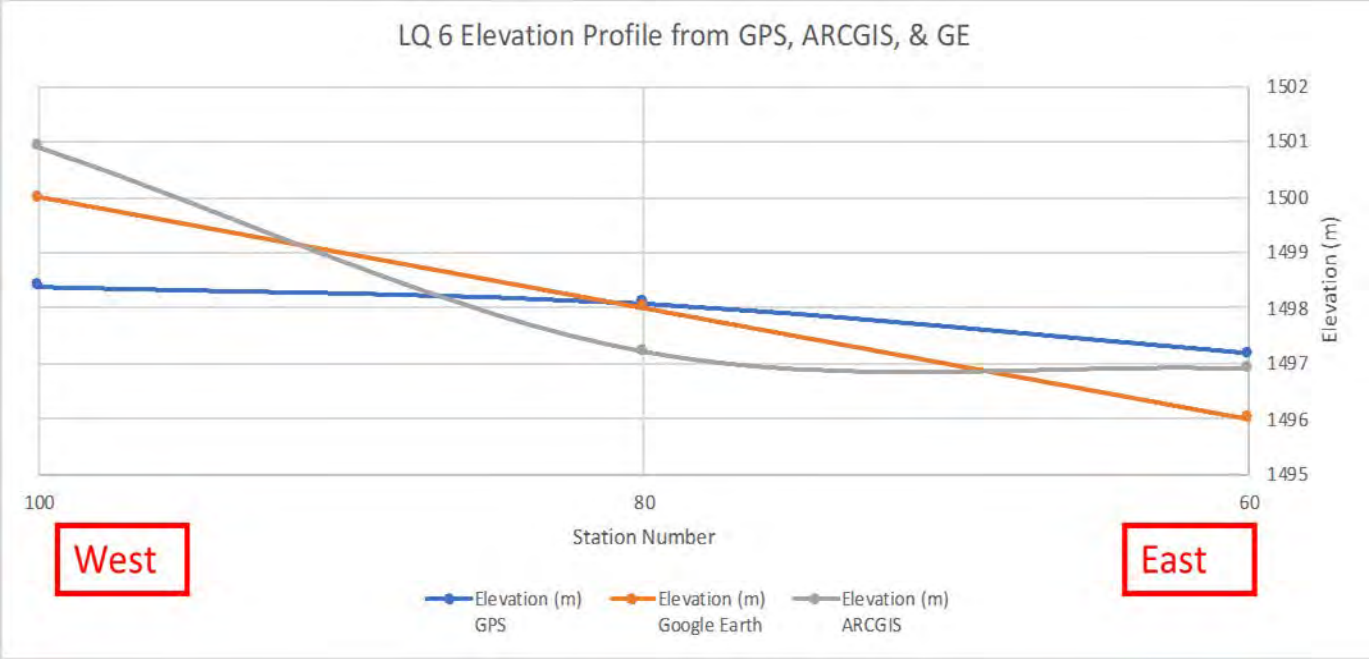

Figure 2.15. Comparison of GPS, ArcGIS and Google Earth Pro elevation profiles from west to east across TEM line LQ6.

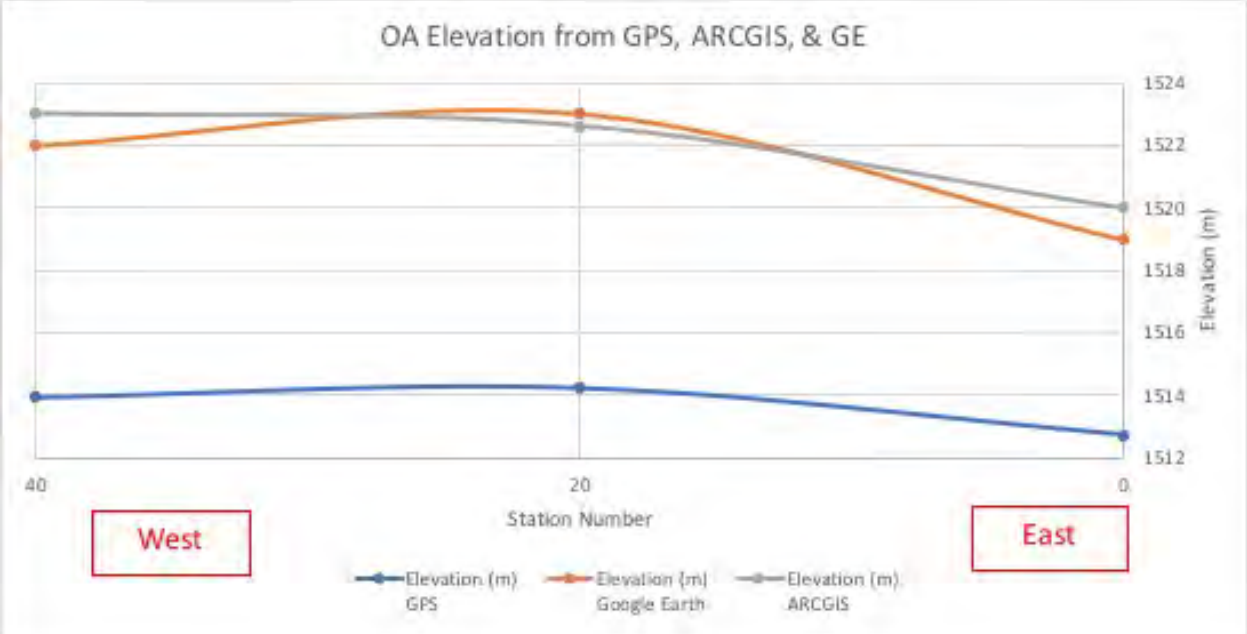

Figure 2.16. Comparison of GPS, ArcGIS and Google Earth Pro elevation profiles from west to east across the TEM line for the Other Adit.

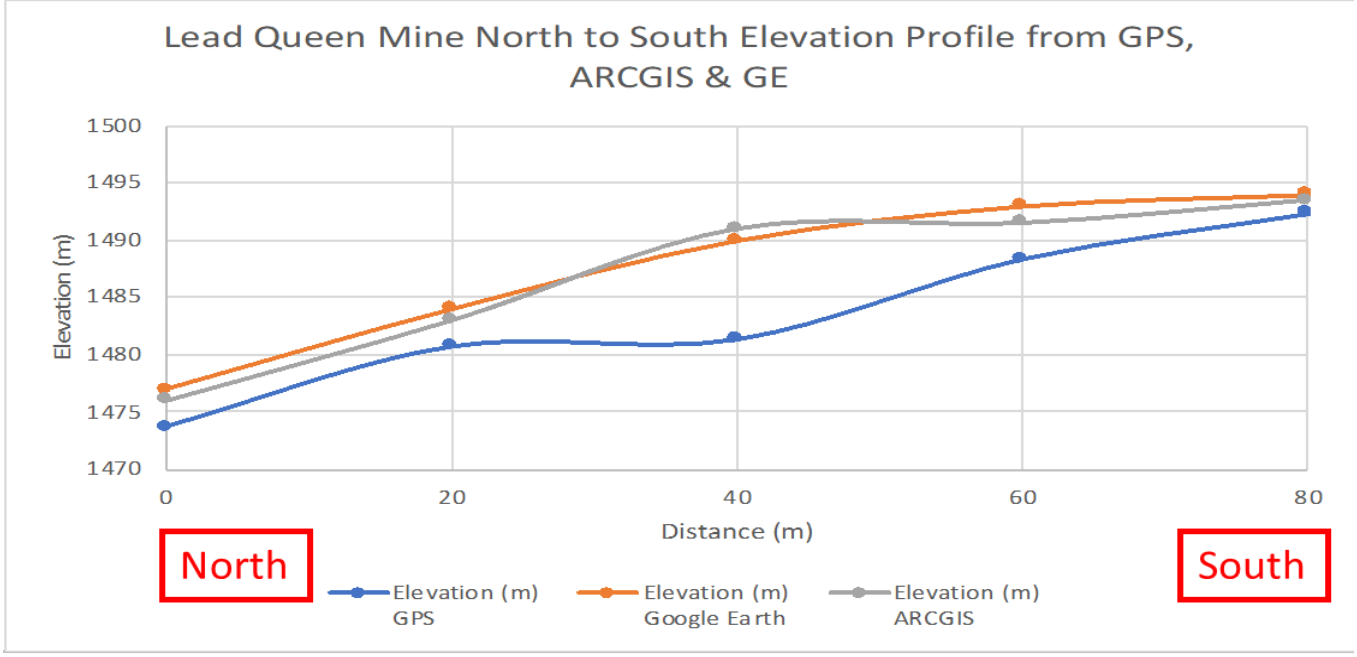

Figure 2.17. Comparison of GPS, ArcGIS and Google Earth Pro elevation profiles from north to south following the projected trend line of the Lead Queen adit.

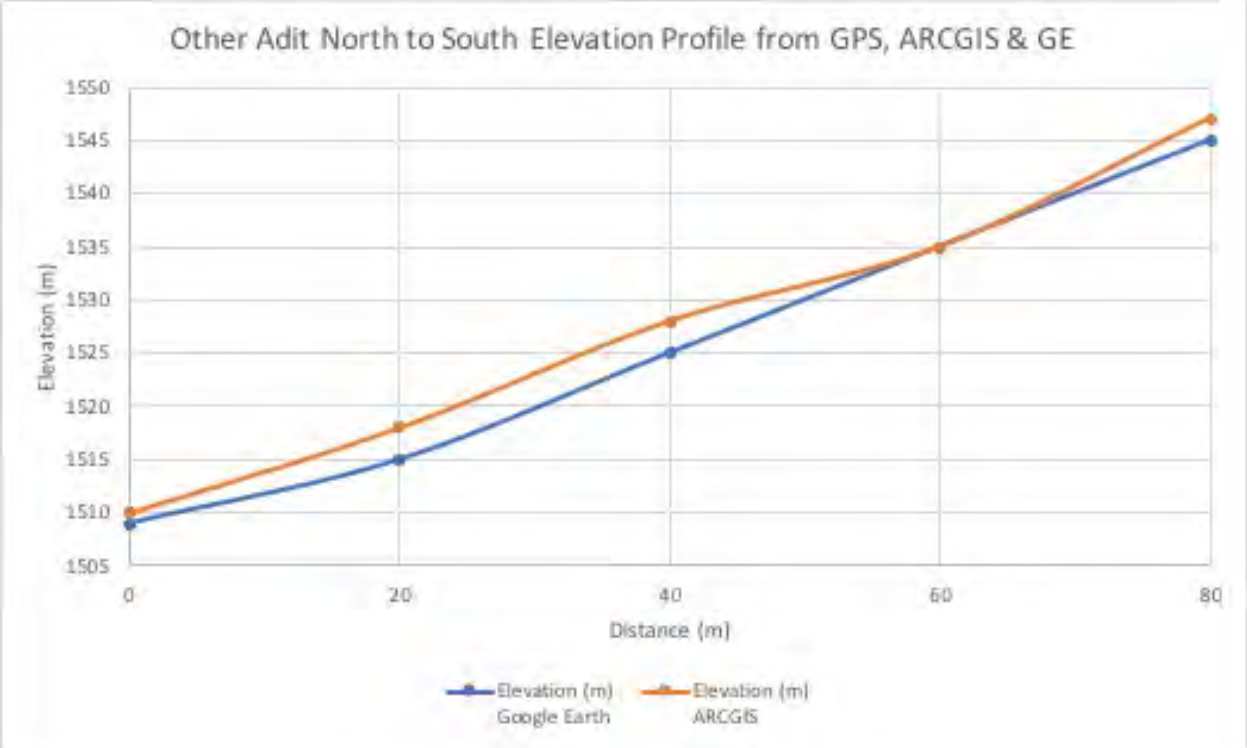

Figure 2.18. Comparison of ArcGIS and Google Earth Pro elevation profiles from north to south following the projected trend line of the Other Adit.

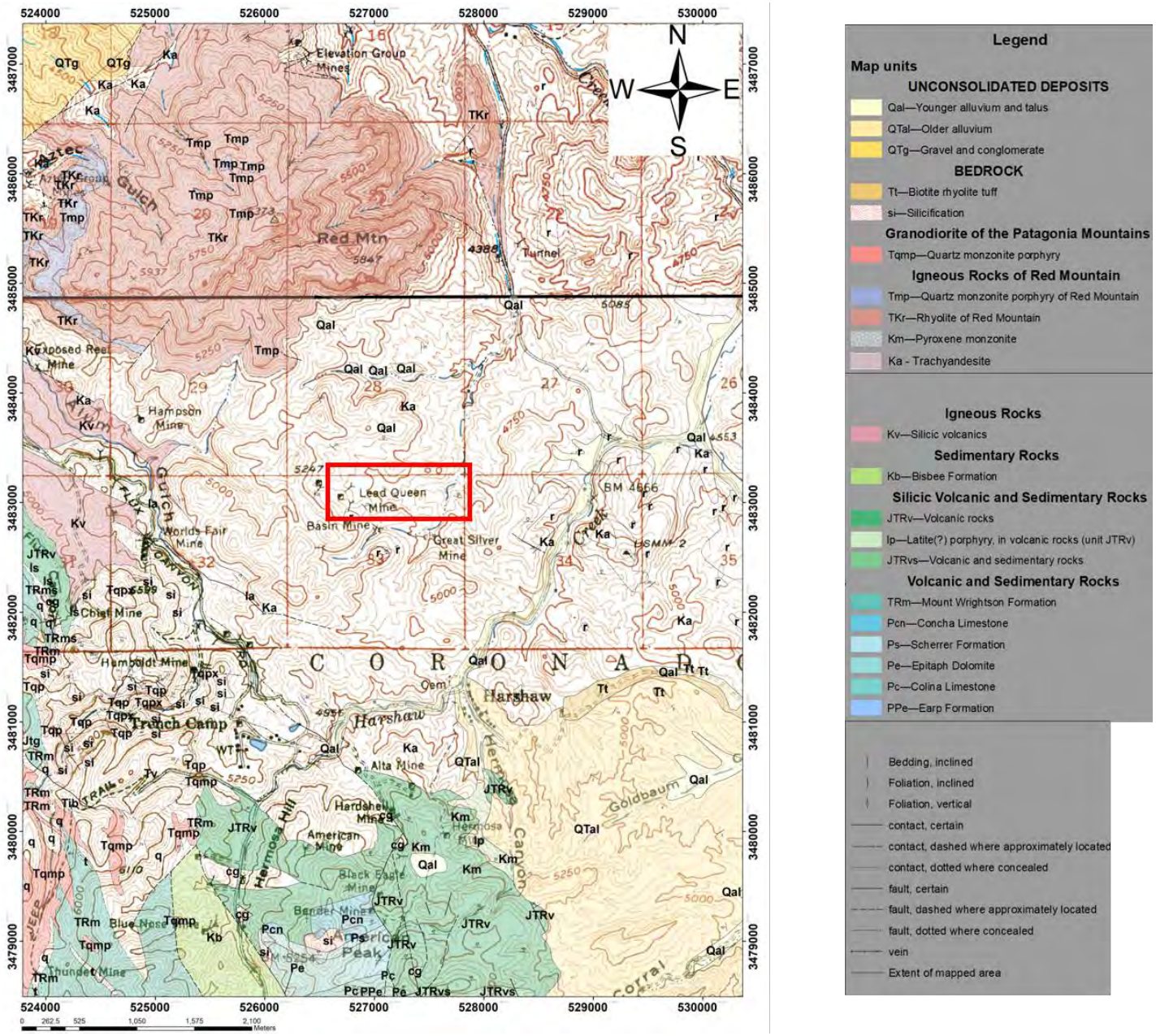

Figure 2.19. Geologic map of region around the Lead Queen mine.

2.9 References

Garmin. 2016. *What is GPS?* Web. Retrieved April 5, 2018. http://www8.garmin.com/aboutGPS/.

U.S. Forest Service. 2017. GPS Tested Accuracies. https://www.fs.fed.us/database/gps/mtdcrept/accuracy/documents/accuracy.pdf. Retrieved April 5, 2018.

Lipman, P.W. 1993. *Geologic map of the Tucson Mountains caldera, southern Arizona*. U.S. Geological Survey. Miscellaneous Investigations Series Map I-2205. 1:24,000.

U.S. Geological Survey. 1995. Jaynes Quadrangle. North American Datum of 1983 (NAD83). World Geodetic System of 1984 (WGS84). 1:24,000.

3. Transient Electromagnetic (TEM) Surveys

3.1 Introduction

The transient electromagnetic (TEM) method is a geophysical technique that provides information on the electrical resistivity of the subsurface of the targeted area. A loop of insulated wire is laid on the ground over a target area, which acts as a transmitter, and is driven by a time varying current (Figure 3.1). “The change in current and the resulting EM field establish an image current within the earth equal in magnitude, but opposite in polarity, to that of the transmitter.” (Zonge, 2018). Conductive material in the earth below interacts with the image current to create secondary magnetic fields which are then measured at the receiver. The depth of exploration depends on the transmitter loop size, with three times the loop size being an acceptable guideline for reliable data. “The TEM method is based on transmitting a time-domain, square-wave signal into a large, ungrounded wire loop and then interrupting the current as fast as possible, causing a rapid change in the magnetic field” (Zonge, 2018). This produces currents in surrounding conducting materials, forming small secondary magnetic fields that are observed in the induced voltages in receiver loops. These induced currents decay rapidly in material with poor conductivity (moderate resistivity) and slowly in material with good conductivity (low resistivity). Material with very poor conductivity (high resistivity) cannot sustain any quantifiable induced current. Modeling software is then used to convert TEM measurements to profiles of resistivity vs depth. This is then used to help identify changes in the subsurface.

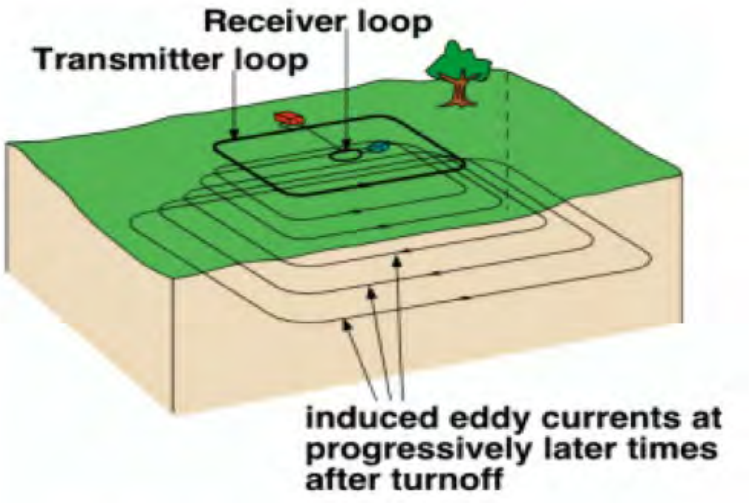

Figure 3.1a. Representation of a standard TEM setup showing the transmitter and receiver loop, as well as the “smoke rings” from the induced eddy currents (Zonge, 2018).

3.2 Field Procedures and Instrumentation

The data were collected on two weekends February 10/11, 2018 and March 3/4, 2018 using a Zonge International GDP – 32 II (Serial # SN-53) multi-function receiver with a Zonge International NT-20 transmitter. The receiver records one transient sounding per loop and computer modeling translates the time into depth. Frequencies were transmitted using the NT - 20 transmitter. The data were transmitted at both 32 Hz and 64 Hz fundamental frequencies. Other parameters are SEM 1-3, 2048 Cycles at 3 amps for 64 Hz and 1024 at 3 amps for 32 Hz on lines LQ2 through LQ6 and for line OA (Other Adit). Line LQ1 used the same current (3Amps) SEM (1-3), same two frequencies but at 512 cycles at 32 Hz and 1024 cycles at 64 Hz due to time constraints.

The TEM arrays consisted of 20 by 20-meter square transmitter loops and a 5 by 5 meter receiver loop in the center of the loop. A standard formula for the depth of investigation is three times the length of a loop side, providing a depth of investigation for this study of approximately 60 meters. Garmin GPSMAP 64ST handheld GPS units were used to record center points for each loop with an allowable 10% line variation due to GPS errors. Six loop lines trending east to west were used to collect data at the Lead Queen adit. Lines LQ1 through LQ4 contained five loops each (0, 20, 40, 60, 80), with the 40-meter loops centered on the adit with two loops on each side. The sides of the squares trend 120° (-300°) perpendicular to the adit and 30° (-210°) parallel to the adit's estimated trend line of -210°. Line LQ5 consisted of four loops (40, 60, 80, 100) with loops 0 and 20 being omitted due to the terrain being too rough for the effective use of TEM. Line LQ6 consisted of three loops (60, 80 and 100) with loops 0, 20 and 40 being omitted due to terrain considerations. The OA array line used 3 loops laid out in an east to west heading of 100˚ (-280˚), perpendicular to the adit trend line of 190 ˚ from the entrance. The three loops were numbered 0, 20 and 40, with loop 20 being centered over OA (Figure 3.2)

Figure 3.1b. Geophysical Data Receiver-32 II: instrument used in collection of data.

3.3 Data Processing

The NanoTEM data obtained in the field were downloaded from the GDP32-II receiver and processed using Zonge International's DATPRO suite of geophysical software, consisting of two main programs, TEMAVG and STEMINV. Field measurements at a typical site consisted of three repeat measurements which were averaged with TEMAVG. The averaged data were then processed and inverted with STEMINV. After the inversions were completed, the measured data were compared with the inverted data to determine if the modeled results were accurate. Smooth-Model and Transient curves of NanoTEM data using STEMINV software are displayed in Figures 3.16-3.22 and the inversion models are shown in Figures 3.3-3.11. The inversion models were then used in Golden Software's Surfer program to generate contour maps of the 6 Ohm-m contour line depth, to provide a 3D image of the subsurface at this depth.

3.4 Interpretation

The inversion models from the NanoTEM survey show a large conductor at depths varying from 20 to 60 meters beneath the surface around the Lead Queen Adit and at around 60 meters for the

Other Adit. Based on Archie's Law, the low-resistivity region could be an area of high fracture porosity and/or highly saturated rock or highly conductive water. This conductor varies significantly in shape and size between the six transects of the area. There is a high resistivity layer on all the inversion models at a depth less than 10 meters, indicting a possible linear feature that extends through all of the inversion models.

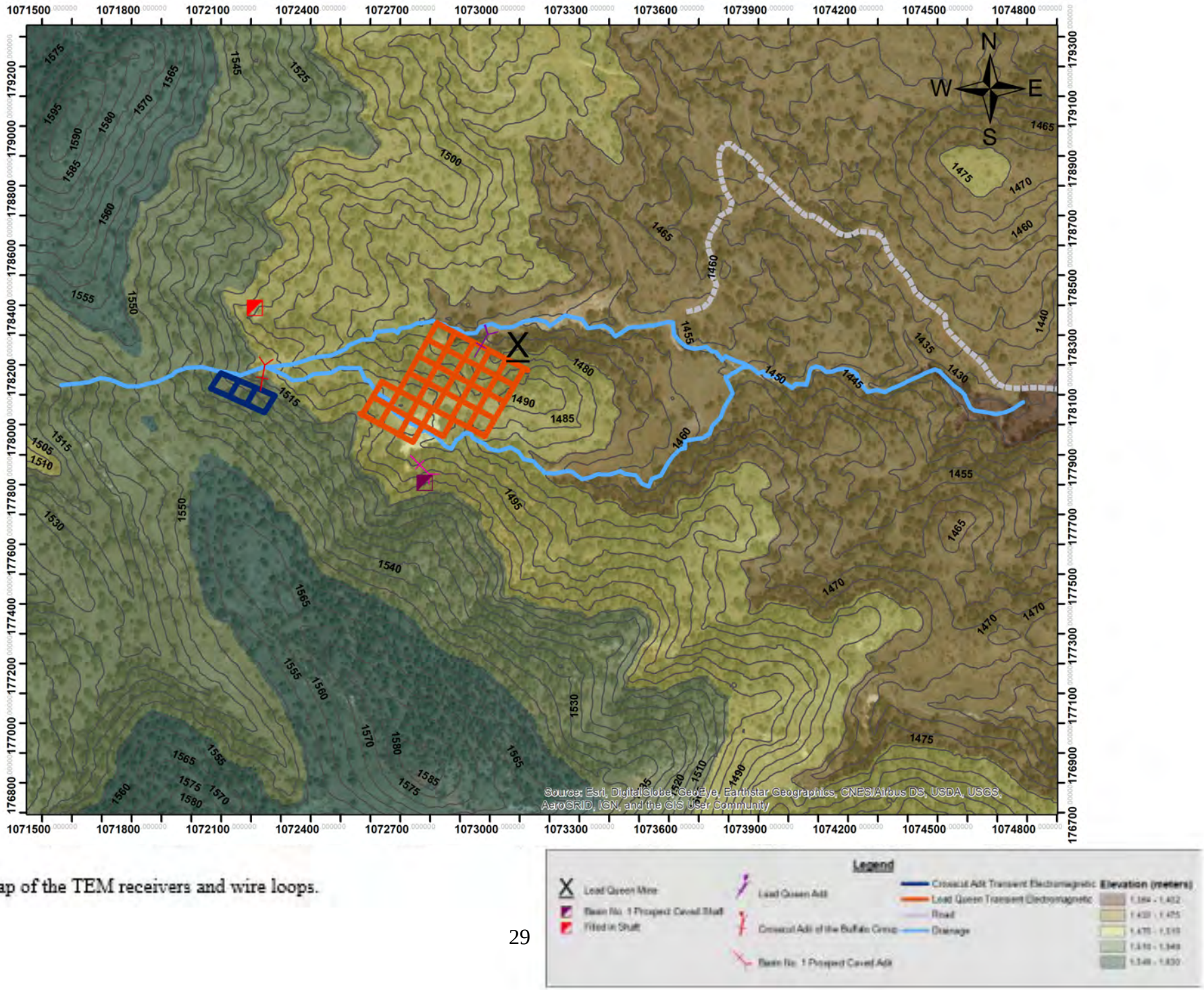

Figure 3.2. Map of the TEM receivers and wire loops.

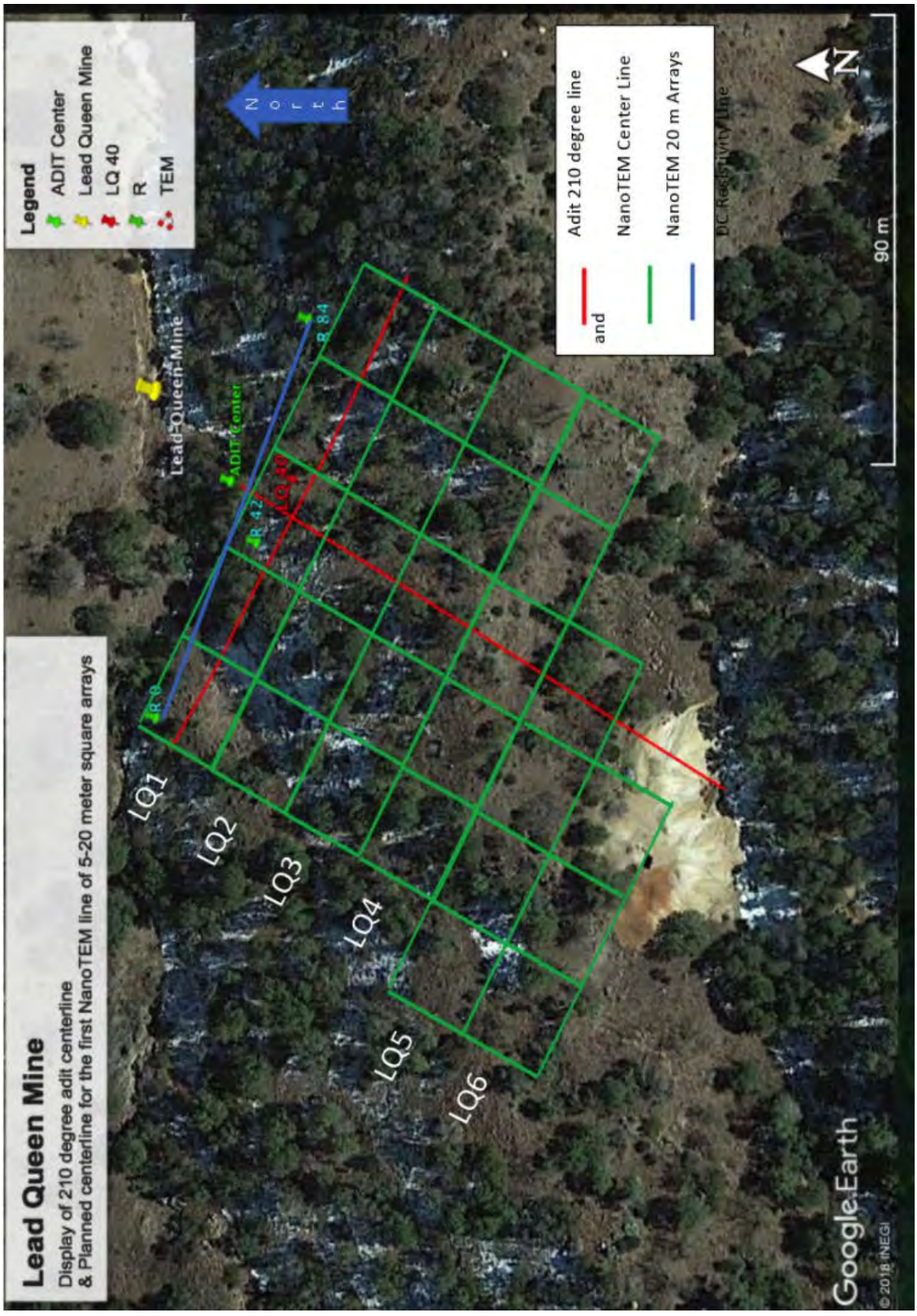

Figures 3.3. Location map for the Lead Queen Adit NanoTEM grids.

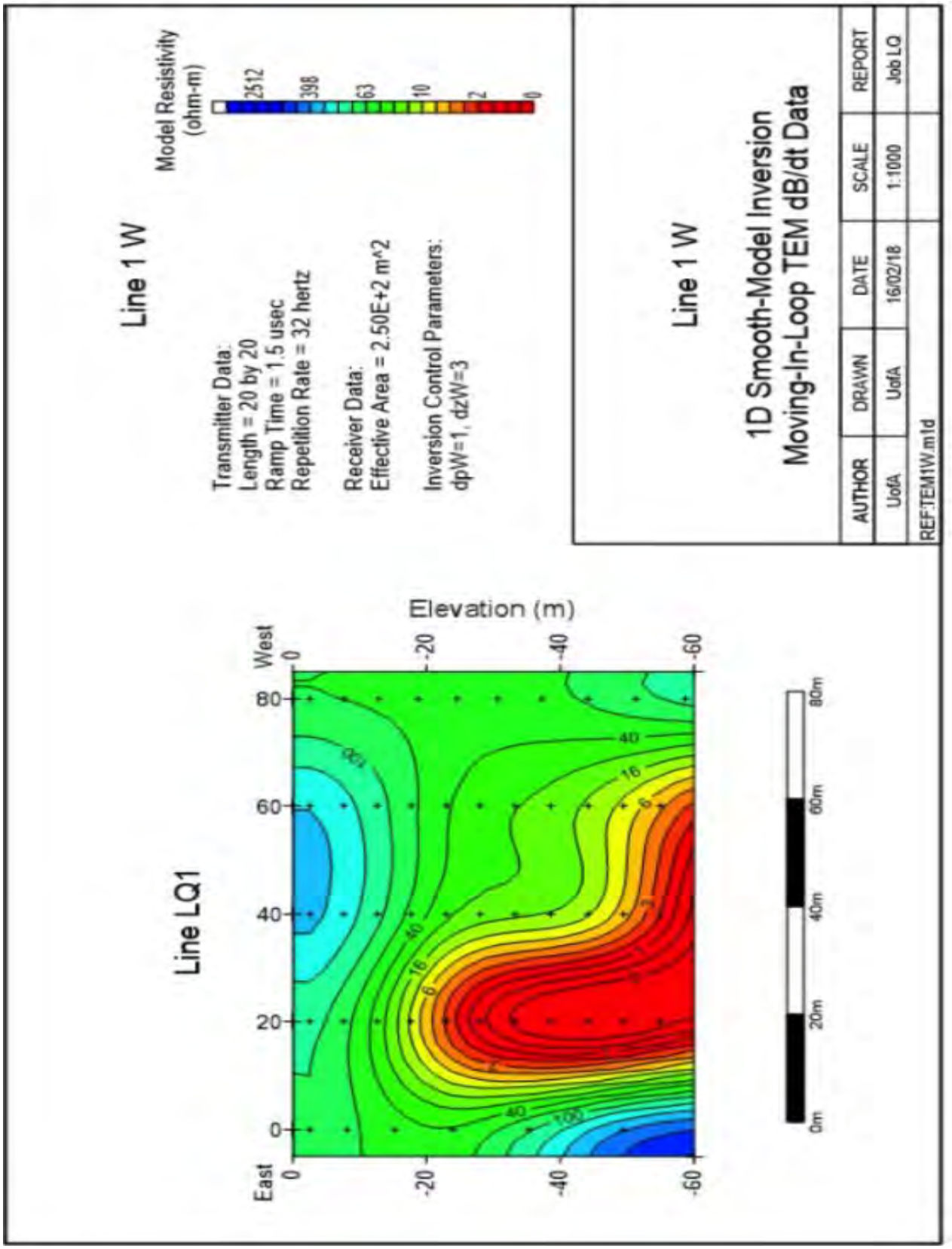

Figure 3.4. Transect 1 for Lead Queen Adit at 32 Hertz

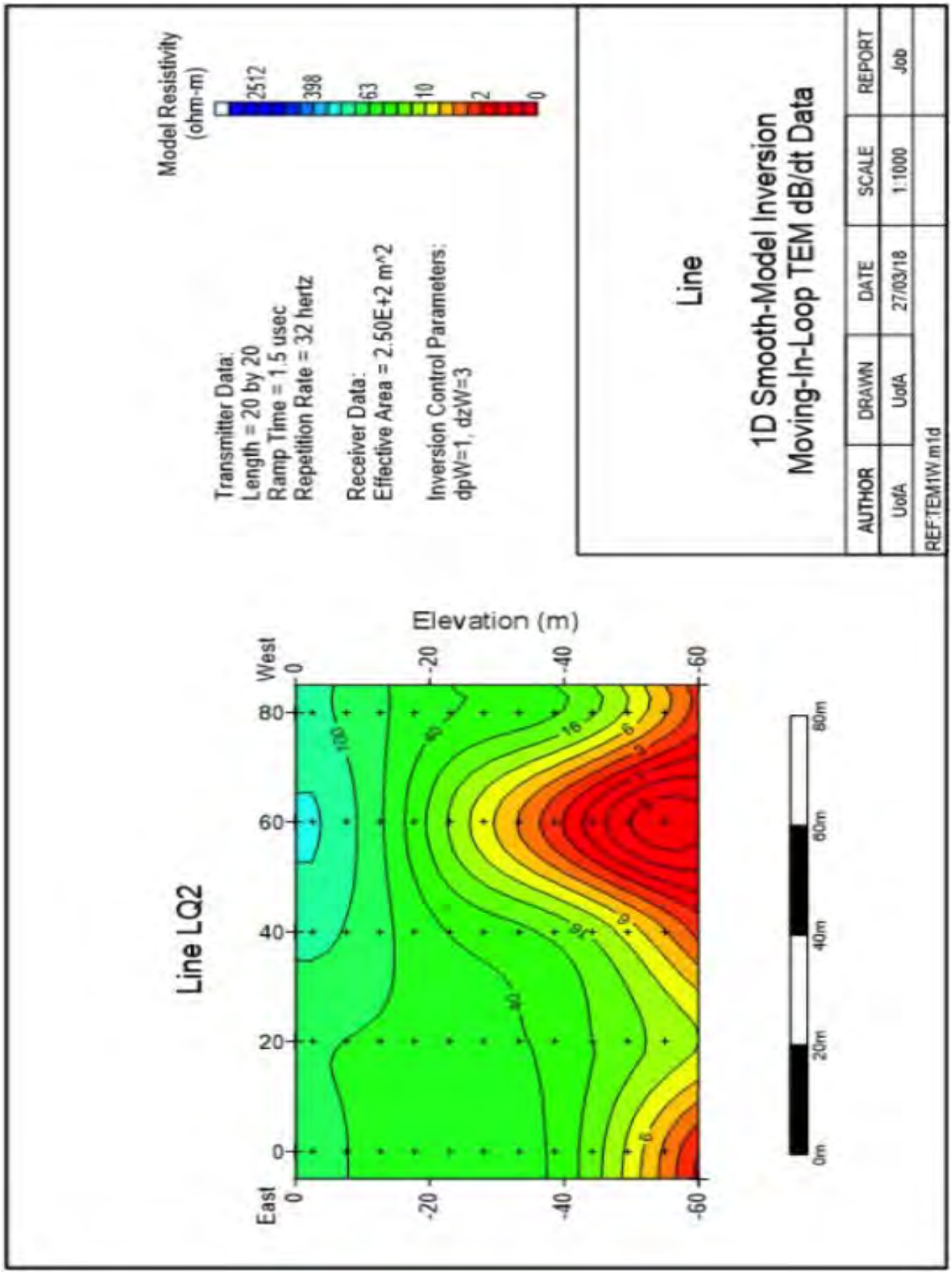

Figure 3.5. Transect 2 for Lead Queen Adit at 32 Hertz

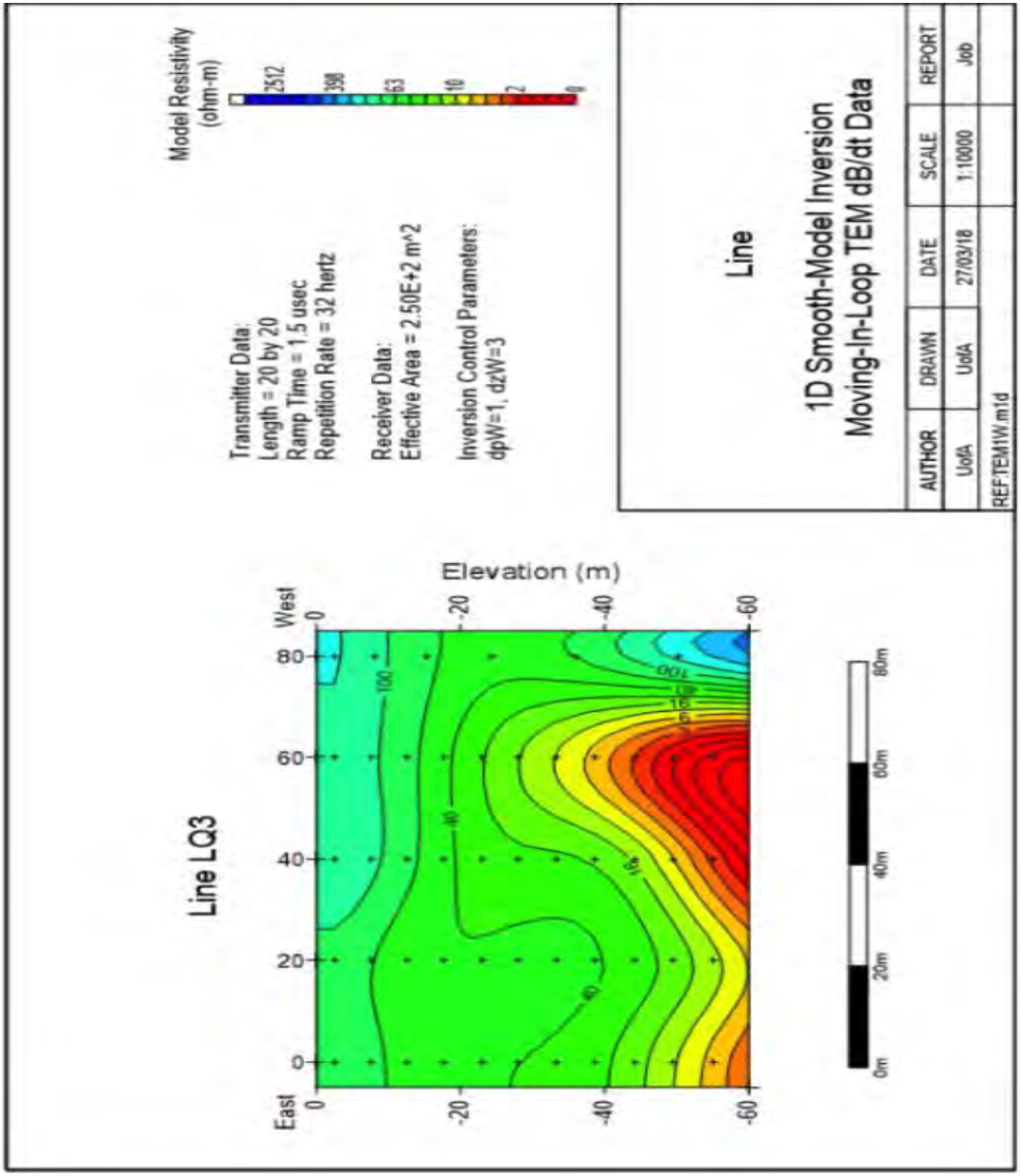

Figure 3.6. Transect 3 for Lead Queen Adit at 32 Hertz

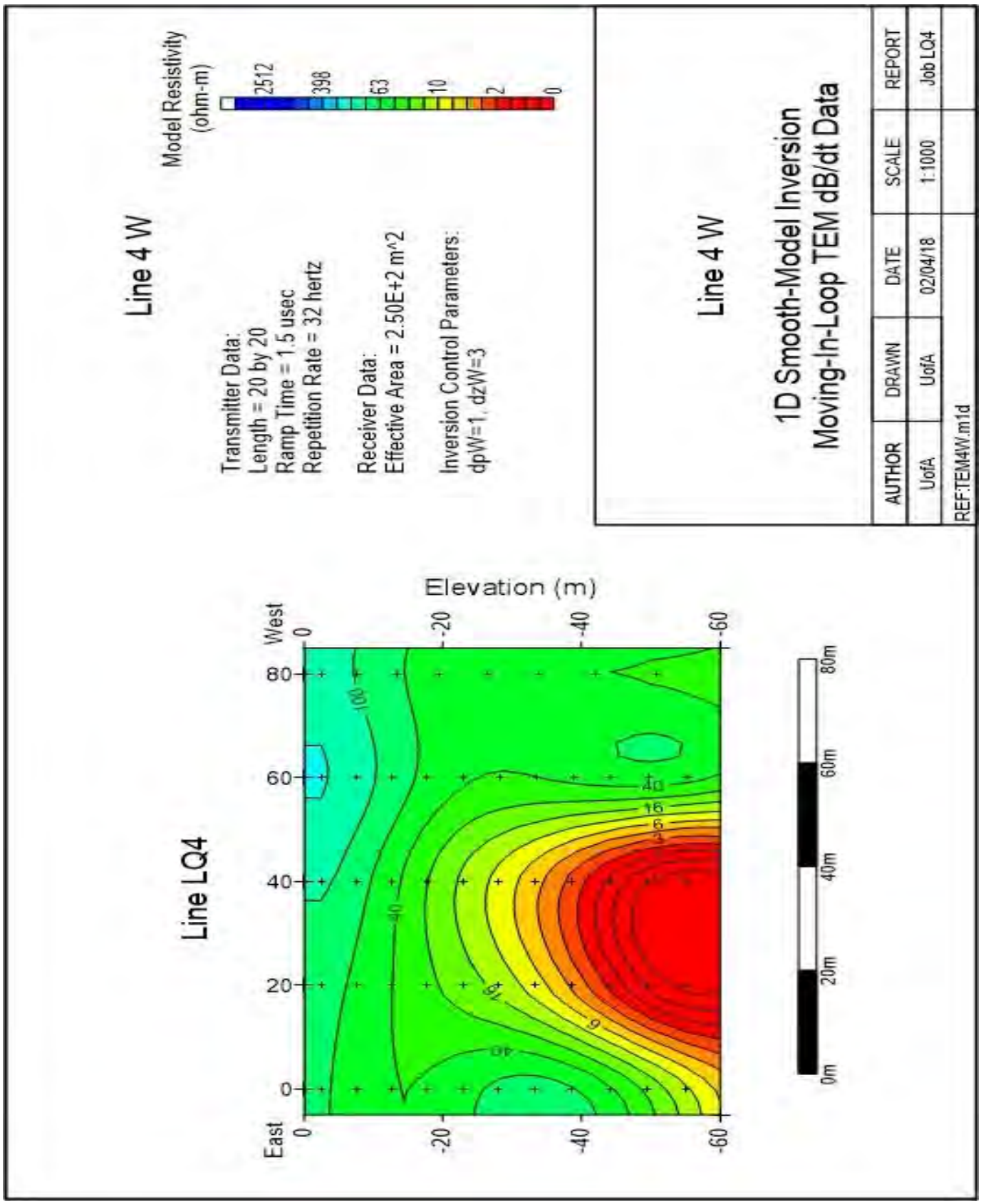

Figure 3.7. Transect 4 for Lead Queen Adit at 32 Hertz

Figure 3.8. Transect 5 for Lead Queen Adit at 32 Hertz

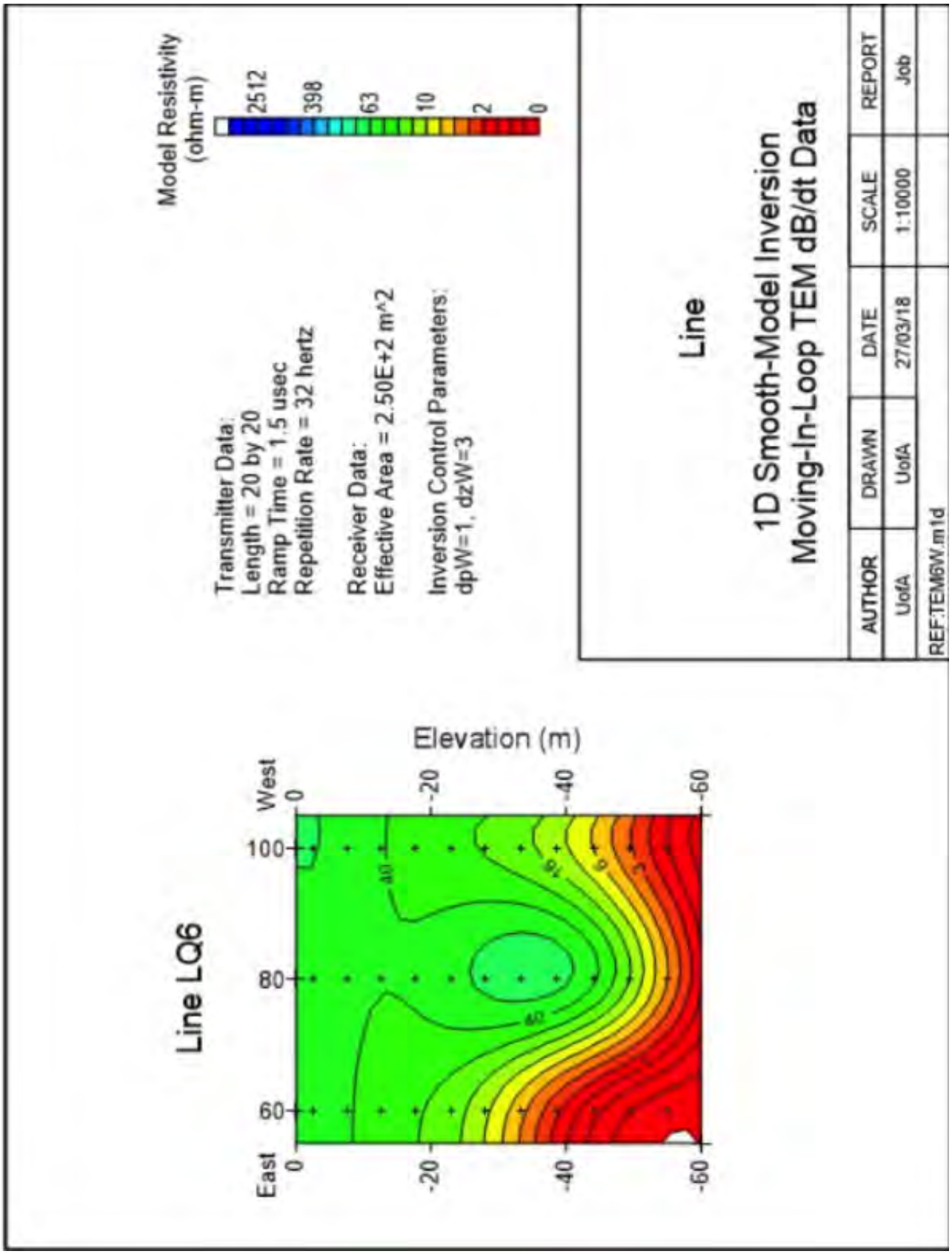

Figure 3.9. Transect 6 for Lead Queen Adit at 32 Hertz

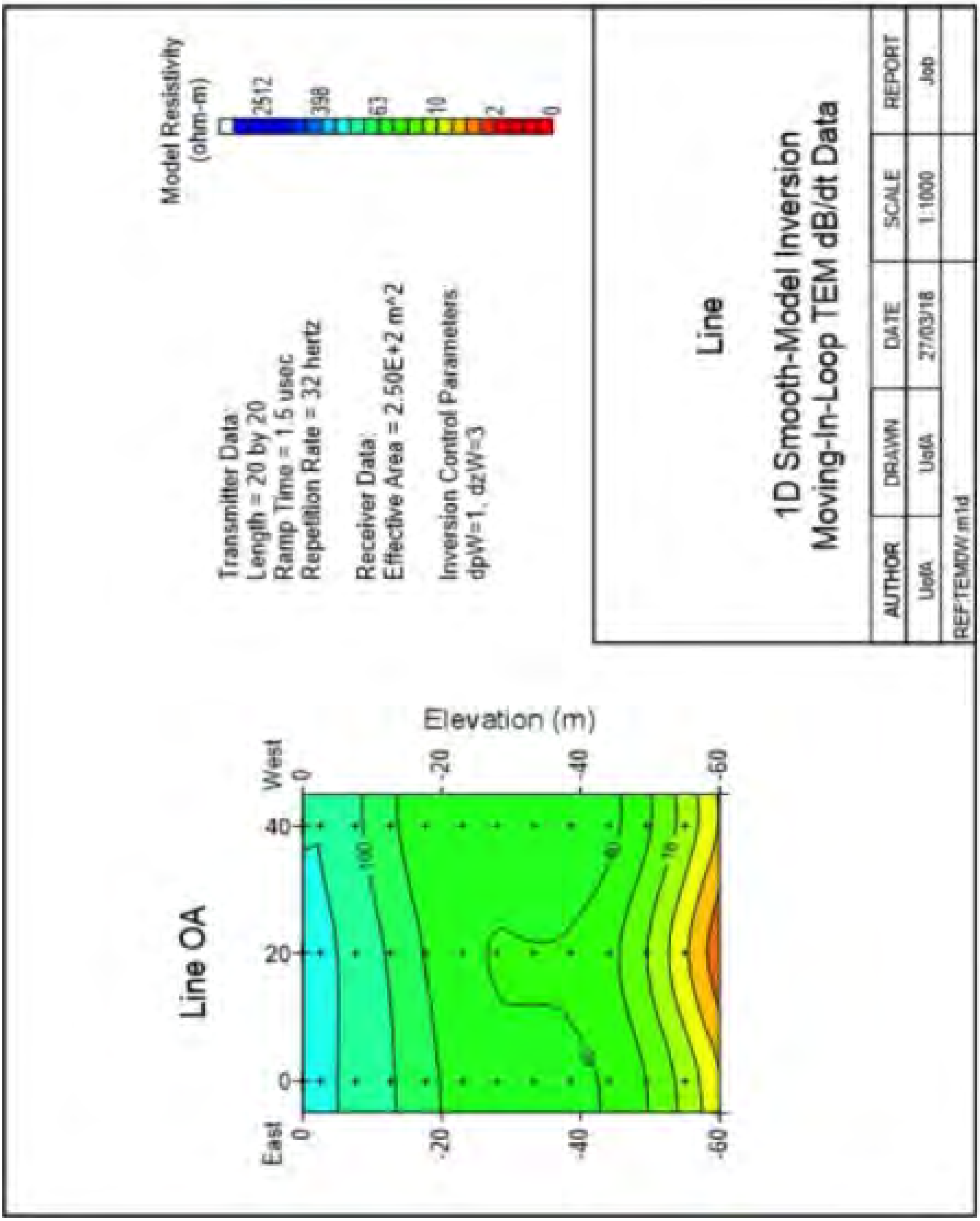

Figure 3.10. Transect 1 for Other Adit at 32 Hertz

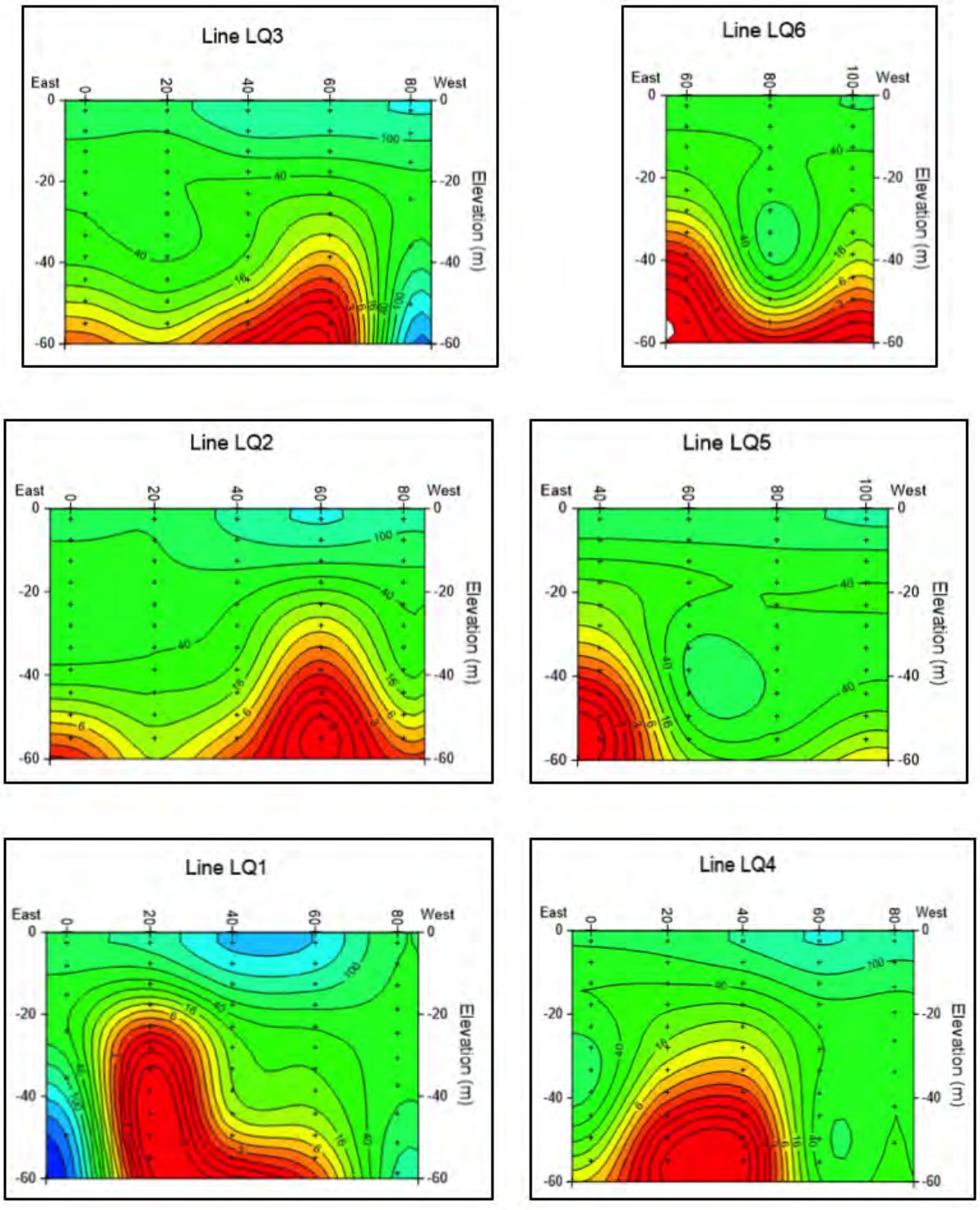

Figure 3.11. All Six transect cross sections from Lead Queen Mine TEM

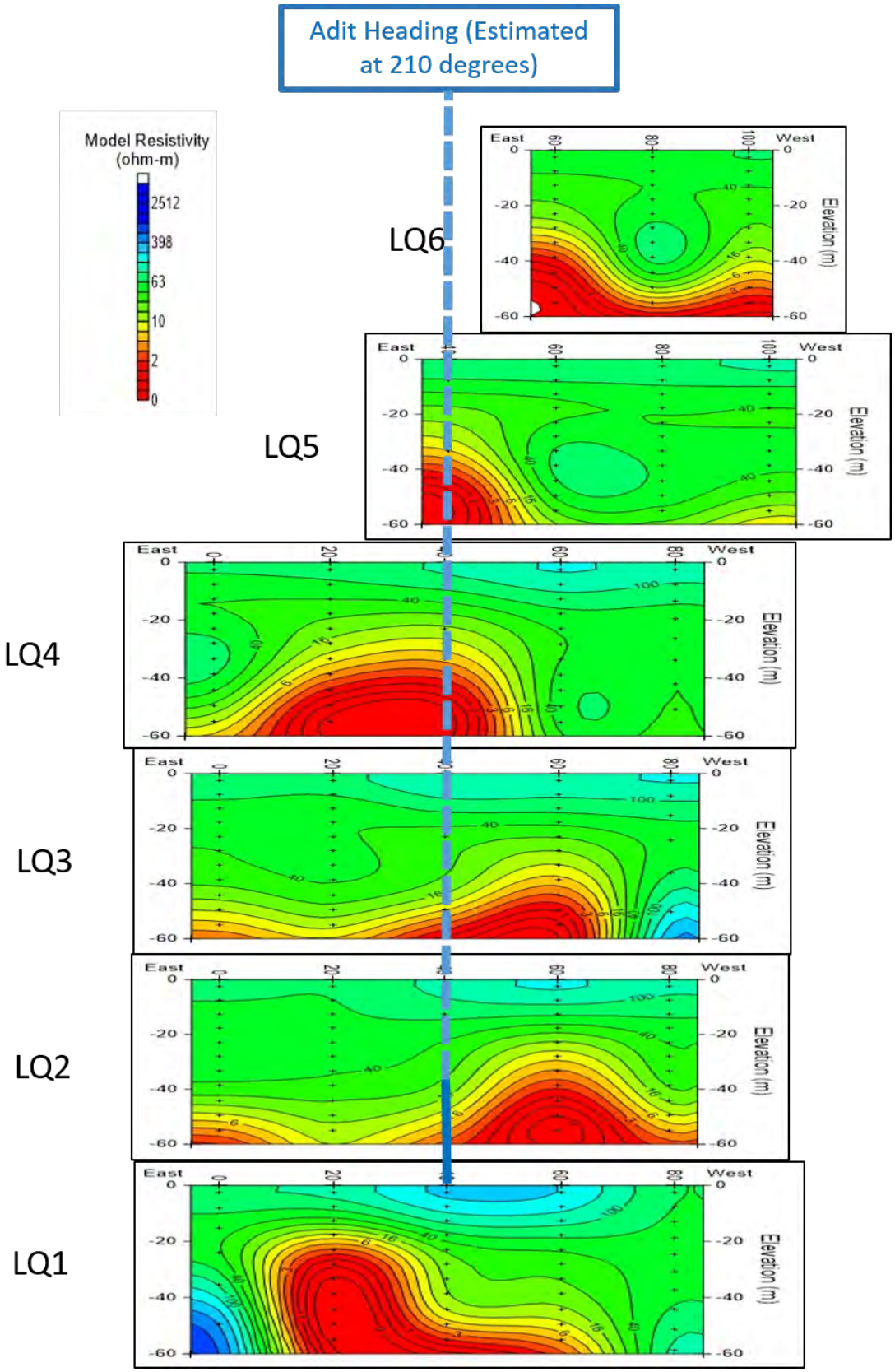

3.12. Transect Cross sections with adit heading measured at 210°

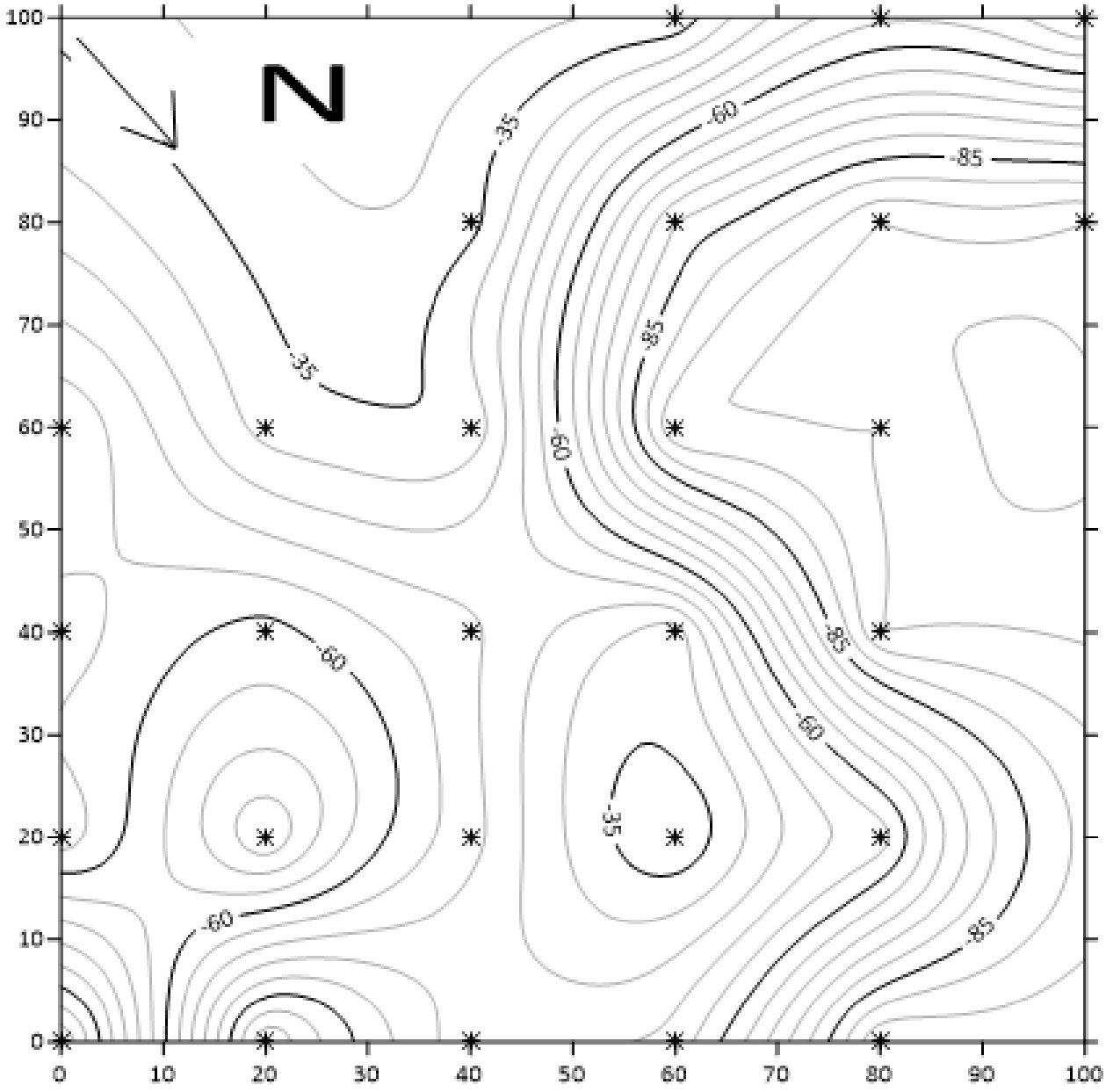

Figure 3.13. Surfer contour of depth from surface to conductive layer created using the original data from the NanoTEM processing. The crosses represent the center points of each loop. Line 0 is line 1 from the NanoTEM data. Line 100 is line 6 from the NanoTEM data

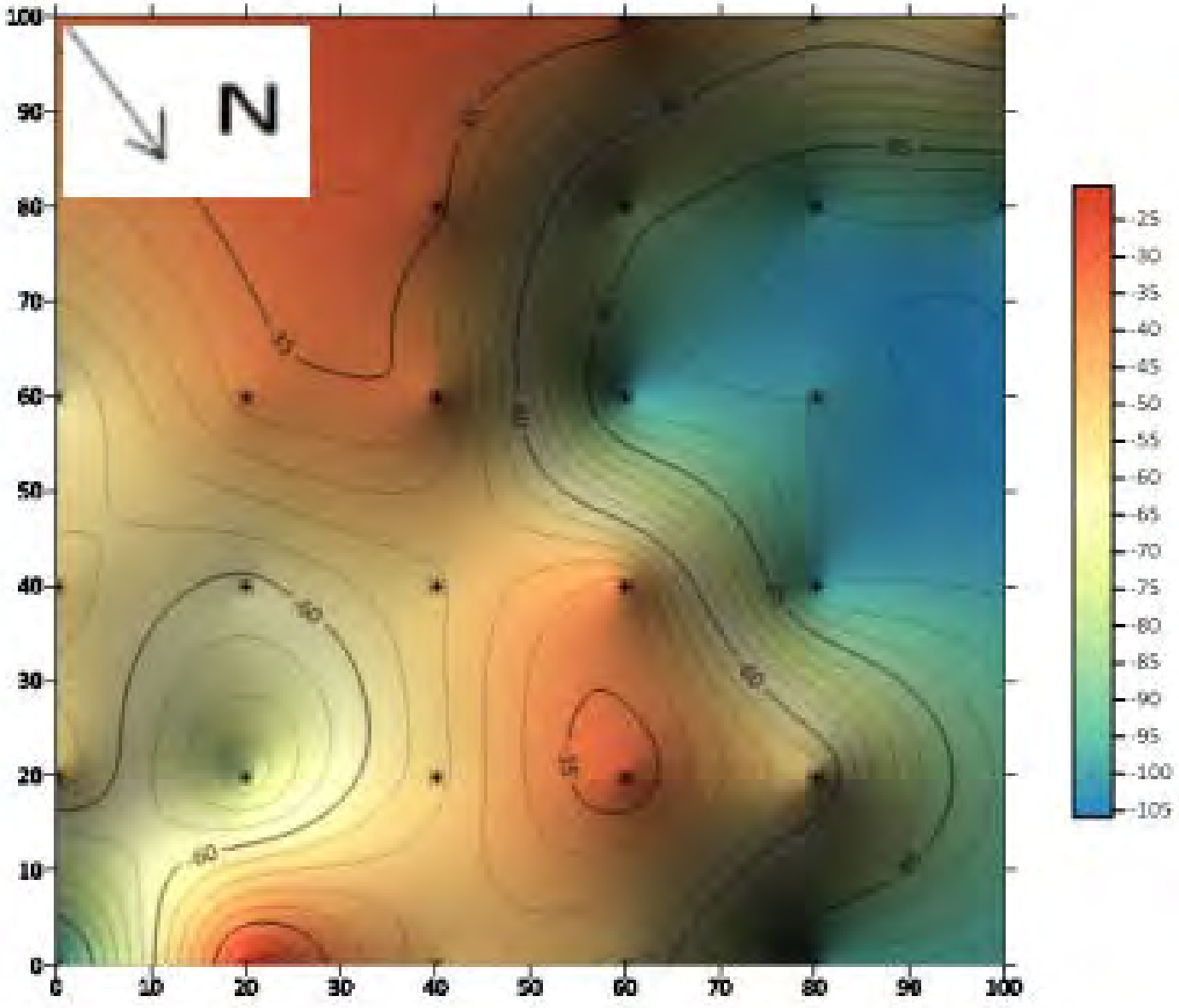

Figure 3.14. Surfer contour of depth from surface to conductive layer with color added

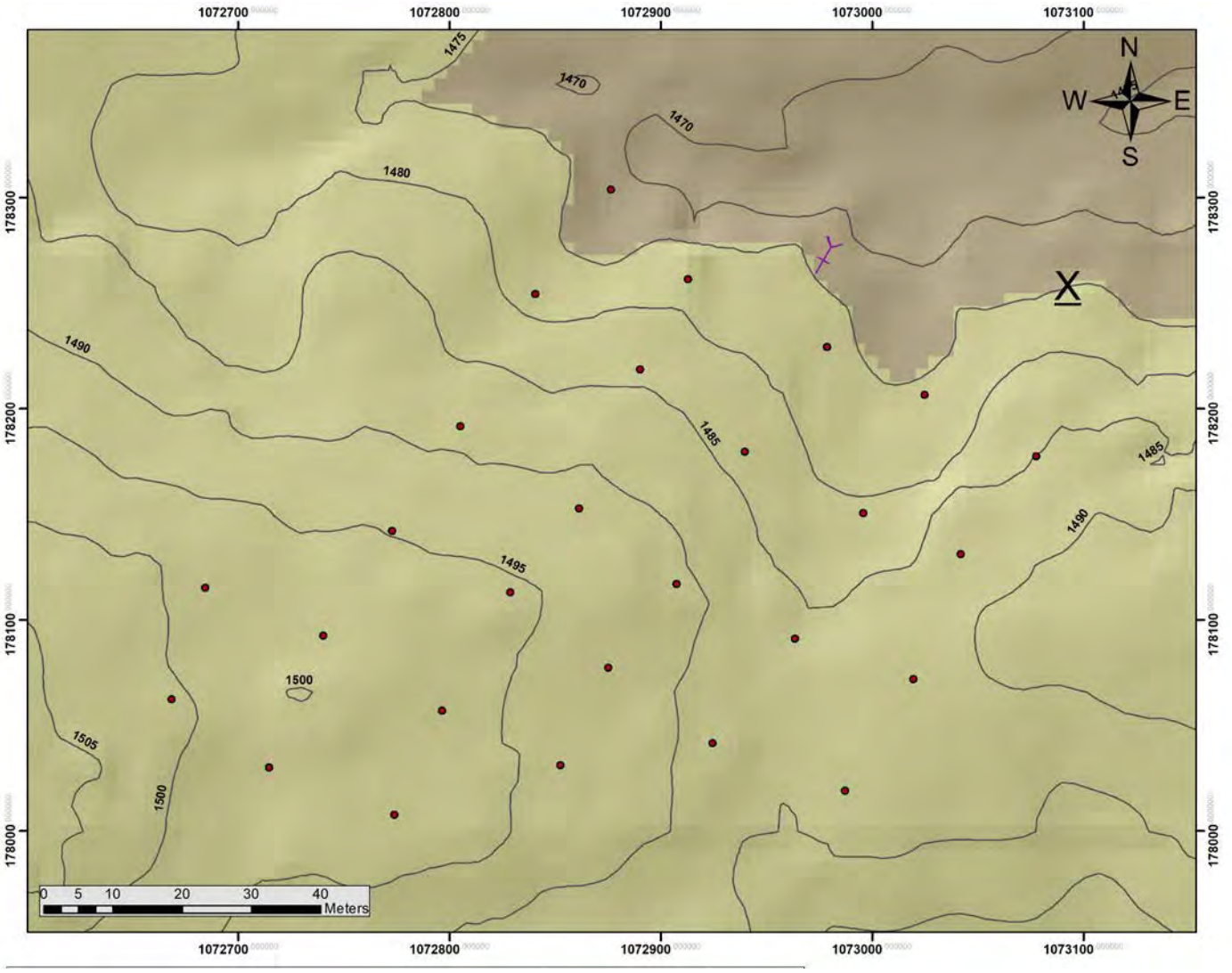

Figure 3.15. Map of TEM lines in reference to sea level

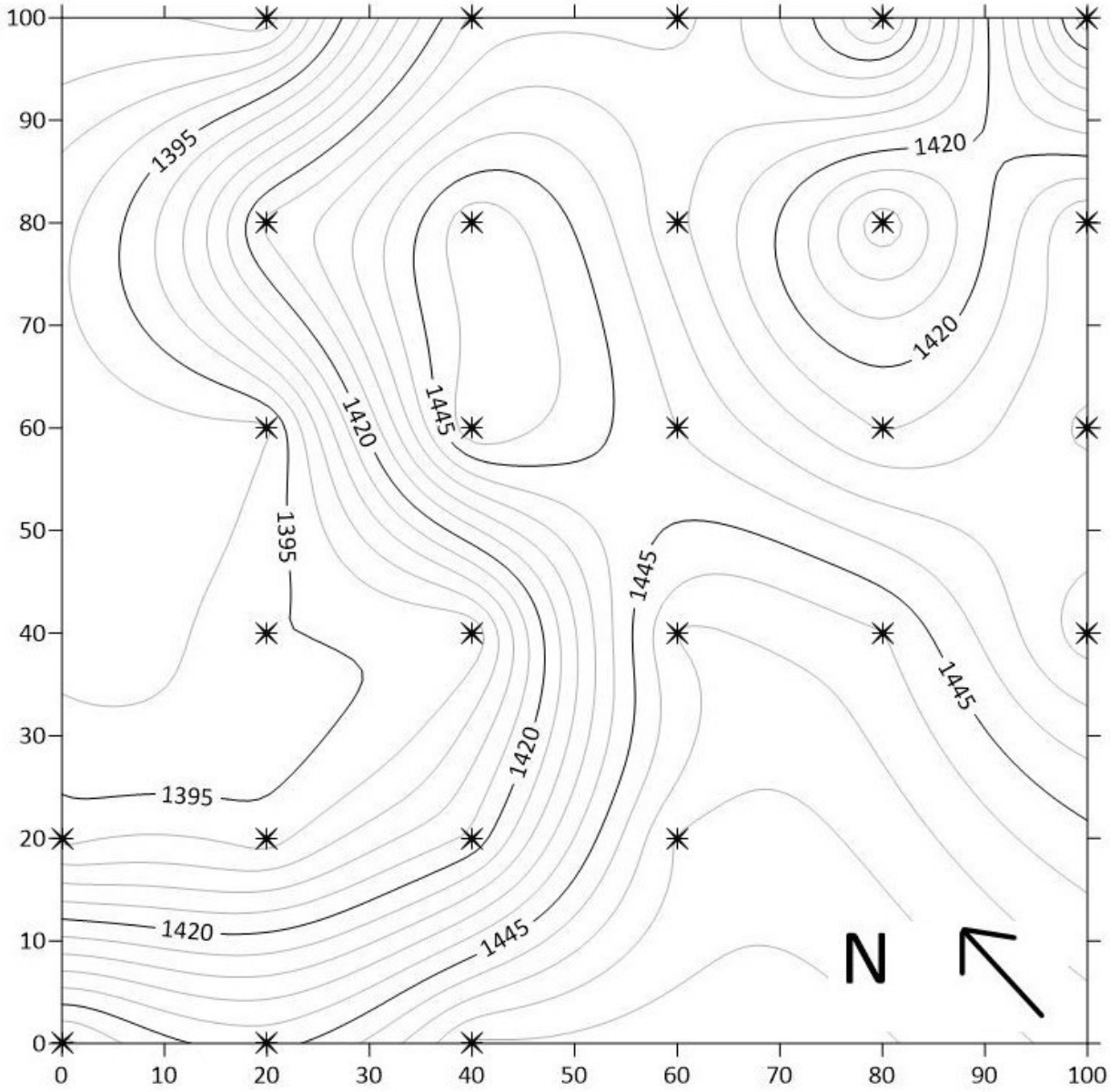

Figure 3.16. Surfer contour of conductive layer elevation in reference to sea level created using the rotated data from the NanoTEM processing. The crosses represent the center points of each loop. Line 0 is line 6 from the NanoTEM data. Line 100 is line 1 from the NanoTEM data.

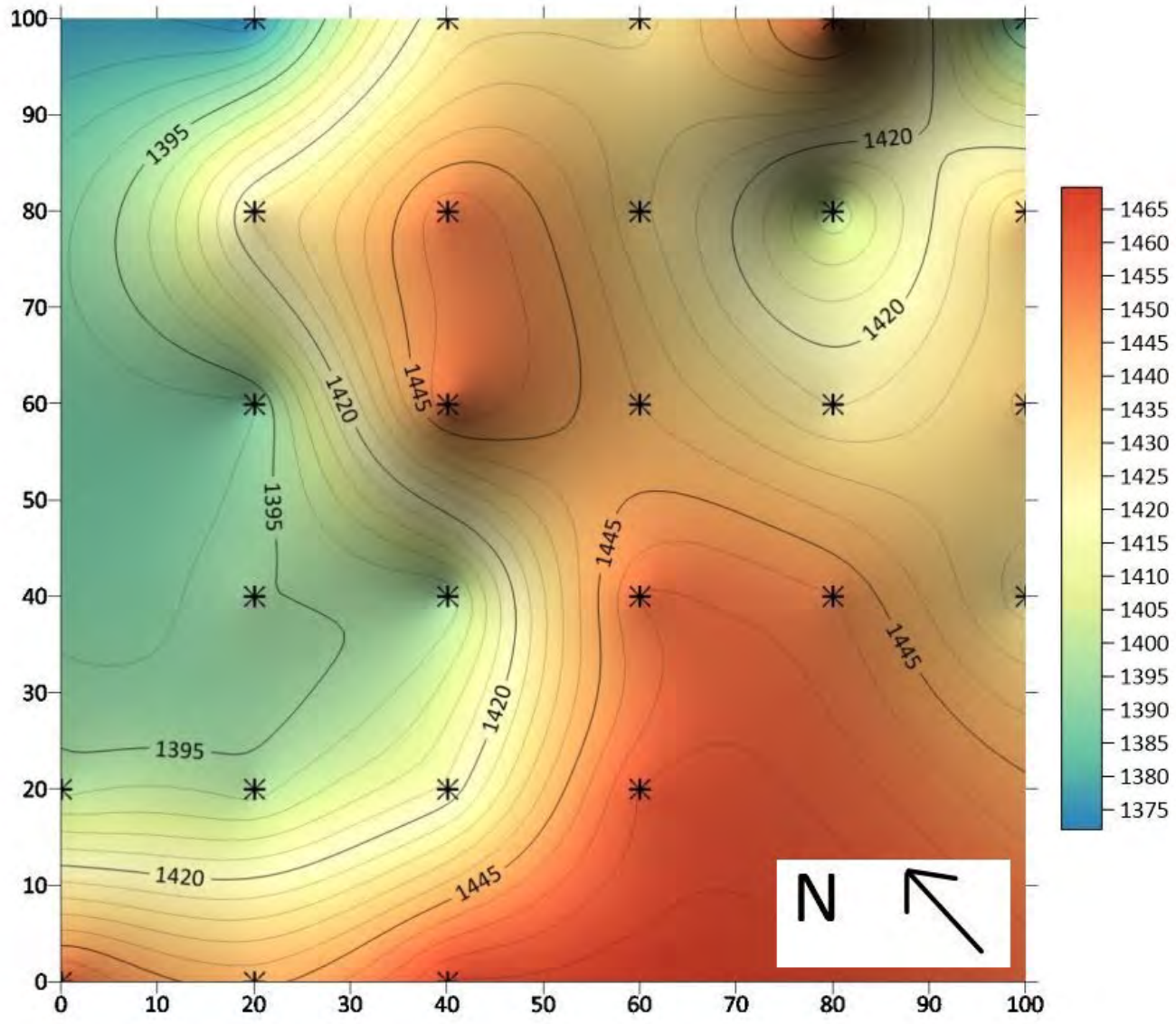

Figure 3.17. Surfer contour of conductive layer elevation in reference to sea level in color

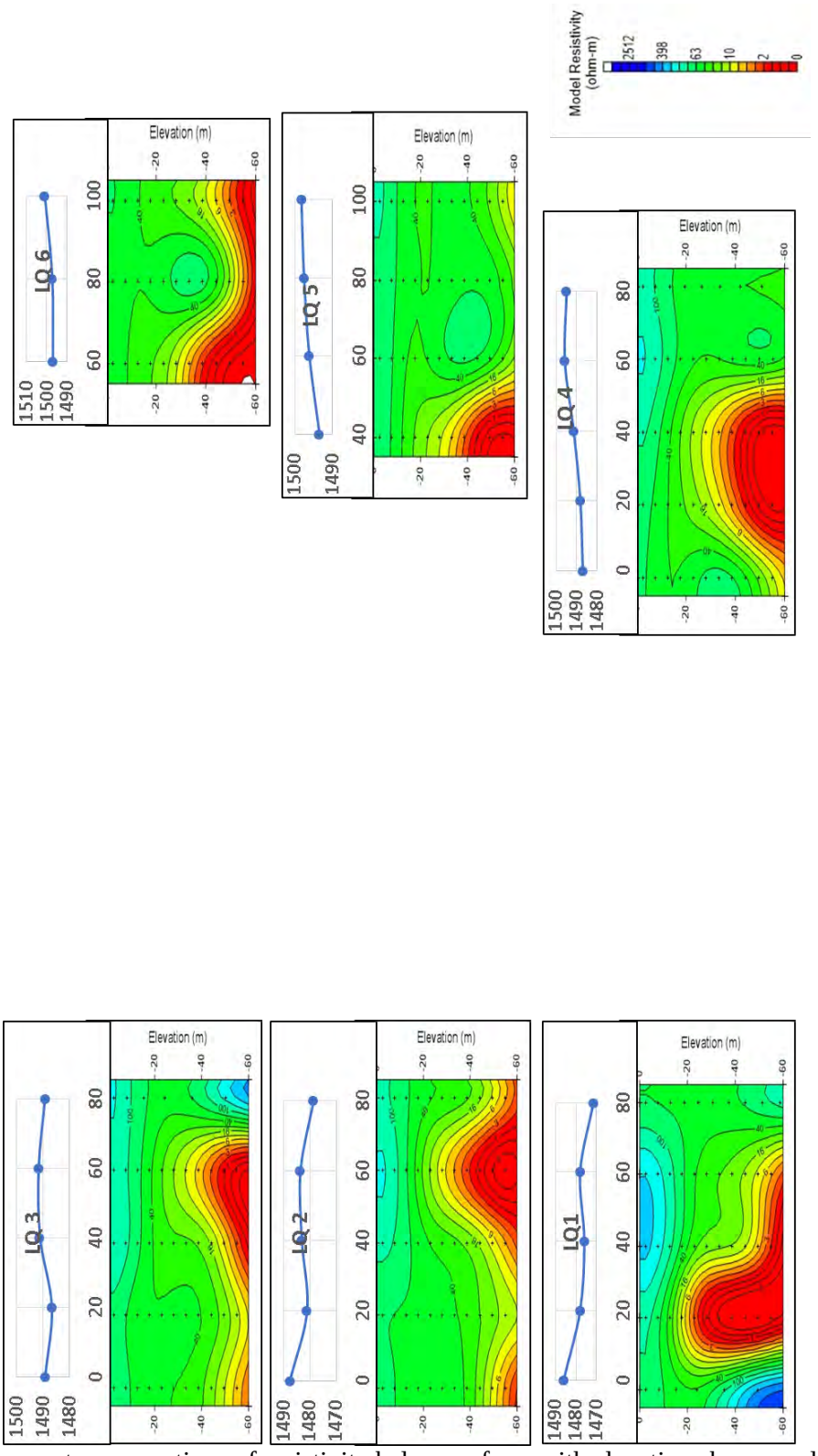

Figure 3.18. Transect cross sections of resistivity below surface, with elevation above sea level of conductive layer plotted above for each line

3.5 References

Zonge International. (2018). TEM geophysical method. *Zonge.com.* Trusted Geophysics. Zonge International. http://zonge.com/geophysical-methods/electrical-em/tem/. Retrieved on April 1, 2018.

3.6 Measured and Calculated transient data plus earth model.

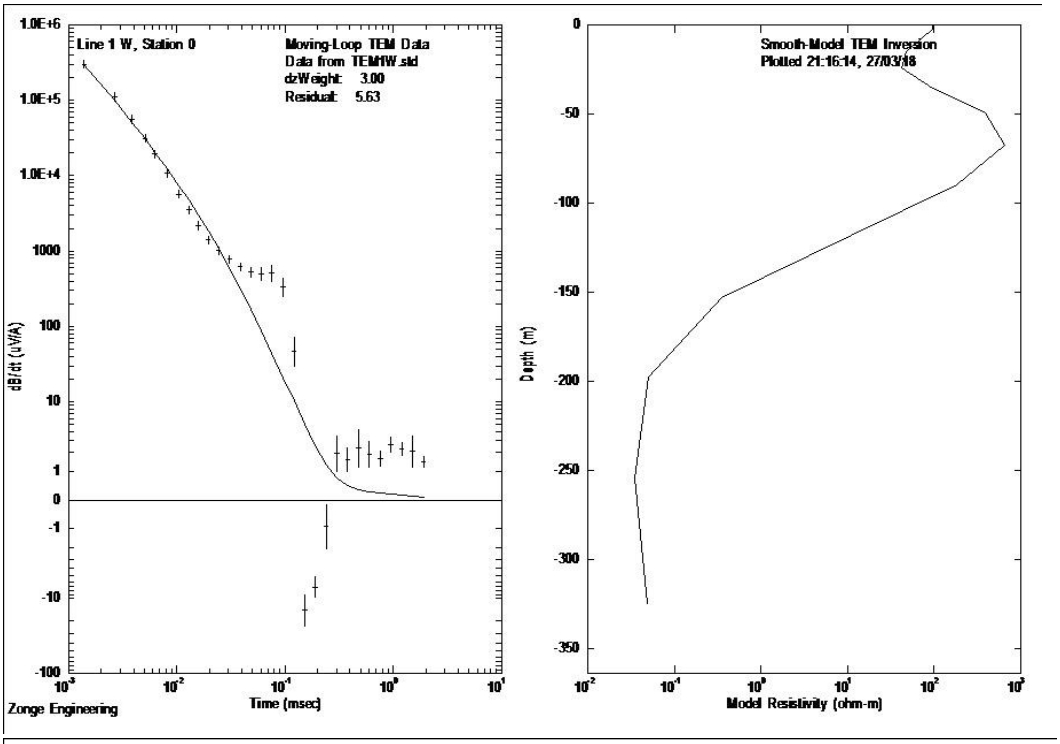

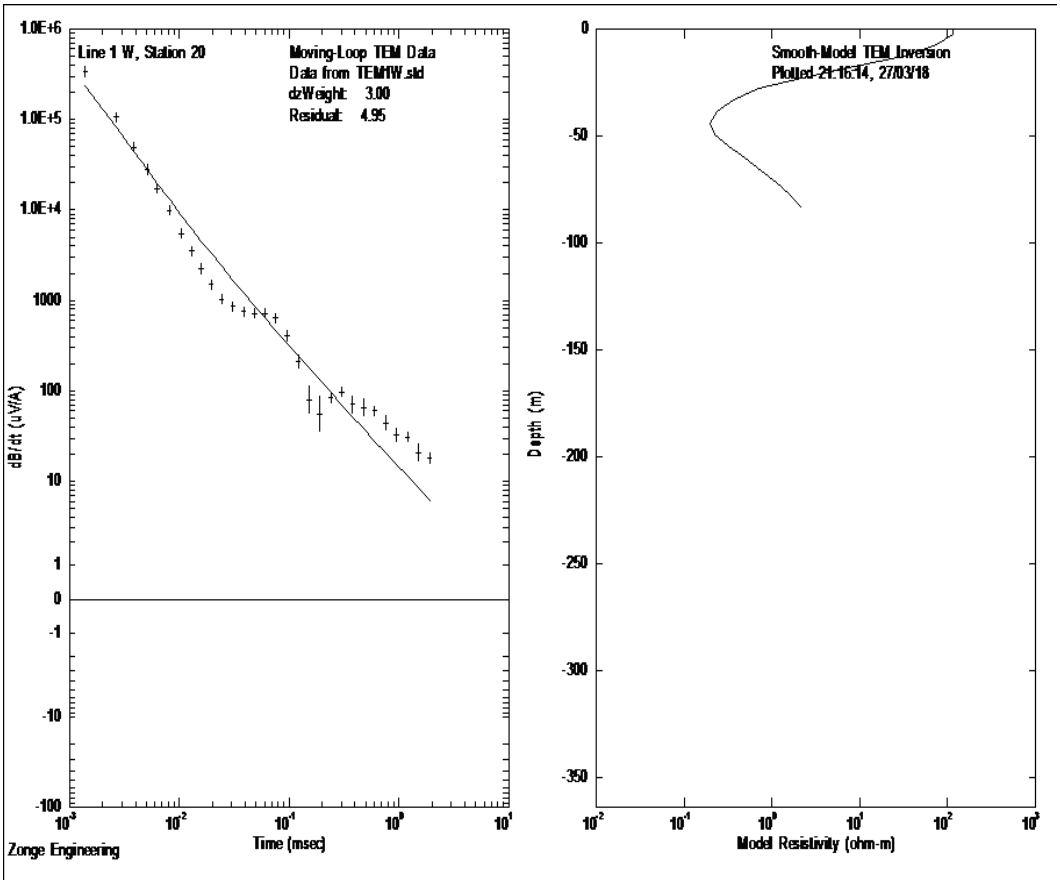

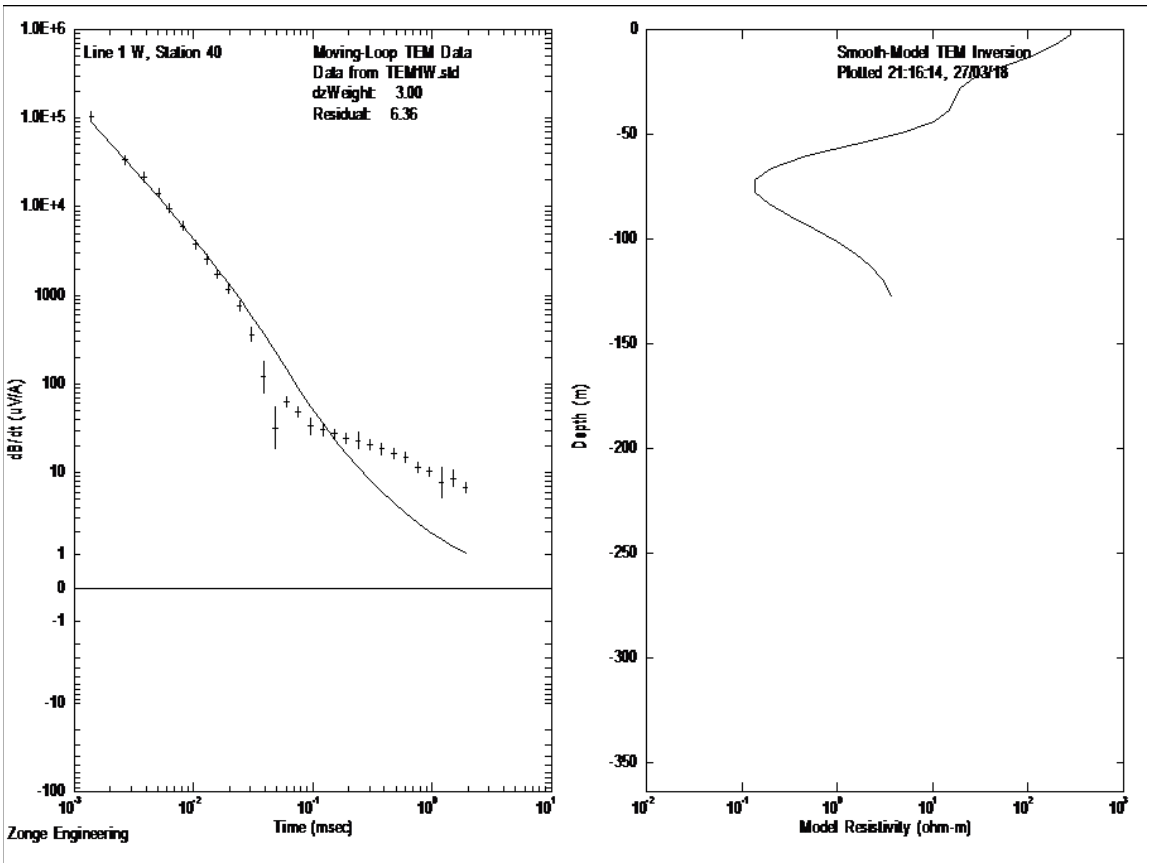
Line 1 W, Station 40
Moving-Loop TEM Data
Data from TEMHW.std
dzWeight: 3.00
Residual: 6.36
dB/dt (uV/A)
Time (msec)
Zonge Engineering
Smooth-Model TEM Inversion
Plotted 21:16:14, 27/03/18
Depth (m)
Model Resistivity (ohm-m)

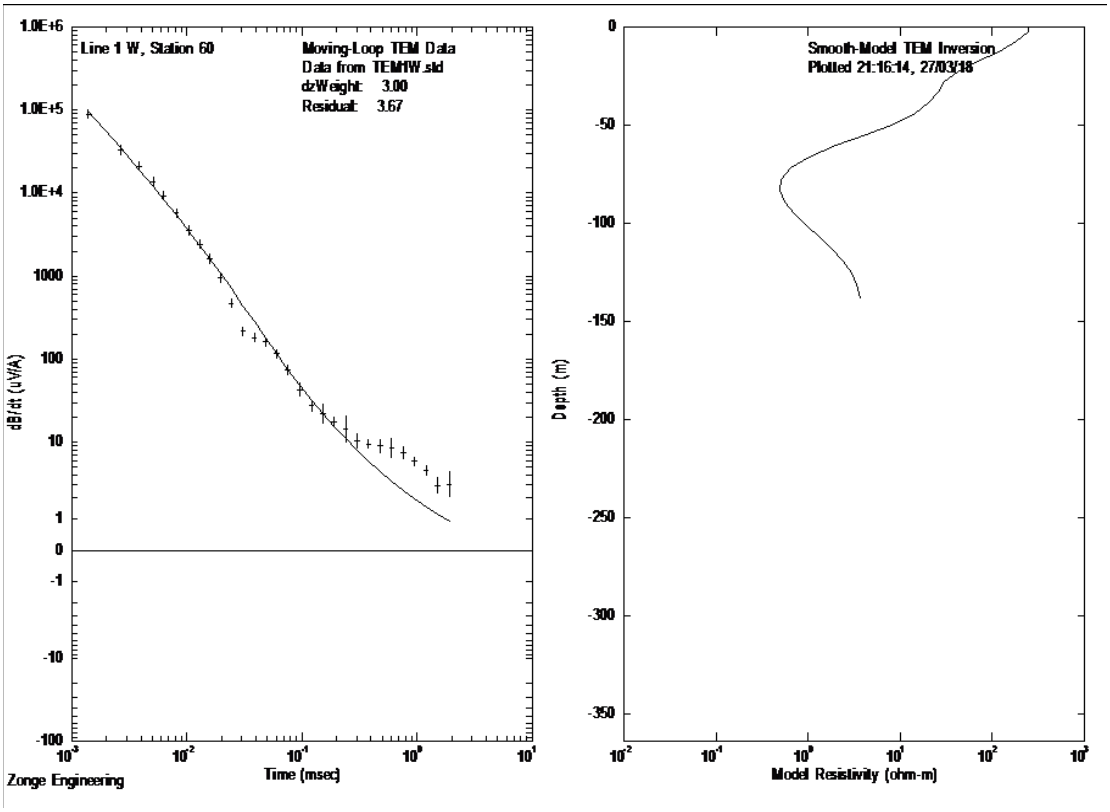
Line 1 W, Station 60
Moving-Loop TEM Data
Data from TEMHW.std
dzWeight: 3.00
Residual: 3.67
dB/dt (uV/A)
Time (msec)
Zonge Engineering
Smooth-Model TEM Inversion
Plotted 21:16:14, 27/03/18
Depth (m)
Model Resistivity (ohm-m)

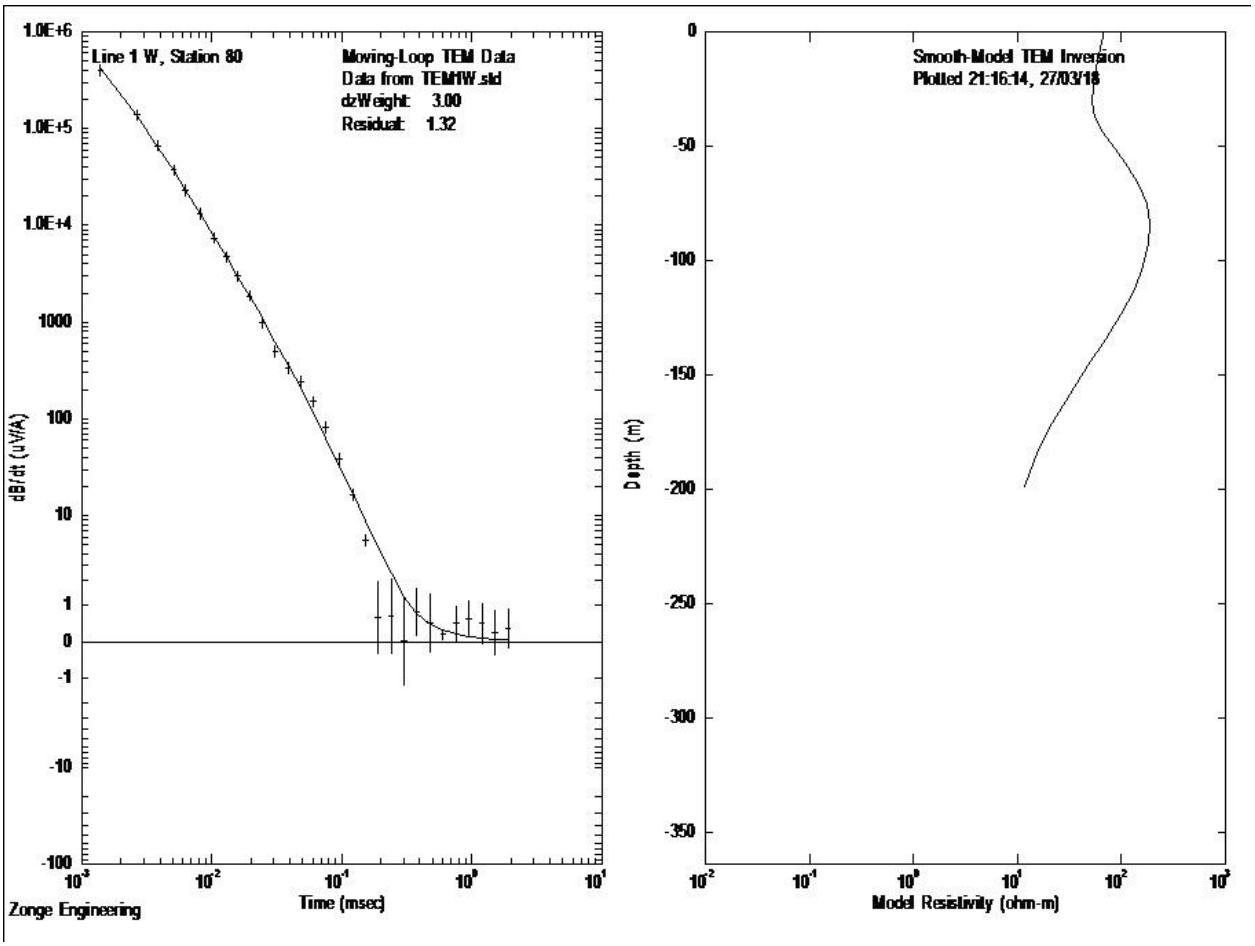

Figure 3.19. Modeled and Transient curve LQ 1 Station 0 - 80

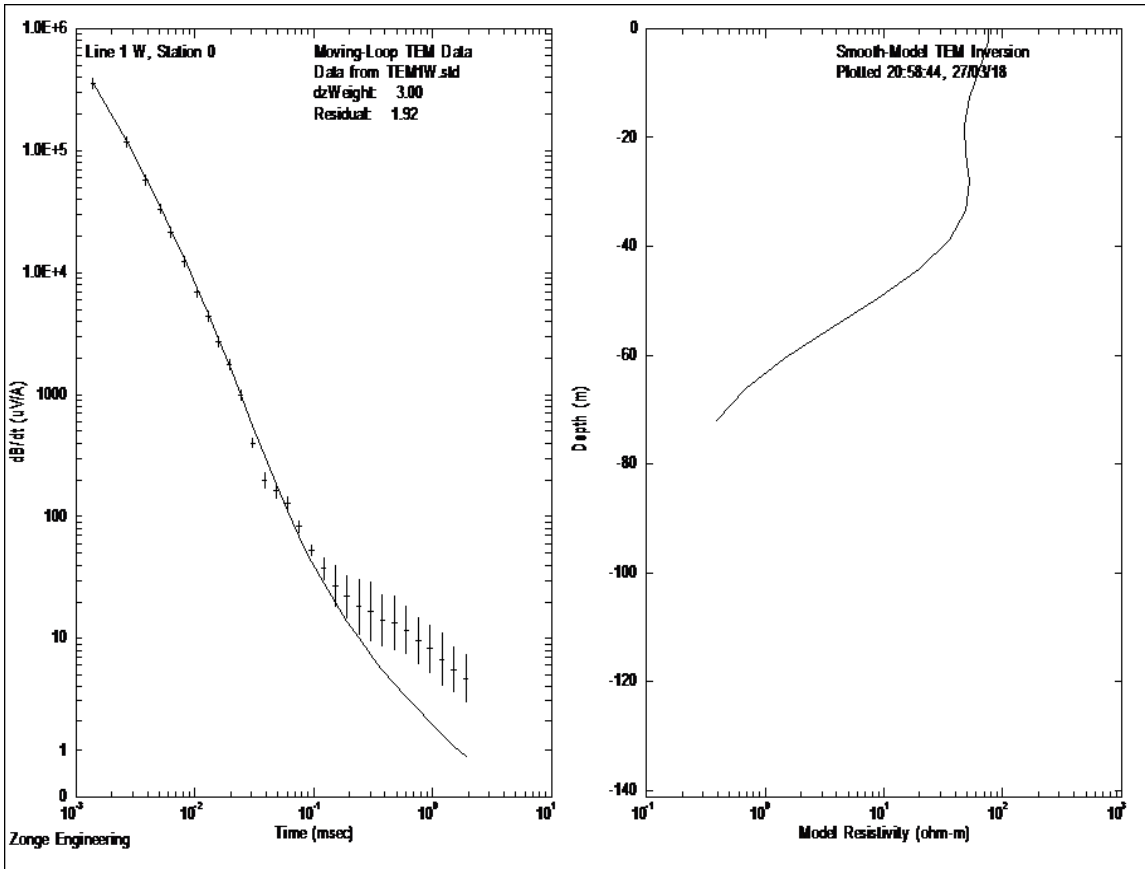
Line 1 W, Station 0
Moving-Loop TEM Data
Data from TEMHW.std
dzWeight: 3.00
Residual: 1.92
dB/dt (uV/A)
Time (msec)
Zonge Engineering
Smooth-Model TEM Inversion
Plotted 20:58:44, 27/03/18
Depth (m)
Model Resistivity (ohm-m)

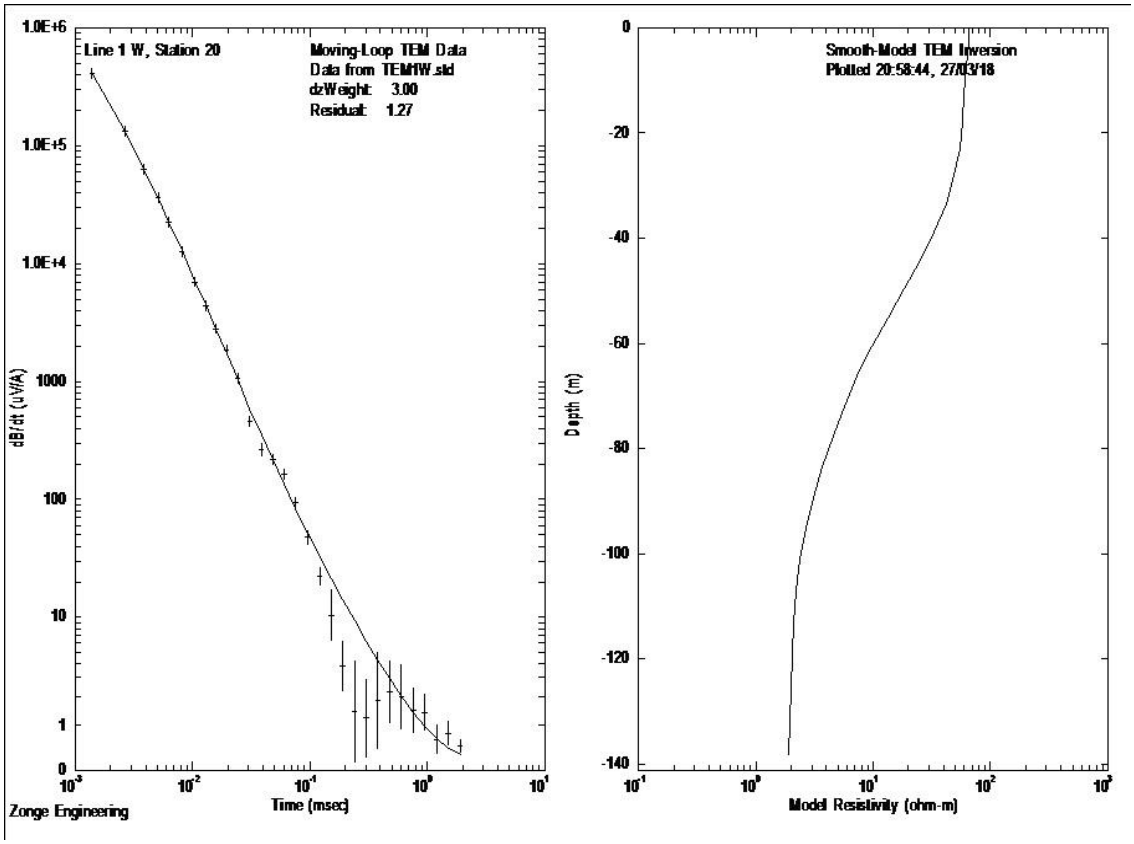
Line 1 W, Station 20
Moving-Loop TEM Data
Data from TEMHW.std
dzWeight: 3.00
Residual: 1.27
dB/dt (uV/A)
Time (msec)
Zonge Engineering
Smooth-Model TEM Inversion
Plotted 20:58:44, 27/03/18
Depth (m)
Model Resistivity (ohm-m)

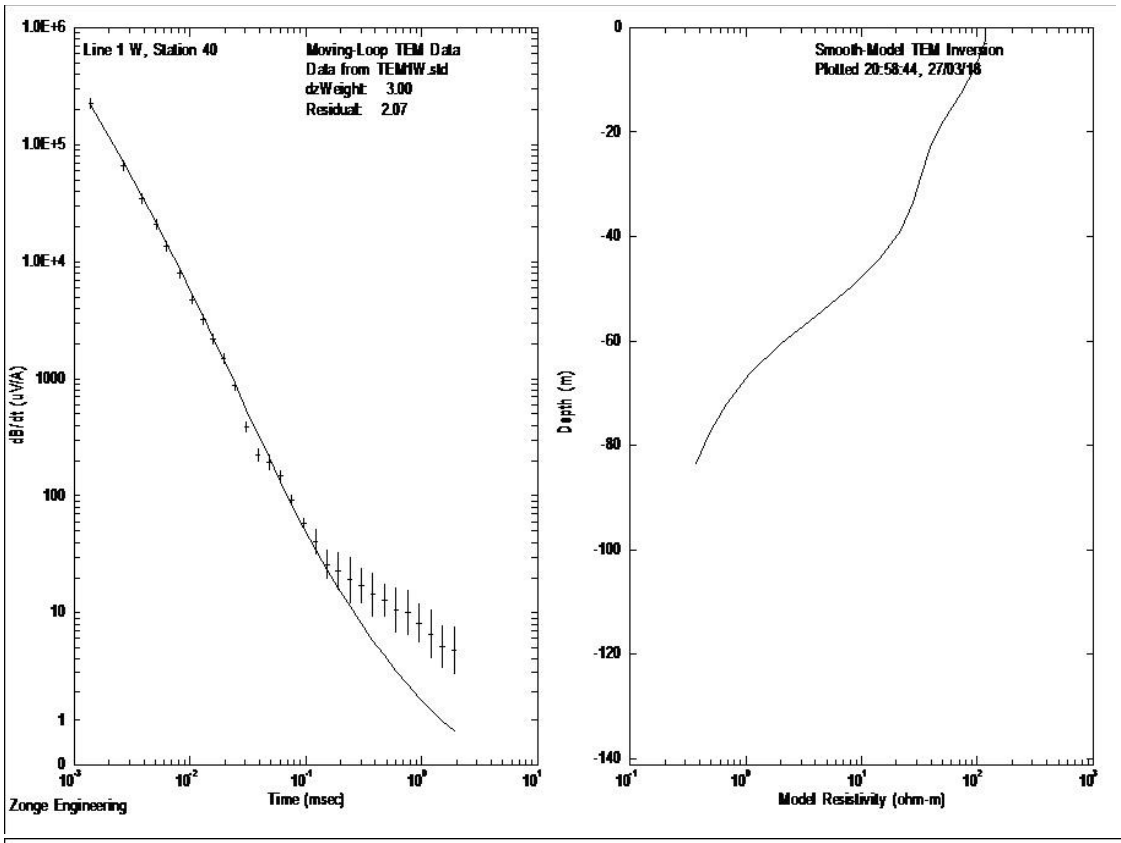
Line 1 W, Station 40
Moving-Loop TEM Data
Data from TEM1W.sld
dzWeight: 3.00
Residual: 2.07
dB/dt (uV/A)
Time (msec)
Zonge Engineering
Smooth-Model TEM Inversion
Plotted 20:58:44, 27/03/18
Depth (m)
Model Resistivity (ohm-m)

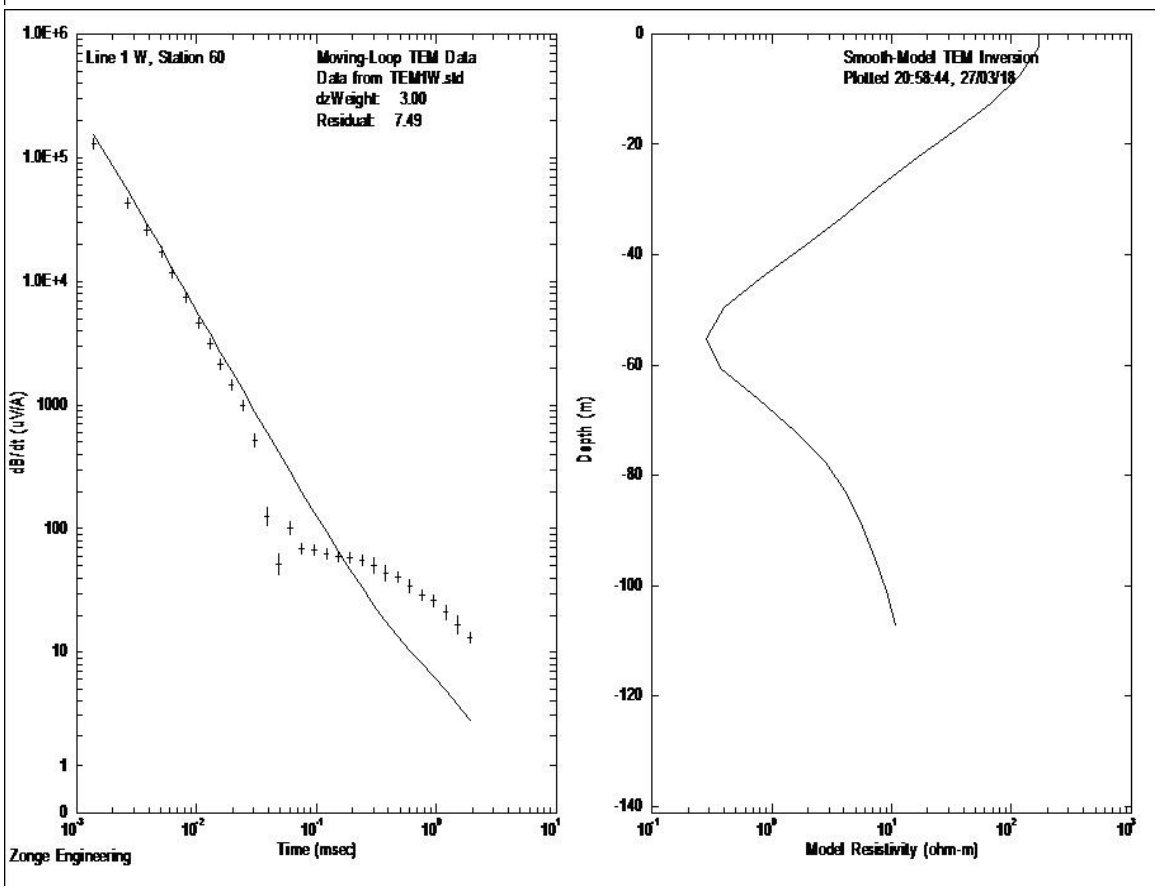
Line 1 W, Station 60
Moving-Loop TEM Data
Data from TEM1W.sld
dzWeight: 3.00
Residual: 7.49
dB/dt (uV/A)
Time (msec)
Zonge Engineering
Smooth-Model TEM Inversion
Plotted 20:58:44, 27/03/18
Depth (m)
Model Resistivity (ohm-m)

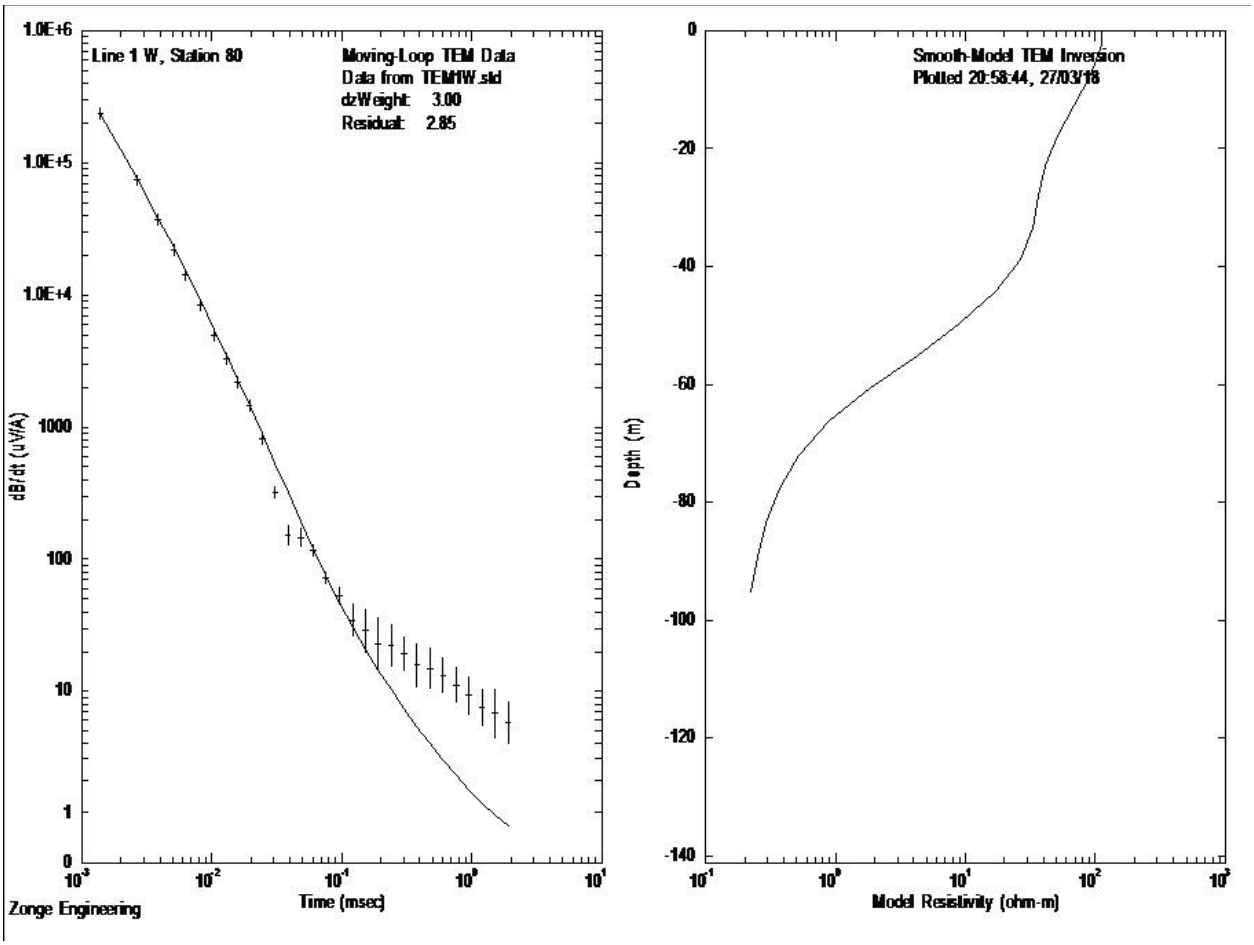

Figure 3.20. Modeled and Transient curves LQ 2 Loop 0-80

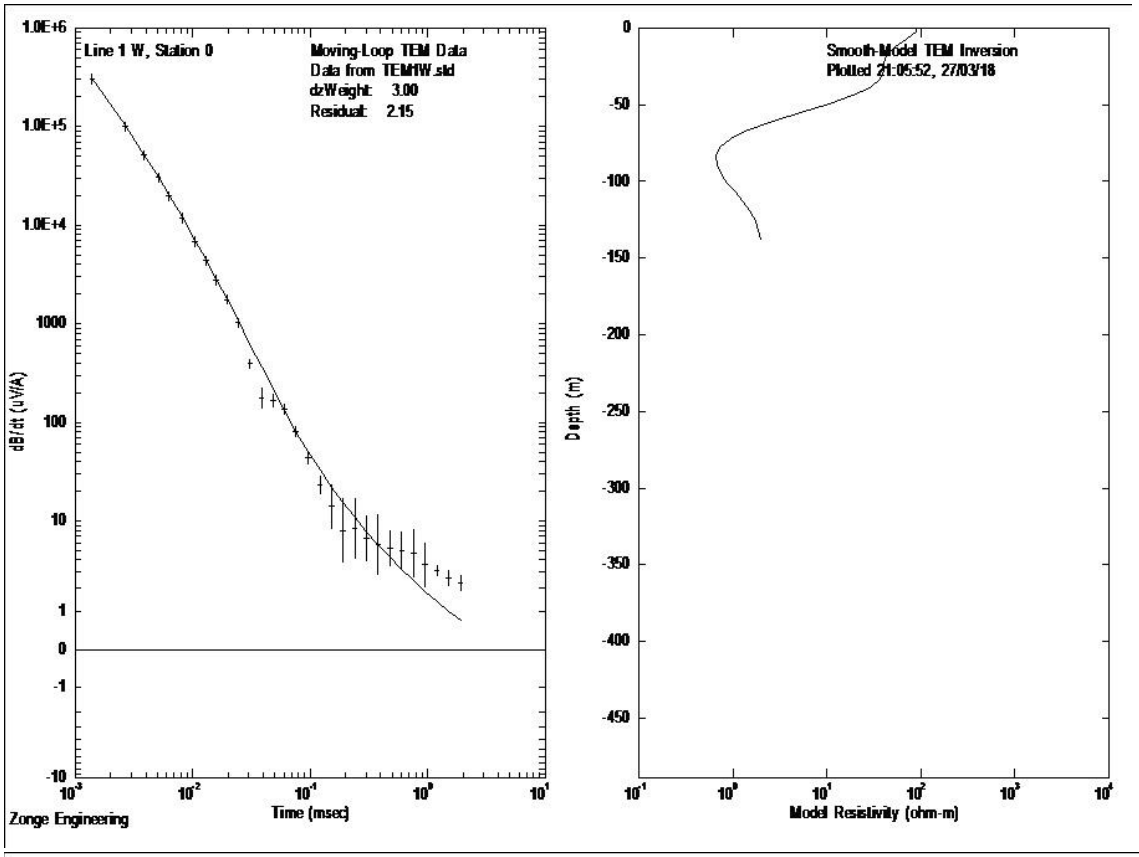
Line 1 W, Station 0
Moving-Loop TEM Data
Data from TEMTW.std
dzWeight: 3.00
Residual: 2.15
dB/dt (uV/A)
Time (msec)
Zonge Engineering
Smooth-Model TEM Inversion
Plotted 21:05:52, 27/03/18
Depth (m)
Model Resistivity (ohm-m)

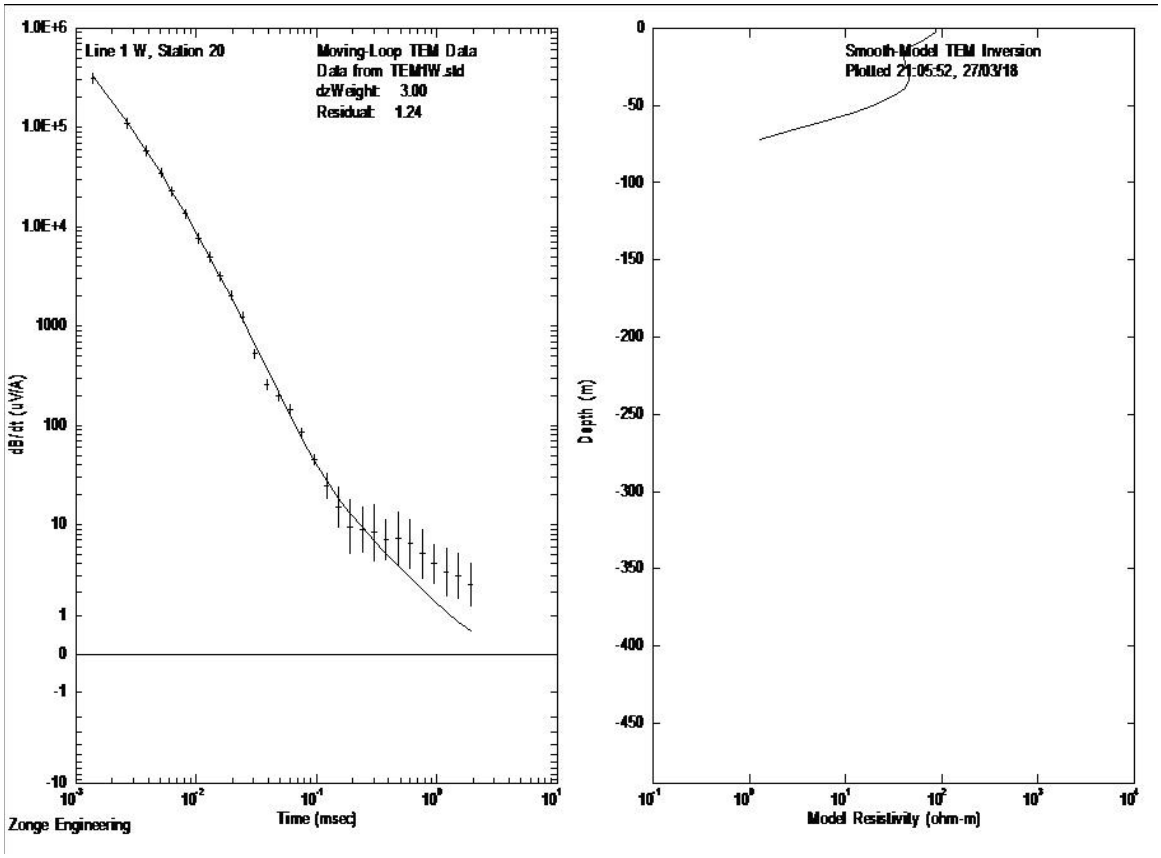
Line 1 W, Station 20
Moving-Loop TEM Data
Data from TEMTW.std
dzWeight: 3.00
Residual: 1.24
dB/dt (uV/A)
Time (msec)
Zonge Engineering
Smooth-Model TEM Inversion
Plotted 21:05:52, 27/03/18
Depth (m)
Model Resistivity (ohm-m)

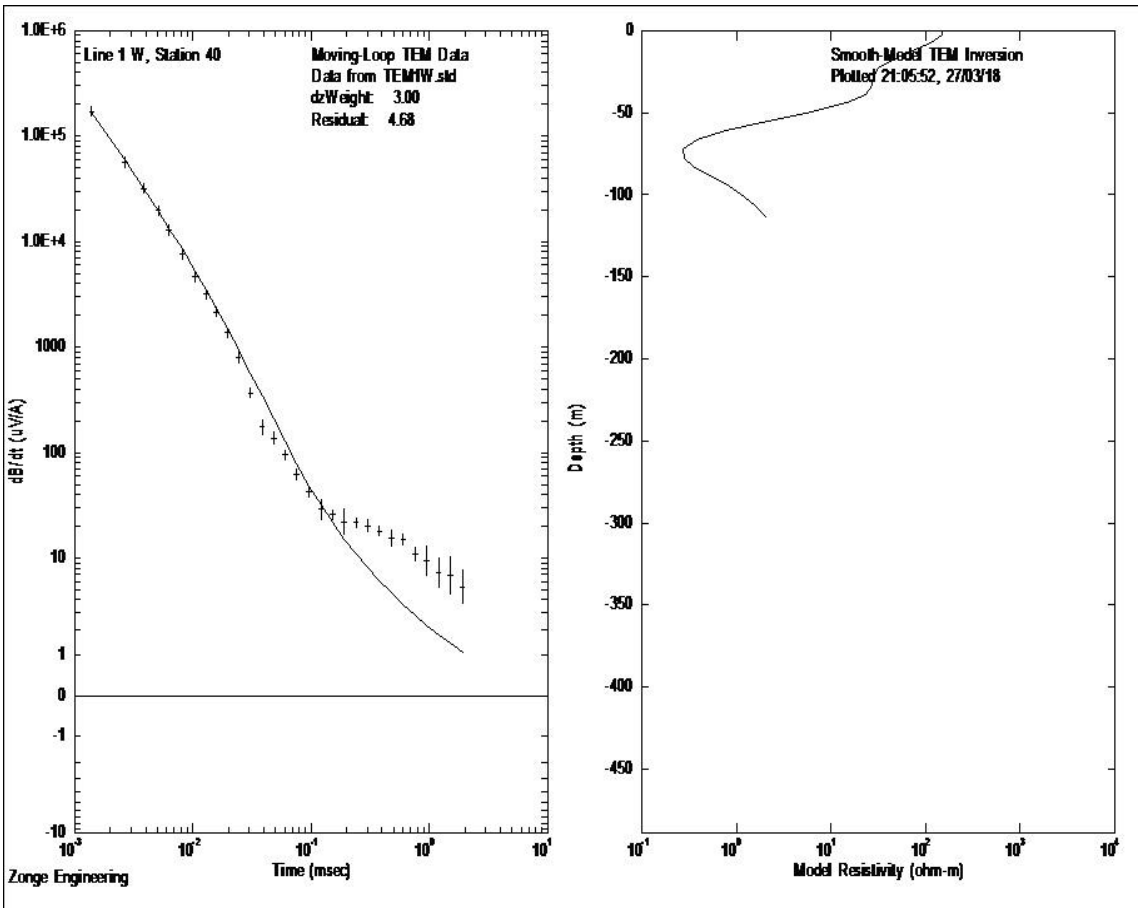
Line 1 W, Station 40
Moving-Loop TEM Data
Data from TEMTW.std
dzWeight: 3.00
Residual: 4.68
dB/dt (uV/A)
Time (msec)
Zonge Engineering
Smooth-Model TEM Inversion
Plotted 21:05:52, 27/03/18
Depth (m)
Model Resistivity (ohm-m)

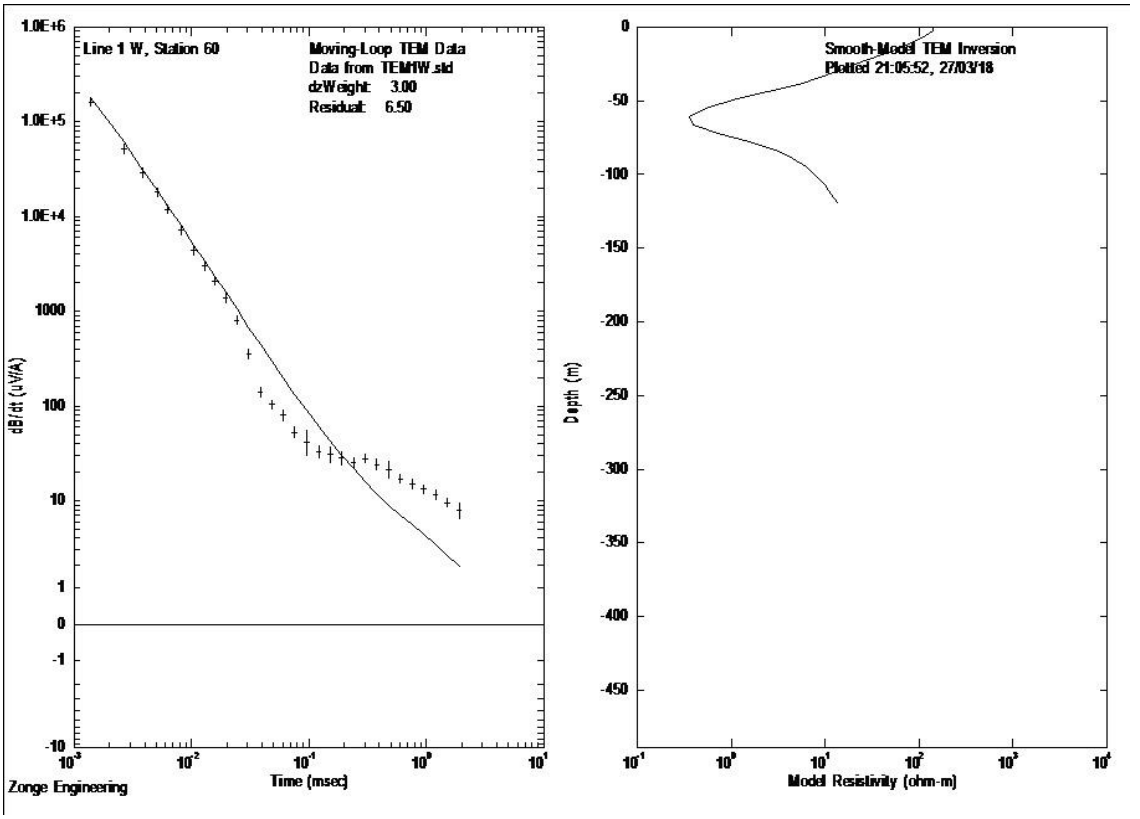
Line 1 W, Station 60
Moving-Loop TEM Data
Data from TEMTW.std
dzWeight: 3.00
Residual: 6.50
dB/dt (uV/A)
Time (msec)
Zonge Engineering
Smooth-Model TEM Inversion
Plotted 21:05:52, 27/03/18
Depth (m)
Model Resistivity (ohm-m)

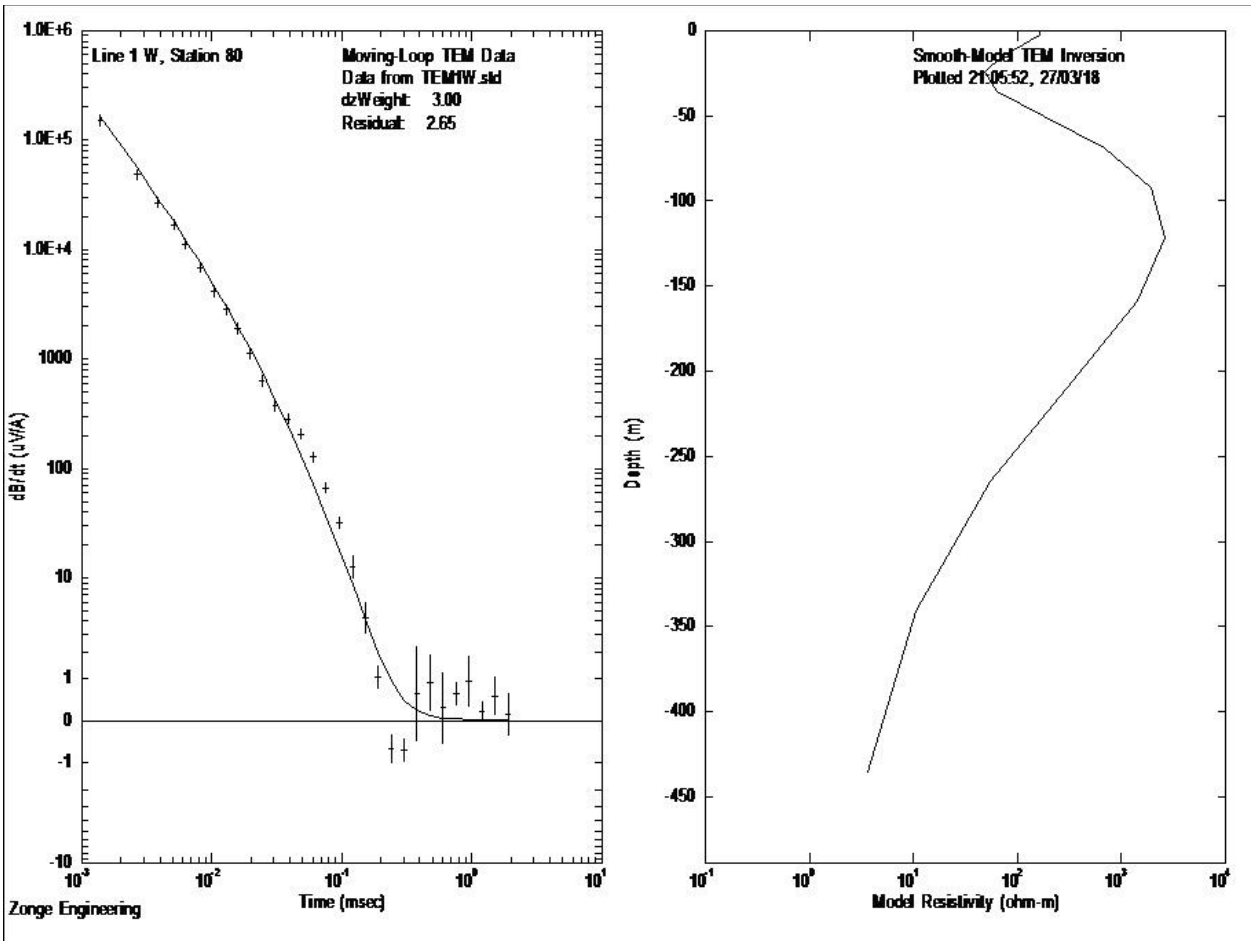

Figure 3.21. Modeled and Transient curves LQ 3 Loop 0-80

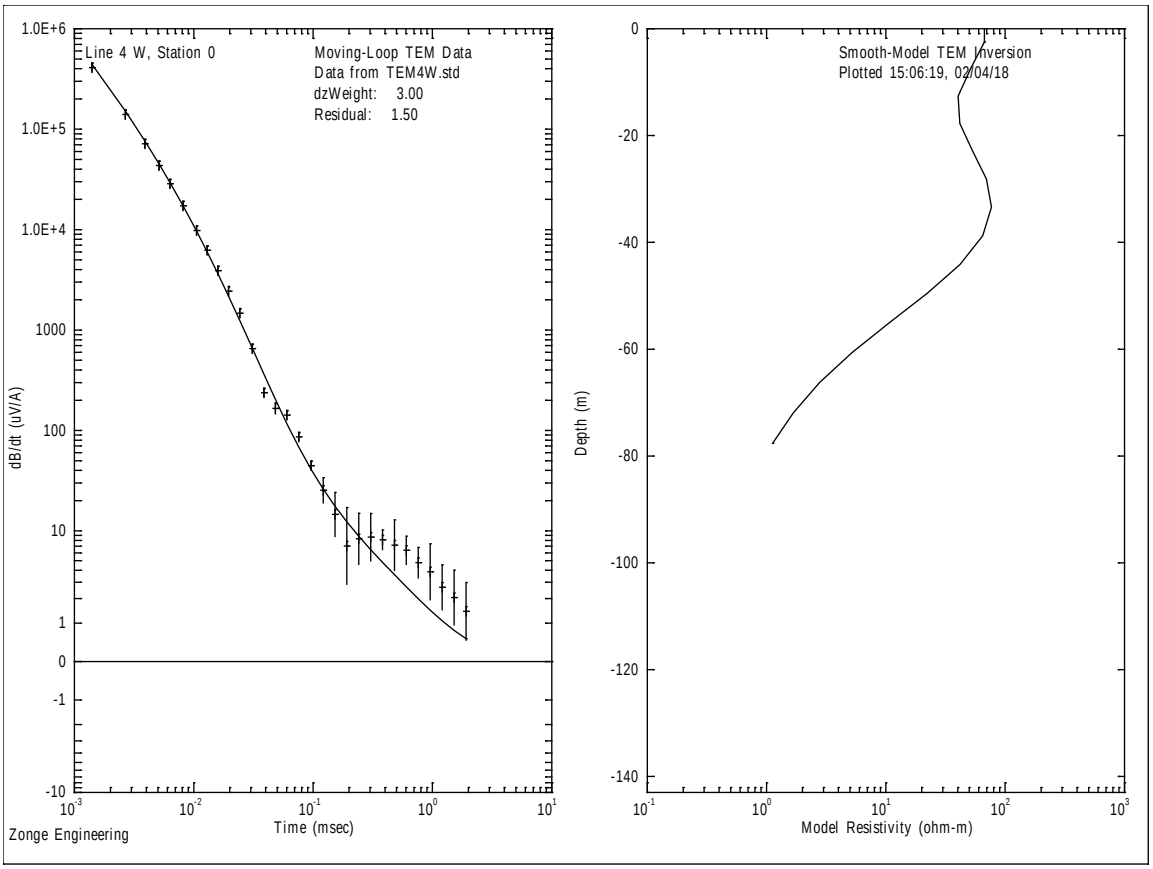
Line 4 W, Station 0
Moving-Loop TEM Data
Data from TEM4W.std
dzWeight: 3.00
Residual: 1.50
dB/dt (uV/A)
Time (msec)
Zonge Engineering
Smooth-Model TEM Inversion
Plotted 15:06:19, 02/04/18
Depth (m)
Model Resistivity (ohm-m)

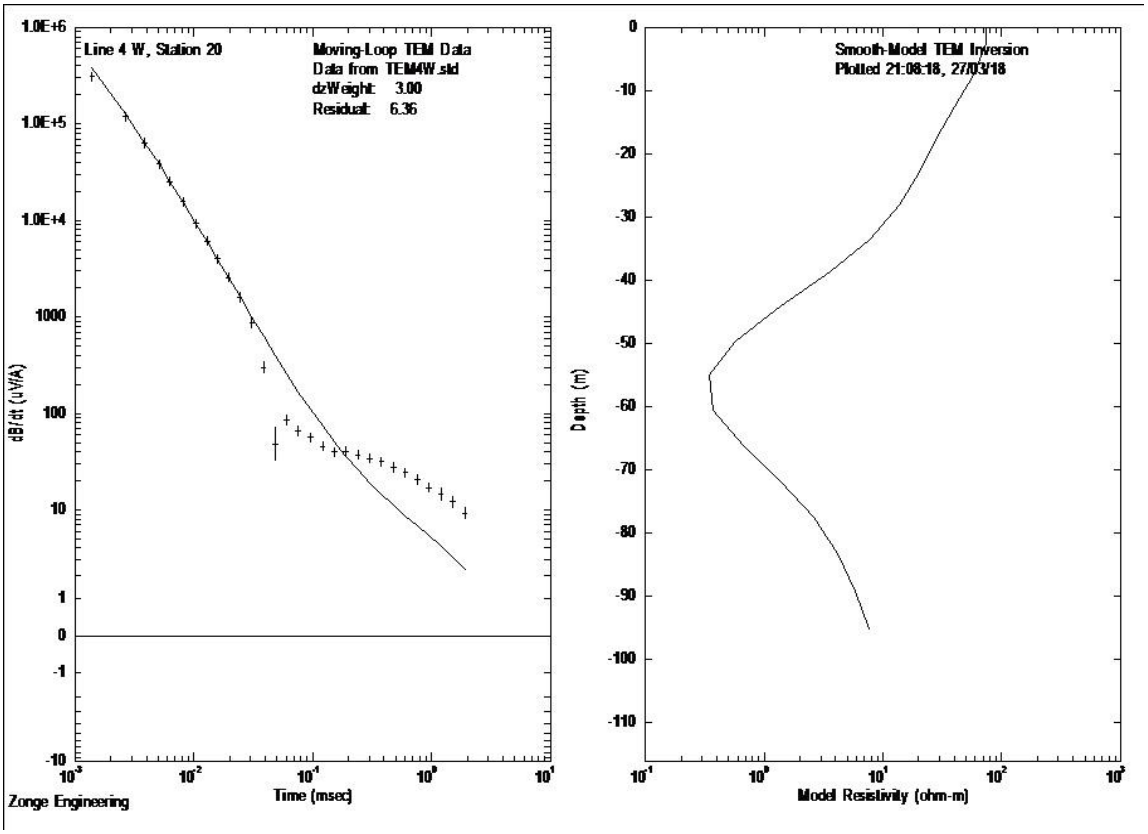
Line 4 W, Station 20
Moving-Loop TEM Data
Data from TEM4W.std
dzWeight: 3.00
Residual: 6.36
dB/dt (uV/A)
Time (msec)
Zonge Engineering
Smooth-Model TEM Inversion
Plotted 21:08:18, 27/03/18
Depth (m)
Model Resistivity (ohm-m)

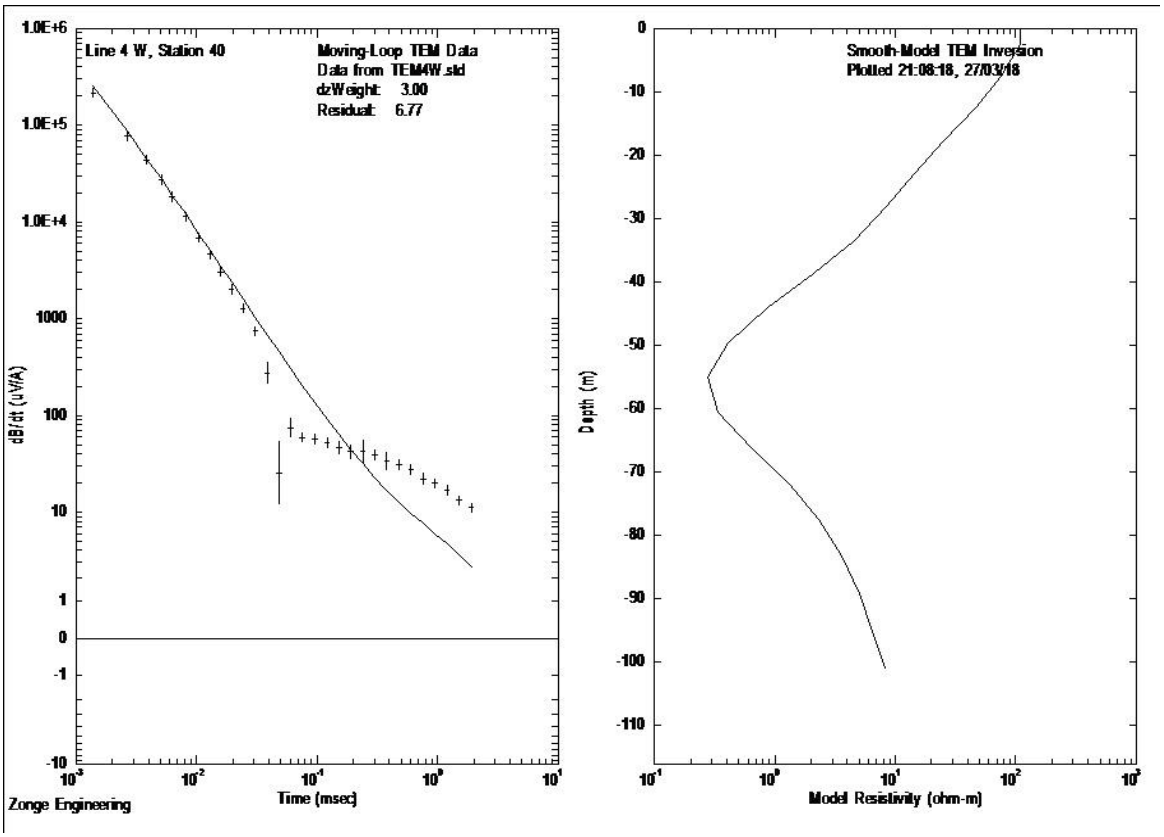
Line 4 W, Station 40
Moving-Loop TEM Data
Data from TEM4W.std
dzWeight: 3.00
Residual: 6.77
dB/dt (uV/A)
Time (msec)
Zonge Engineering
Smooth-Model TEM Inversion
Plotted 21:08:18, 27/03/18
Depth (m)
Model Resistivity (ohm-m)

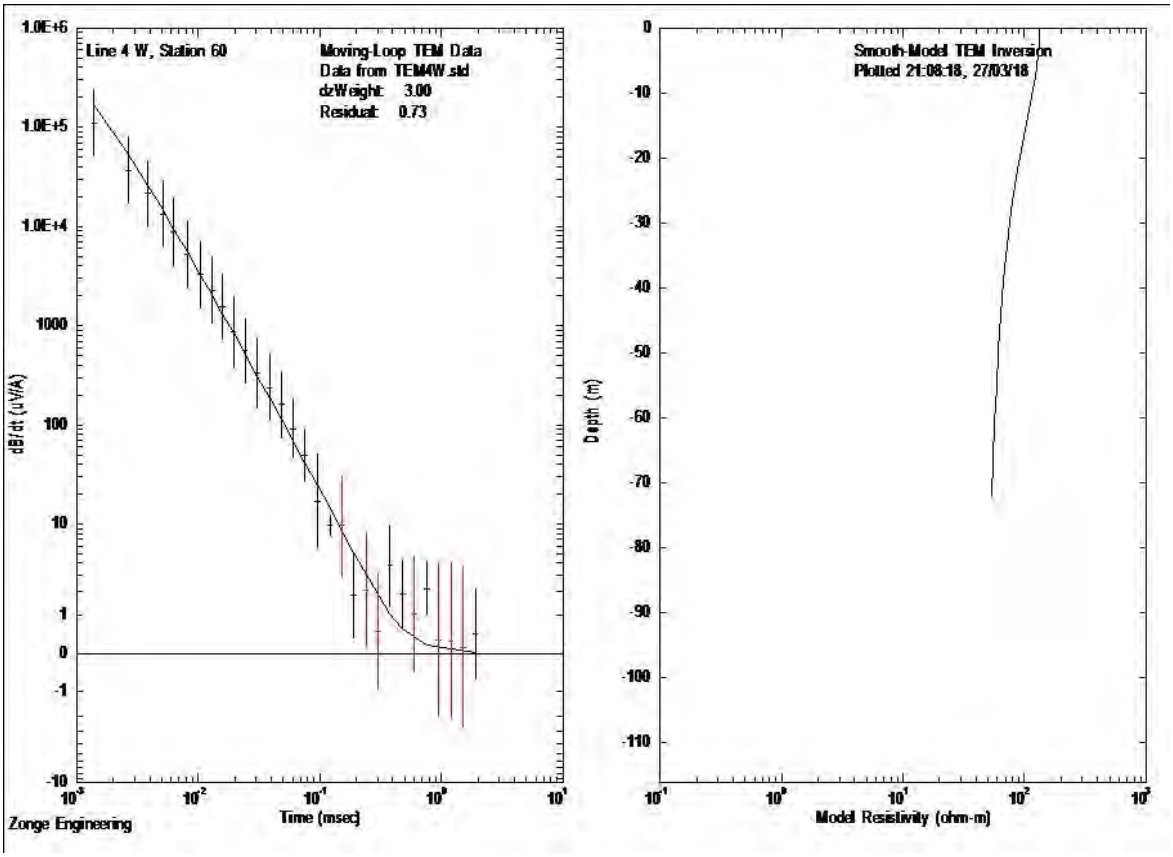
Line 4 W, Station 60
Moving-Loop TEM Data
Data from TEM4W.std
dzWeight: 3.00
Residual: 0.73
dB/dt (uV/A)
Time (msec)
Zonge Engineering
Smooth-Model TEM Inversion
Plotted 21:08:18, 27/03/18
Depth (m)
Model Resistivity (ohm-m)

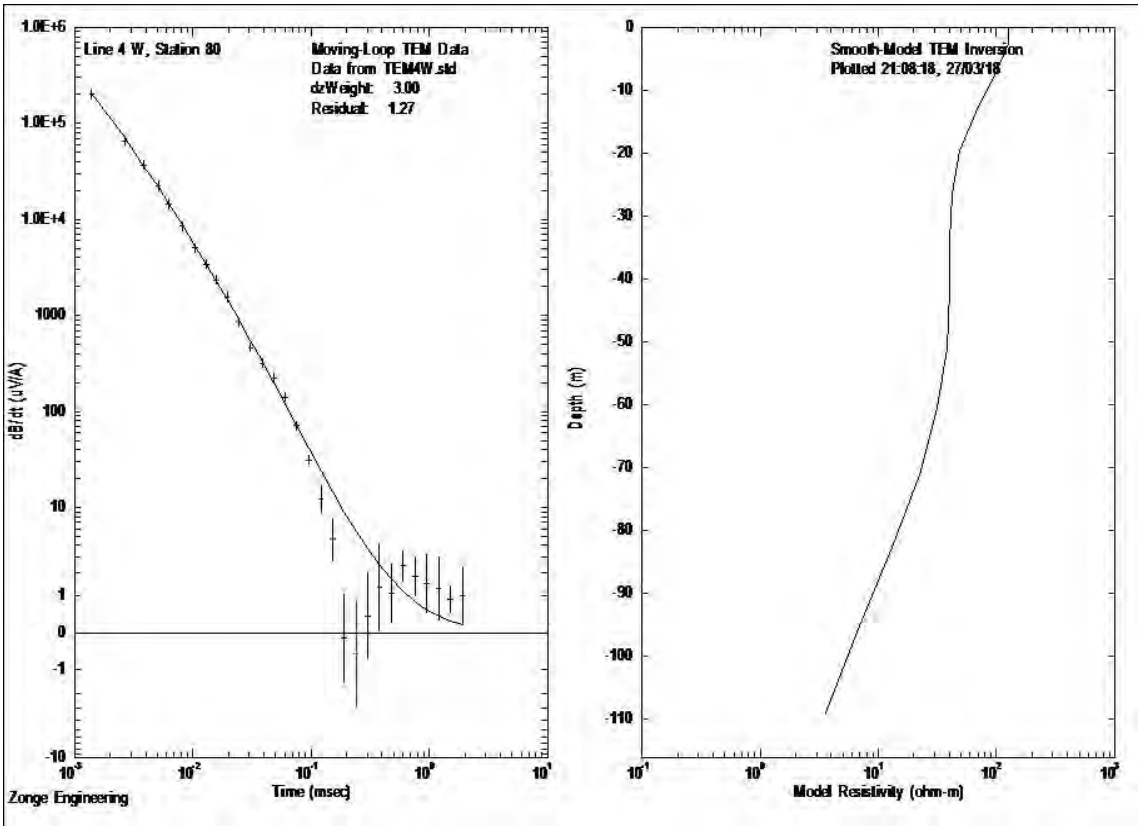

Figure 3.22. Modeled and Transient curves for LQ4 Loop 20-80

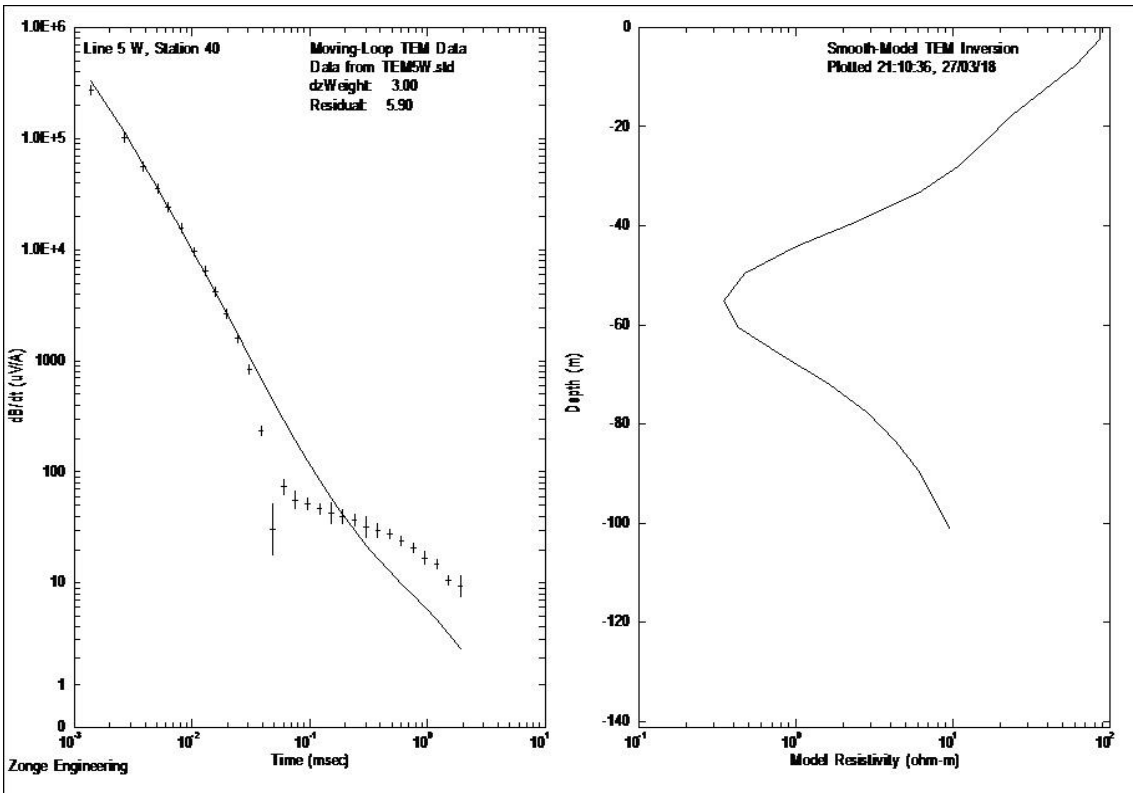
Line 5 W, Station 40
Moving-Loop TEM Data
Data from TEM5W.std
dzWeight: 3.00
Residual: 5.90
dB/dt (uV/A)
Time (msec)
Zonge Engineering
Smooth-Model TEM Inversion
Plotted 21:10:36, 27/03/18
Depth (m)
Model Resistivity (ohm-m)

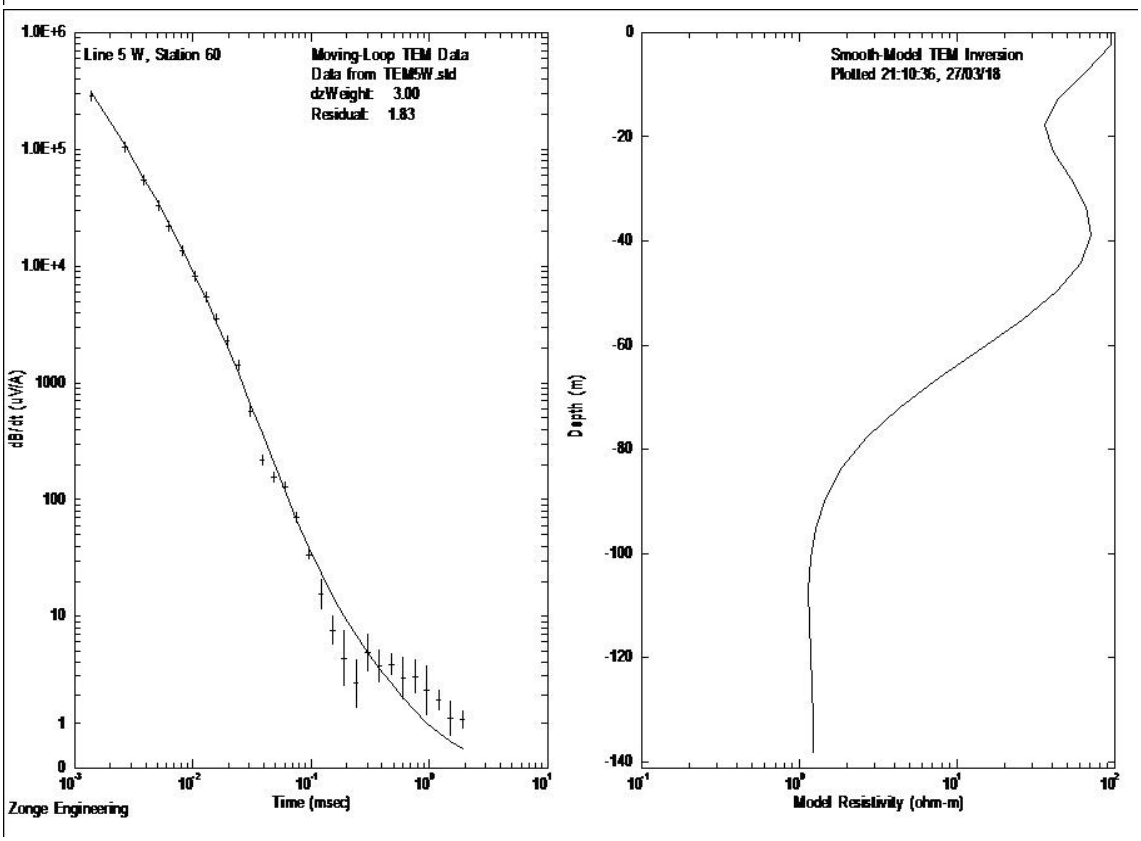
Line 5 W, Station 60
Moving-Loop TEM Data
Data from TEM5W.std
dzWeight: 3.00
Residual: 1.83
dB/dt (uV/A)
Time (msec)
Zonge Engineering
Smooth-Model TEM Inversion
Plotted 21:10:36, 27/03/18
Depth (m)
Model Resistivity (ohm-m)

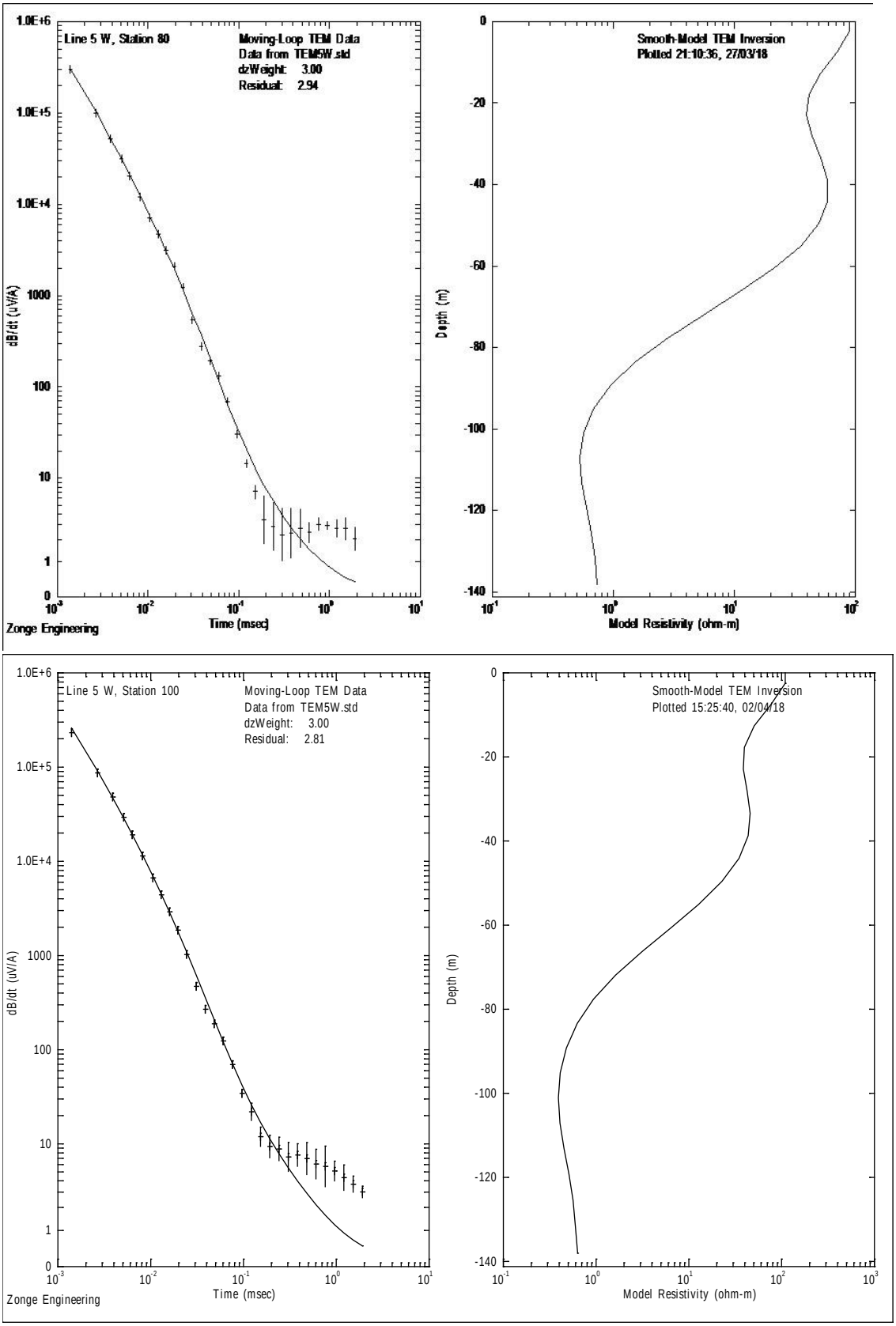

Figure 3.23. Modeled and Transient curves for LQ 5 Loop 40-100

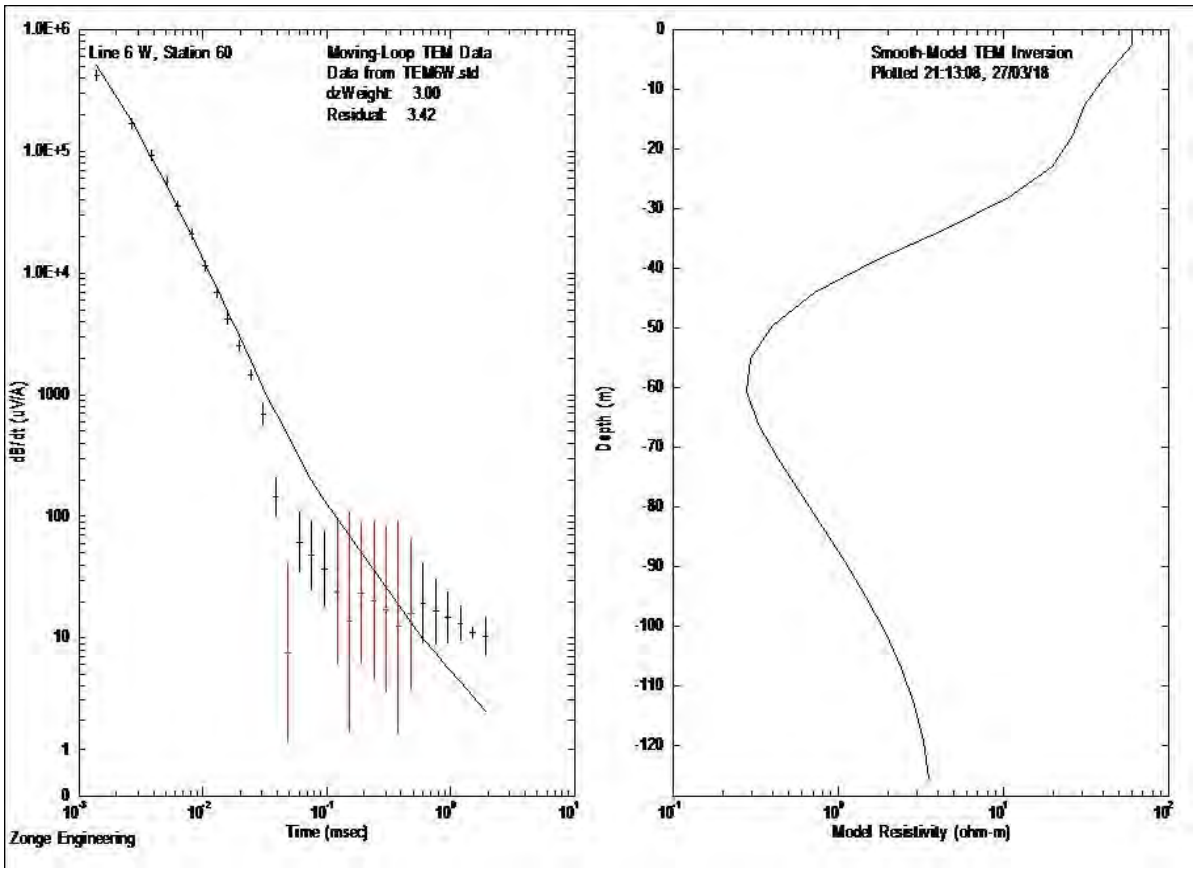
Line 6 W, Station 60
Moving-Loop TEM Data
Data from TEM6W.std
dzWeight: 3.00
Residual: 3.42
dB/dt (uV/A)
Time (msec)
Zonge Engineering
Smooth-Model TEM Inversion
Plotted 21:13:08, 27/03/18
Depth (m)
Model Resistivity (ohm-m)

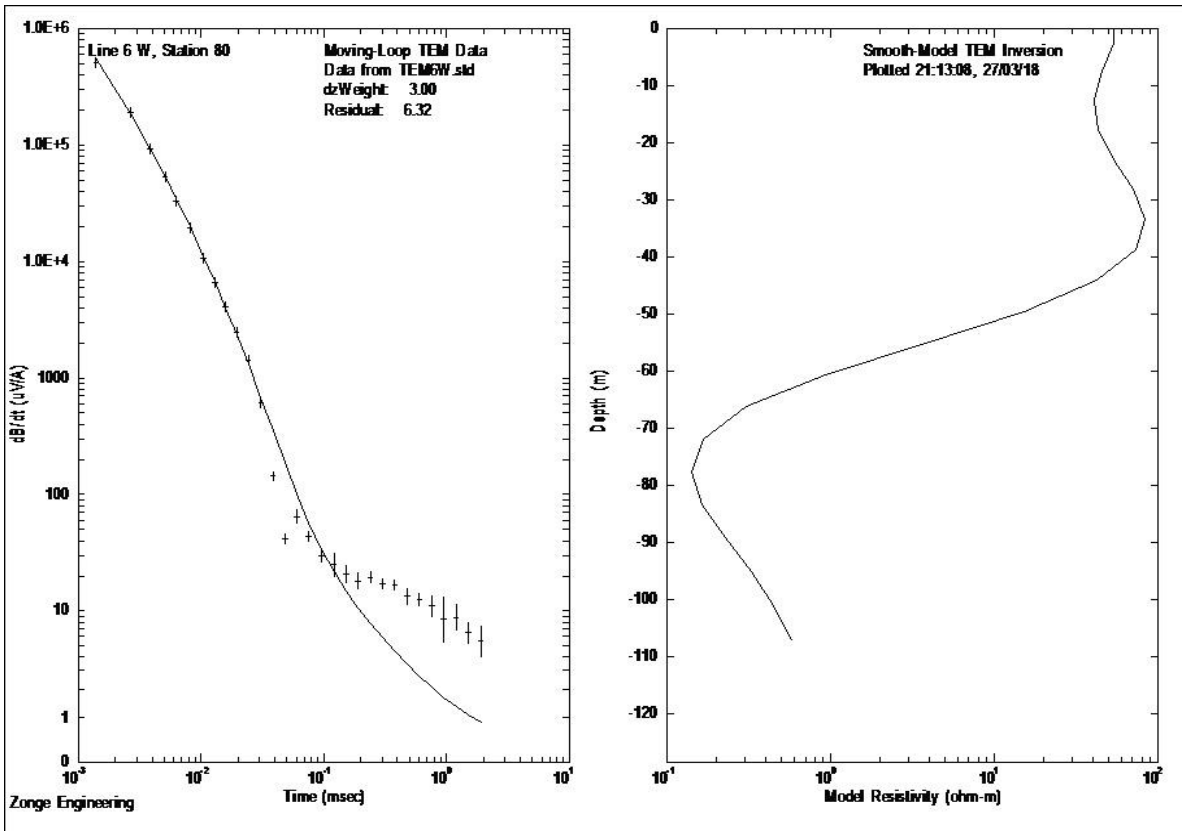
Line 6 W, Station 80
Moving-Loop TEM Data
Data from TEM6W.std
dzWeight: 3.00
Residual: 6.32
dB/dt (uV/A)
Time (msec)
Zonge Engineering
Smooth-Model TEM Inversion
Plotted 21:13:08, 27/03/18
Depth (m)
Model Resistivity (ohm-m)

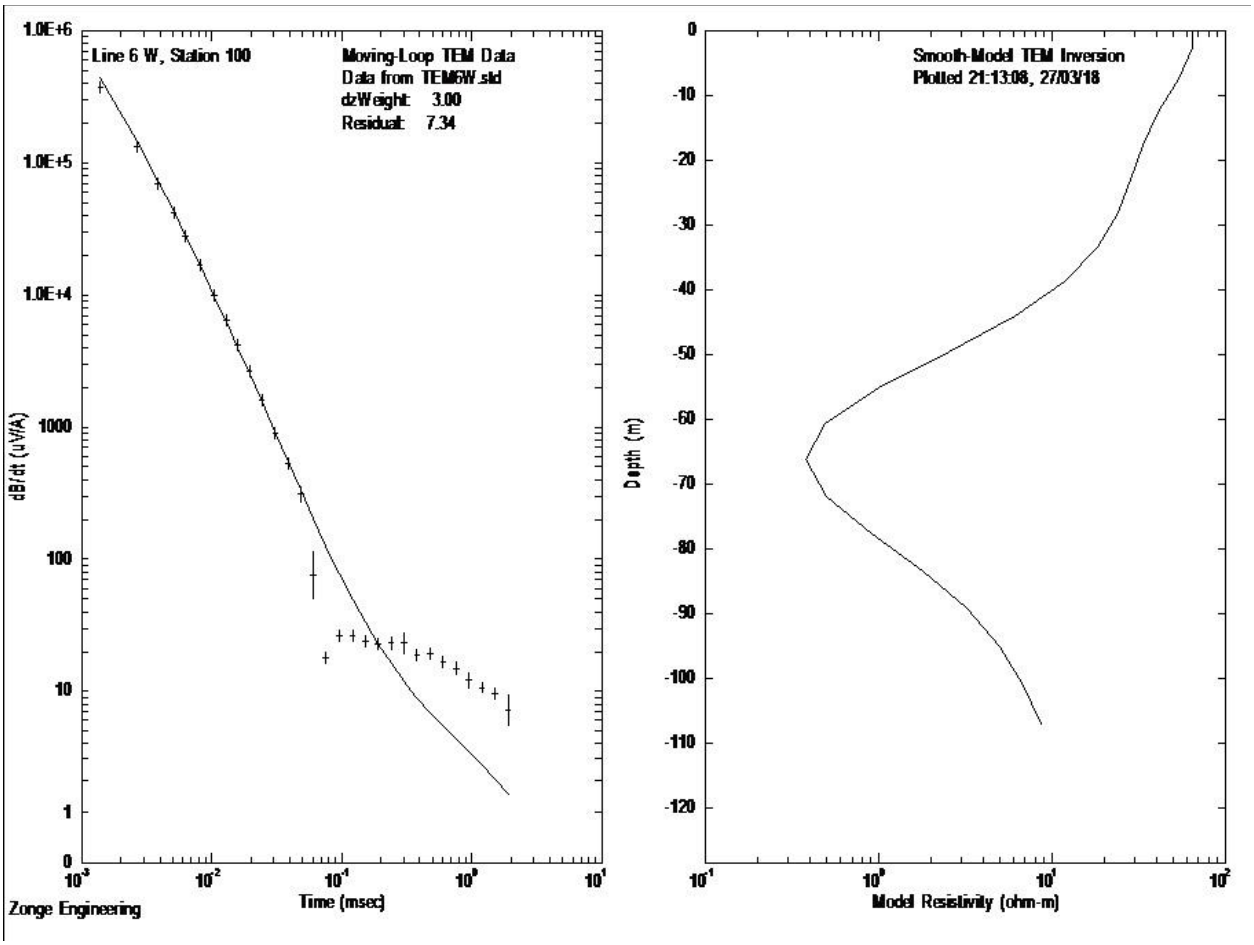

Figure 3.24. Modeled and Transient curves for LQ 6 60-100

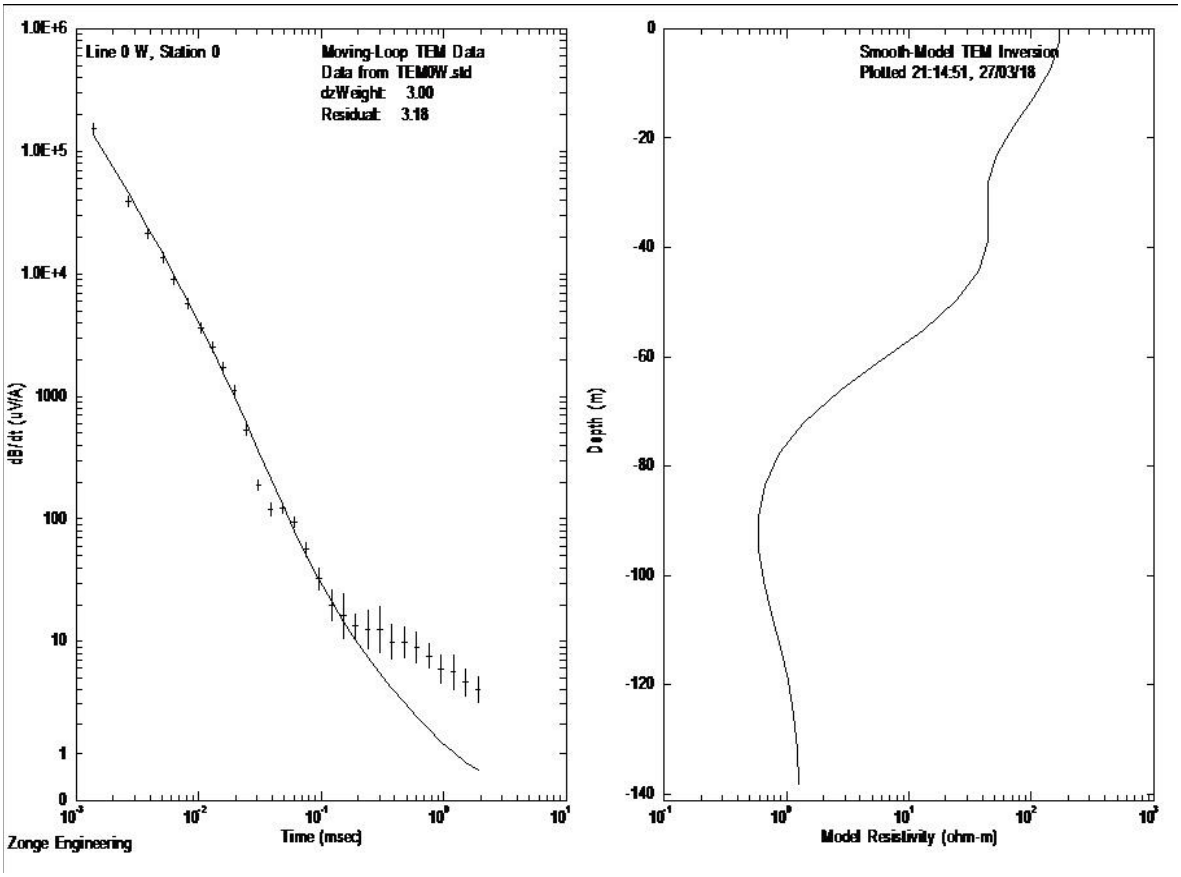
Line 0 W, Station 0
Moving-Loop TEM Data
Data from TEM0W.std
dzWeight: 3.00
Residual: 3.18
dB/dt (uV/A)
Time (msec)
Zonge Engineering
Smooth-Model TEM Inversion
Plotted 21:14:51, 27/03/18
Depth (m)
Model Resistivity (ohm-m)

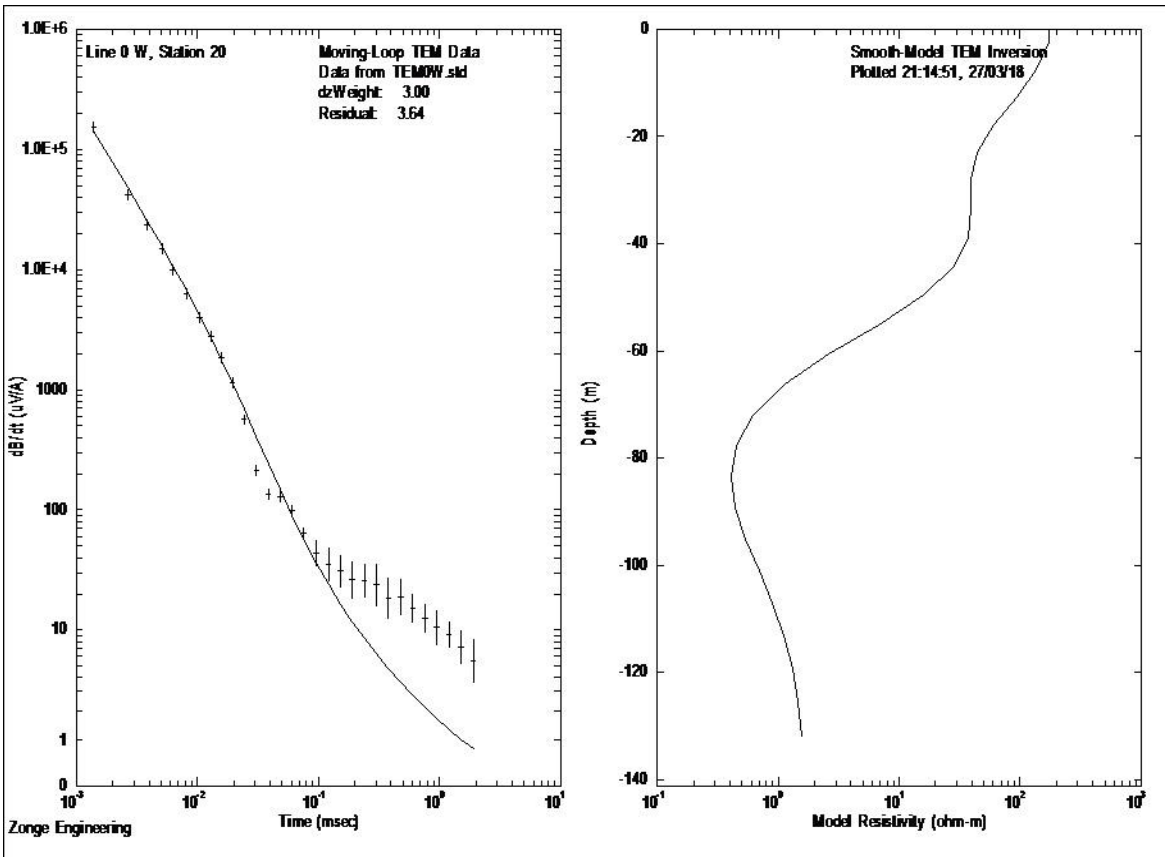
Line 0 W, Station 20
Moving-Loop TEM Data
Data from TEM0W.std
dzWeight: 3.00
Residual: 3.64
dB/dt (uV/A)
Time (msec)
Zonge Engineering
Smooth-Model TEM Inversion
Plotted 21:14:51, 27/03/18
Depth (m)
Model Resistivity (ohm-m)

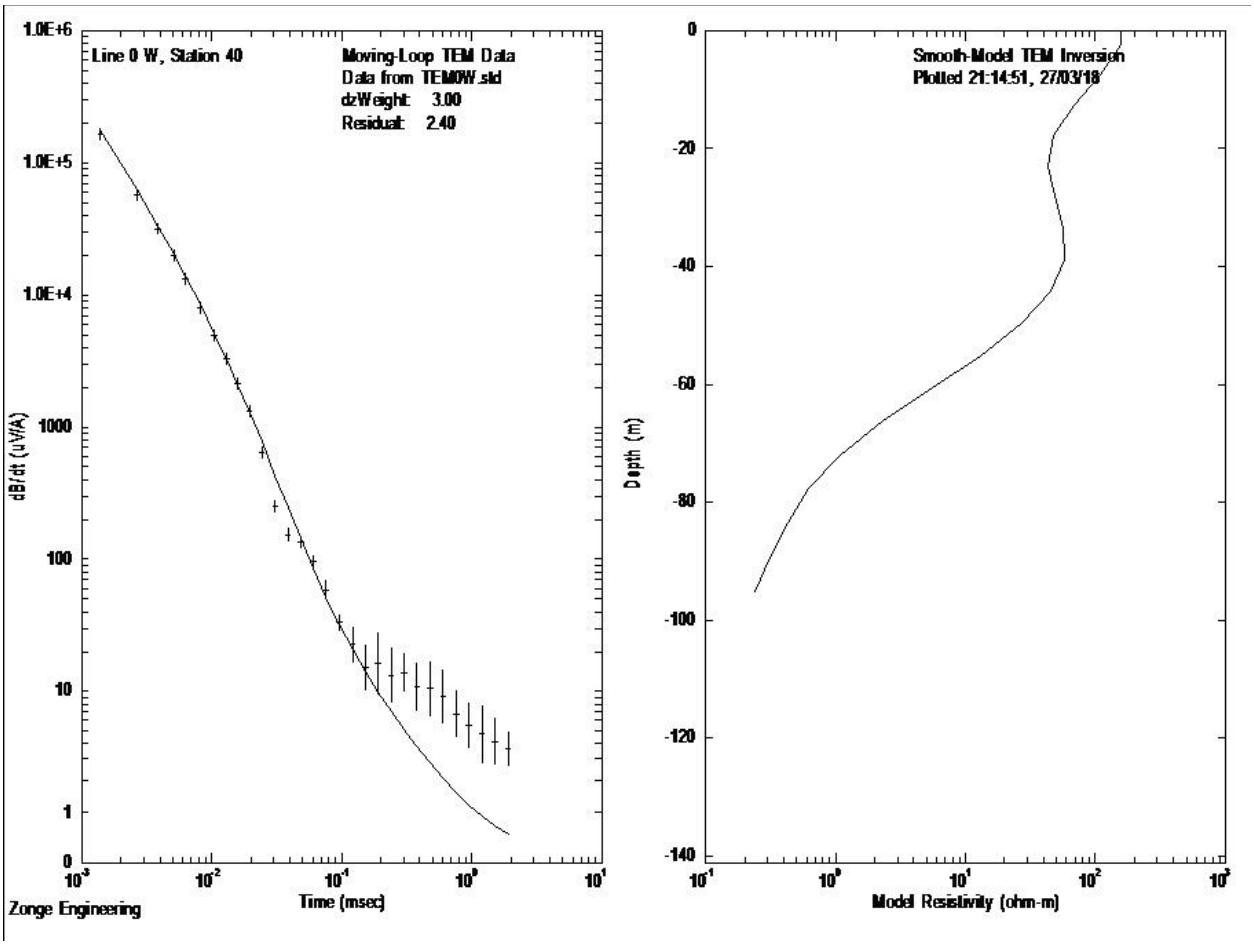

Figure 3.25. Modeled and Transient curves for Other Adit Loop 0-40

4. DC Resistivity

4.1 Introduction

The DC Resistivity method relies on the input of current into the ground, which results in differences in electric potential that are measurable at the surface. Using Ohm's Law relationship, where resistance is proportional to potential divided by current, the apparent resistivity ρ_a can be calculated. Apparent resistivity is the resistivity that would theoretically yield the measured values in an electrically homogenous and isotropic area. Resistivity ρ is defined as:

$$\rho = \frac{\delta R * \delta A}{\delta L}$$

Where δR, δA, and δL are the respective resistance, cross-sectional area, and length of a solid (Figure 4.1).

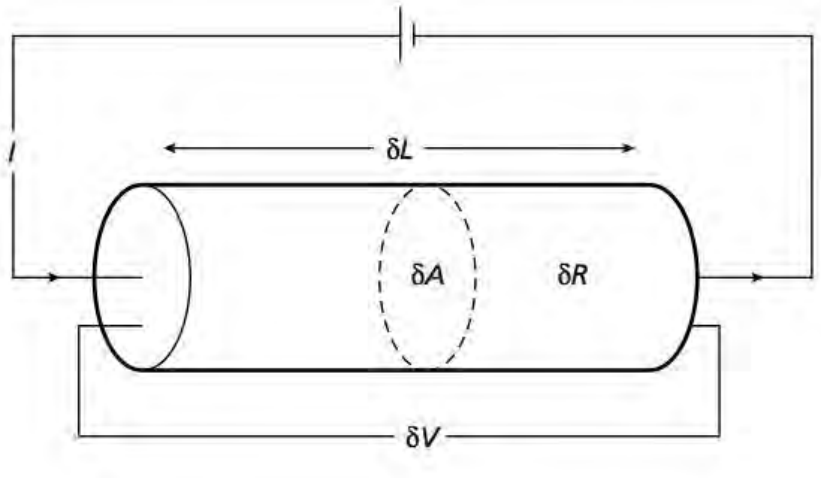

Figure 4.1 The parameters necessary to define resistivity for a solid cylinder (Kearey et al., 2002).

The true resistivity of a rock unit is a bulk property of the rock and is a measure of the resistance it has to the transmission of electrical current. Most rock-forming minerals are effective insulators, therefore if dry they will not conduct electricity. In the Earth, the pore spaces of rocks are usually filled with water, so the resistivity of the rock is directly proportional to the porosity

and the amount of water the rock contains. This means that current is conducted through the passage of ions through areas where water is present in the rock, such as pore spaces and fractures. As a result, the resistivity depends heavily on the porosity and water saturation of the rock, as shown in Archie's Law, an empirical formula for resistivity:

$$\rho = \frac{a\rho_w}{\varphi^m S_W^n}$$

Where a is an empirical constant, ρ_w is the resistivity of pore water, φ is the fractional porosity, s_w is the fractional water saturation, and m and n are empirical constants. Since these factors change between rock types and locations, resistivity is a highly variable property. This can also be useful because certain rock types still exhibit approximate ranges of resistivity that can aid in identification (Figure 4.2).

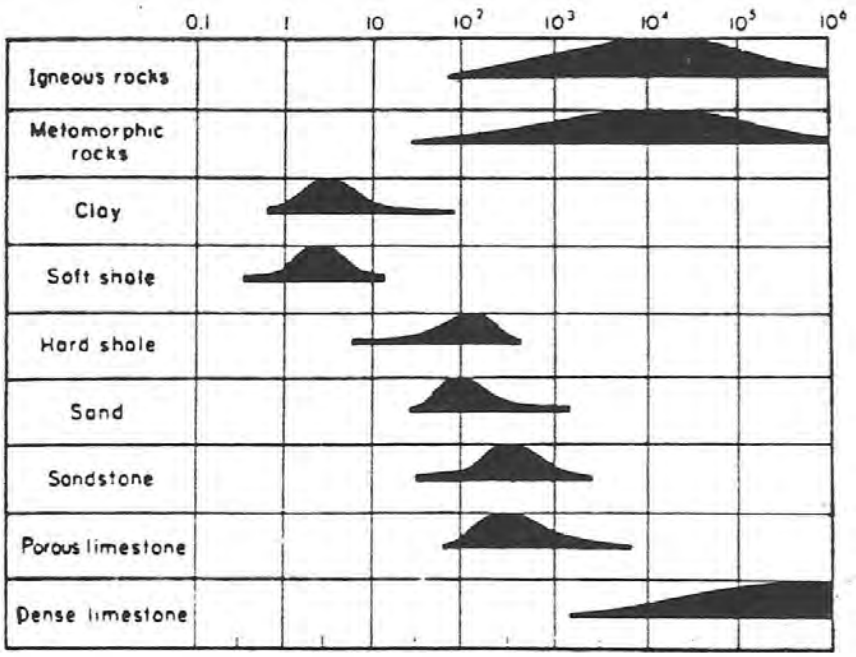

Figure 4.2. Approximate resistivity ranges for a number of rock types. Resistivities (in Ohm- m) are listed on a log scale (Sharma, 1986).

The exact process for calculating apparent resistivities from the measured currents and potentials depends on the geometry of the electrode configuration used to introduce the currents into the ground. In this study the Dipole-Dipole Array was used (Figure 4.3).

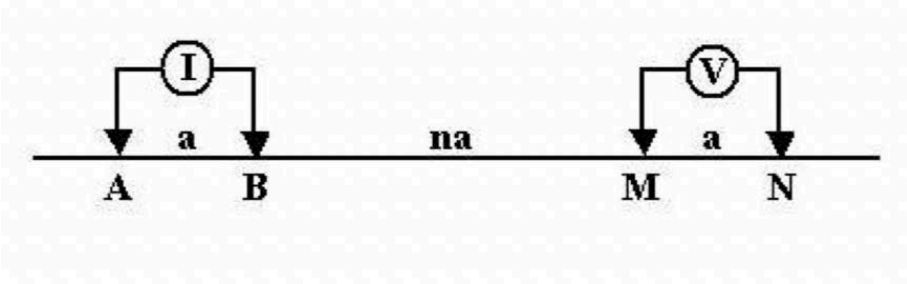

Figure 4.3 Example of a Dipole-Dipole array. "I" represents the current source, "V" represents the measured potential, and *A*, *M*, *N*, and *B* represent the electrodes (Gasperikova and Morrison, 2016).

A common method of presenting resistivity measurements is the pseudosection, in which readings are plotted to reflect the depth of penetration. Figure 4.4 shows how a pseudosection is constructed for the dipole-dipole array. Measured resistivity values are plotted at the intersections of lines sloping at 45° from the centers of the potential and current electrode pairs. Values are thus plotted at depths which reflect the increasing depth of penetration as the length of the dipole separation increases. The values are then contoured. Pseudosections only give an approximate representation of the resistivity response distribution at depth. The depth of investigation (DOI) depends on the length of the electrode line with 0.2 time the line length being an acceptable guideline for reliable data. The DOI for the DC Resistivity line was calculated at 16.8 meters using the formula of 0.2 * the array length of 84 meters.

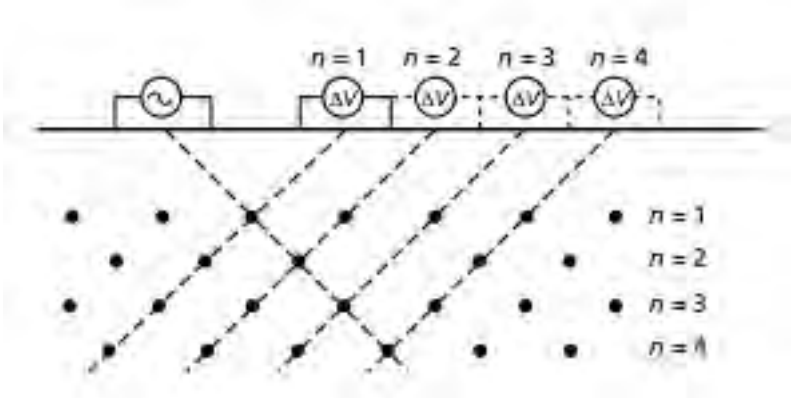

Figure 4.4. The construction of pseudosection using dipole-dipole DC resistivity results. n is the relative spacing between the current and potential electrode pairs. (Kearey et al., 2002).

The apparent resistivity is given by the equation:

$$\rho_a = \frac{V}{I} * \pi * a * n(n+1)(n+2)$$

Where ρ_a is the apparent resistivity, V/I is the impedance (Ohms), a is the distance between electrodes (spacing) and n is the number of spacings (multiples of a).

4.2 Instrumentation and Field Procedures

A single DC Resistivity line using a Dipole-Dipole array was used in this study. The array consisted of 28 stainless steel electrode stakes that were driven into the ground at 3-meter intervals along an 84-meter line that ran in an east-west heading of 120° (or 300°), perpendicular to the Lead Queen adit and roughly in line with the center points of the LQ1 Nano-TEM line. The adit was centered on the 42-meter electrode of the resistivity line (Figure 4.5). This was connected to an Advanced Geosciences Inc. (AGI) Sting R1 resistivity meter, S/N SI000607 with an AGI Swift Resistivity switch box, S/N SB000607 (Figure 4.6), with automatic switching between channels to isolate the individual electrodes for multiple electrode sender and receiver configurations to provide a more detailed subsurface map. The maximum voltage used was 400 volts and 200 milliamps and the system was powered by a 12-volt deep cycle battery.

Figure 4.5. AGI Sting/Swift Smart Electrode System (Photo courtesy of AGI)

4.3 Analysis of Data

Data collected by the AGI Swift-Sting system on the second day of field work, Feb 11th, 2018 were processed using AGI's EarthImager 2D software and inversion methods. Inversion is an analytical process that uses computationally intensive numerical methods to derive an earth model from the measured apparent resistivities at each point in a survey. Therefore, inversion is used to create a more accurate representation of subsurface electrical properties in order to find a geologic solution for the subsurface. While inversion is a valuable tool for interpretation, it is important to remember its limitations. A good inversion model should correlate relatively well with the observed apparent resistivity pseudosection, but inversion models may introduce artifacts that are not necessarily supported by the observed data. One way to determine the quality of an inversion model is to use forward modeling to reverse the process and build a calculated apparent resistivity pseudosection. The accuracy of the inversion model is determined by the similarity between the calculated and observed pseudosections; the more similar the

pseudosections, the more accurate the inversion model. Figures 4.7 and 4.8 show the measured and calculated pseudosections and the inversion model. Figure 4.7 is the original model prepared by Jamie Macy of the USGS, which displays depth from surface and Figure 4.8 is the model calculated by elevation above sea level. Based on the high degree of similarity between the measured and calculated pseudosections, the inversion model for this study should be accurate. Additionally, the root mean square (RMS) of 4.75 percent means the predicted and measured apparent resistivity data correlates well (Figure 4.9).

The resistivity model shows a highly resistive area about four meters wide at the location of the adit between 36 meters and 40 meters with a conductive layer about 2 meters below it on the DC Resistivity line (Figure 4.10). Based on Archie's Law, the high-resistivity section could be an area of decreased porosity and/or decreased water saturation, conversely the section with low resistivity below it could be an area of increased porosity and/or increased water saturation. Using Google Earth Pro, an elevation above sea level of 1474 meters was determined as the floor of the adit, which is approximately equal to the top of this conductive layer. The area directly under this conductive area may be obscured by the higher conductivity at the floor of the adit. Additionally, on either side of the adit location, at an elevation of 1470 meters to 1473 meters, there are areas of low resistivity in the range of 300-1000 Ω-m indicating either low porosity, or water saturation, or water with high resistivity. Another prominent feature of the inversion model is the area of very low resistivity on the east and west sides of the model that extend across the bottom of the model.

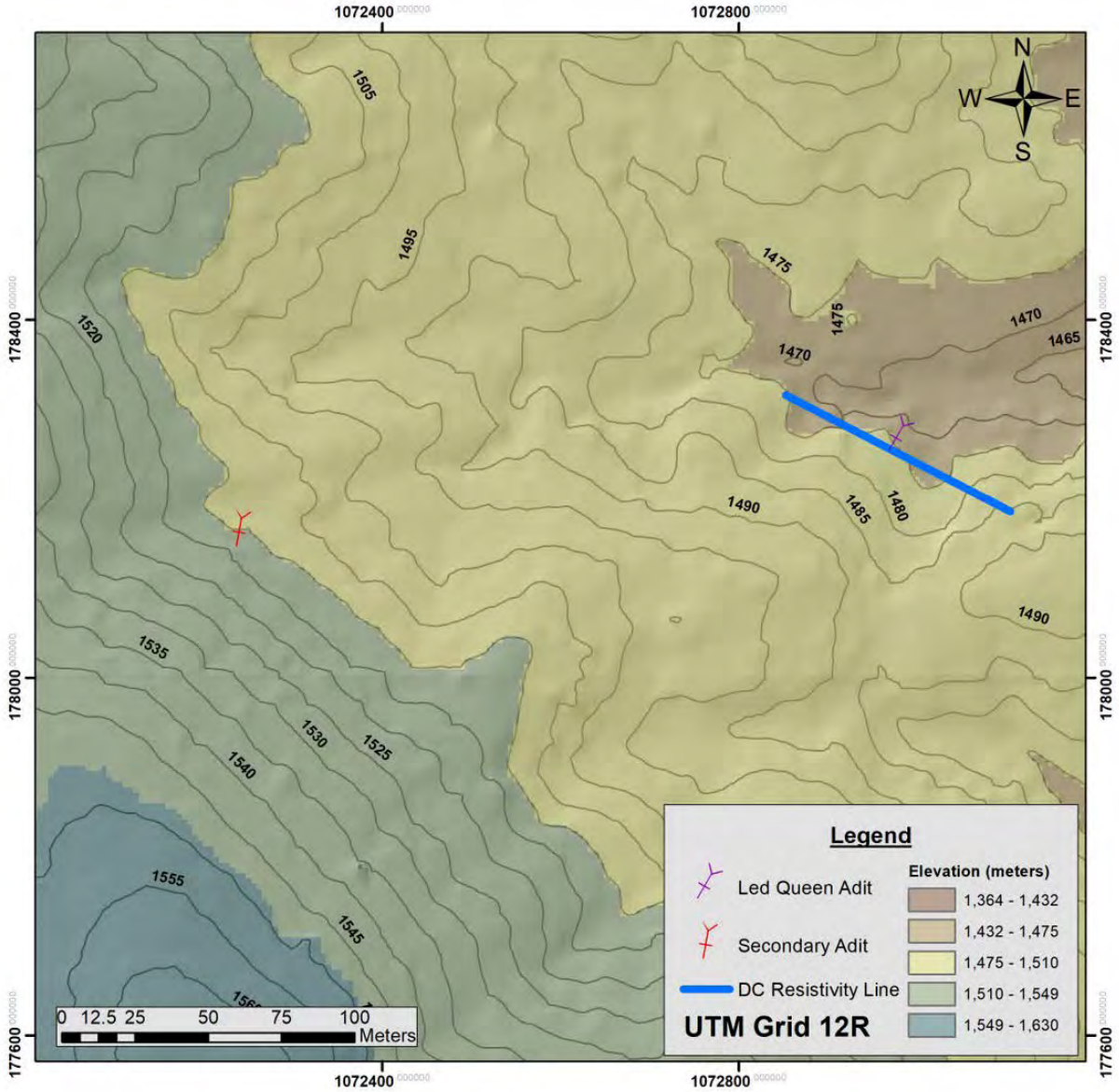

Figure 4.6. Map of the DC Resistivity array line used at the Lead Queen Mine site. The blue line represents the 84-meter-long array line, which was at a heading of 120° or 300°, perpendicular to the main adit and roughly in line with the centers of the LQ1 NanoTEM line.

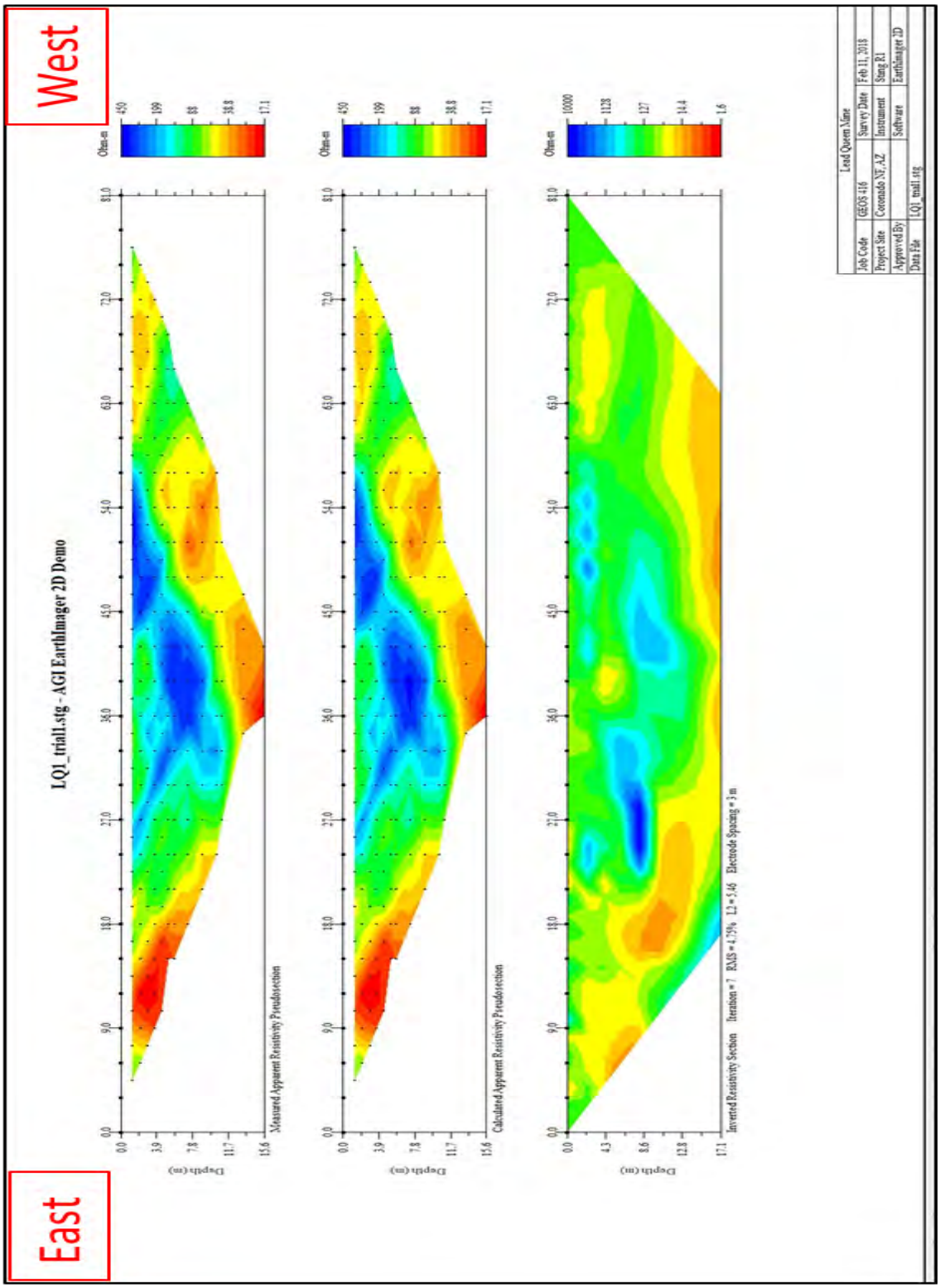

Figure 4.7. DC Resistivity line. Original electrical resistivity inversion prepared by Jamie Macy (USGS). The left and middle images contain the measured apparent and calculated apparent resistivity pseudosections and the right image is the inverted resistivity model. The measured and calculated are almost identical, indicating the model provided a good fit solution.

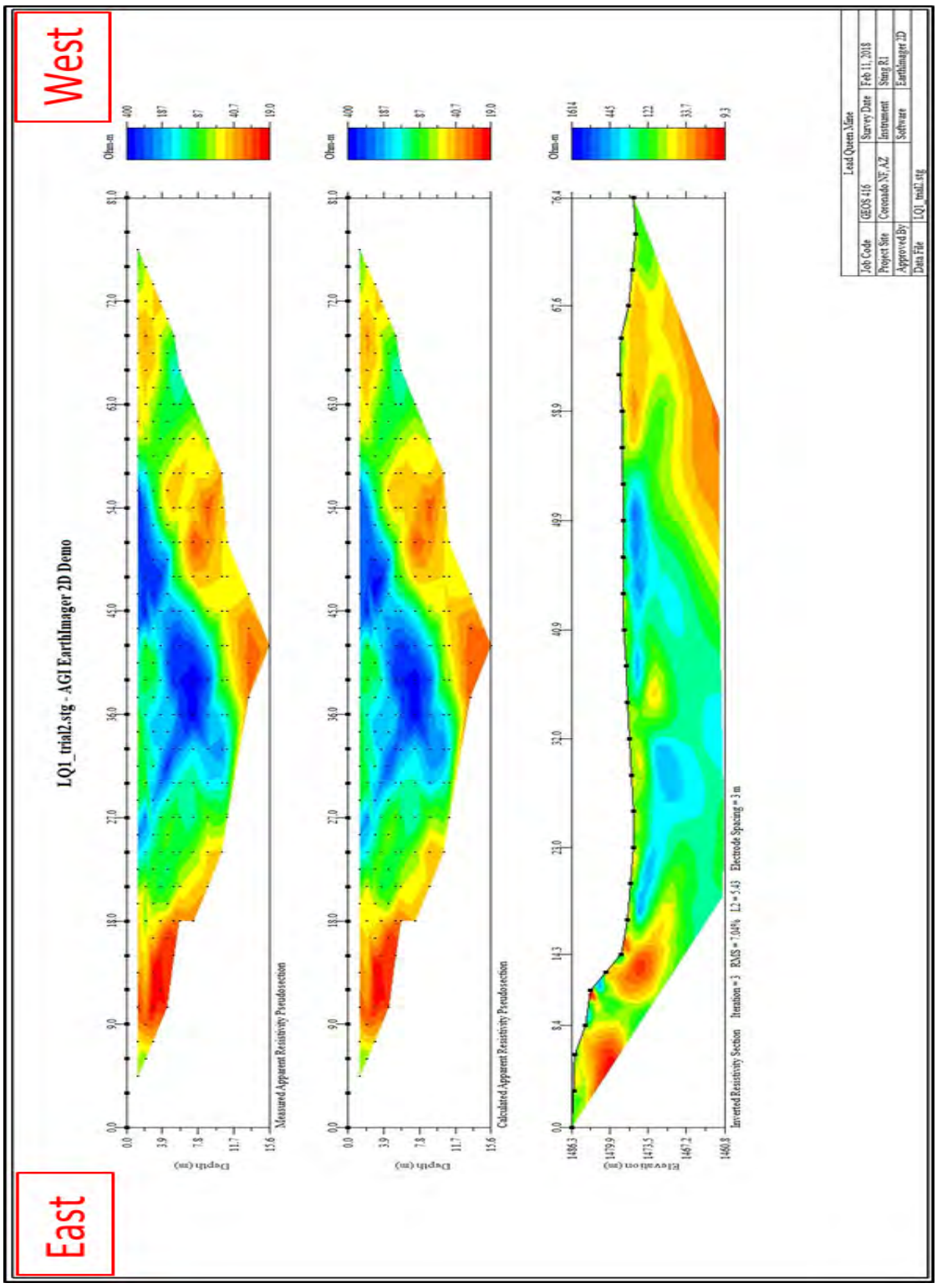

Figure 4.8. DC Resistivity line, electrical resistivity inversion with elevation compensation. The left and middle images contain the measured apparent and calculated apparent resistivity pseudosections and the right image is the inverted resistivity model. The measured and calculated are almost identical, indicating the model provided a good fit solution.

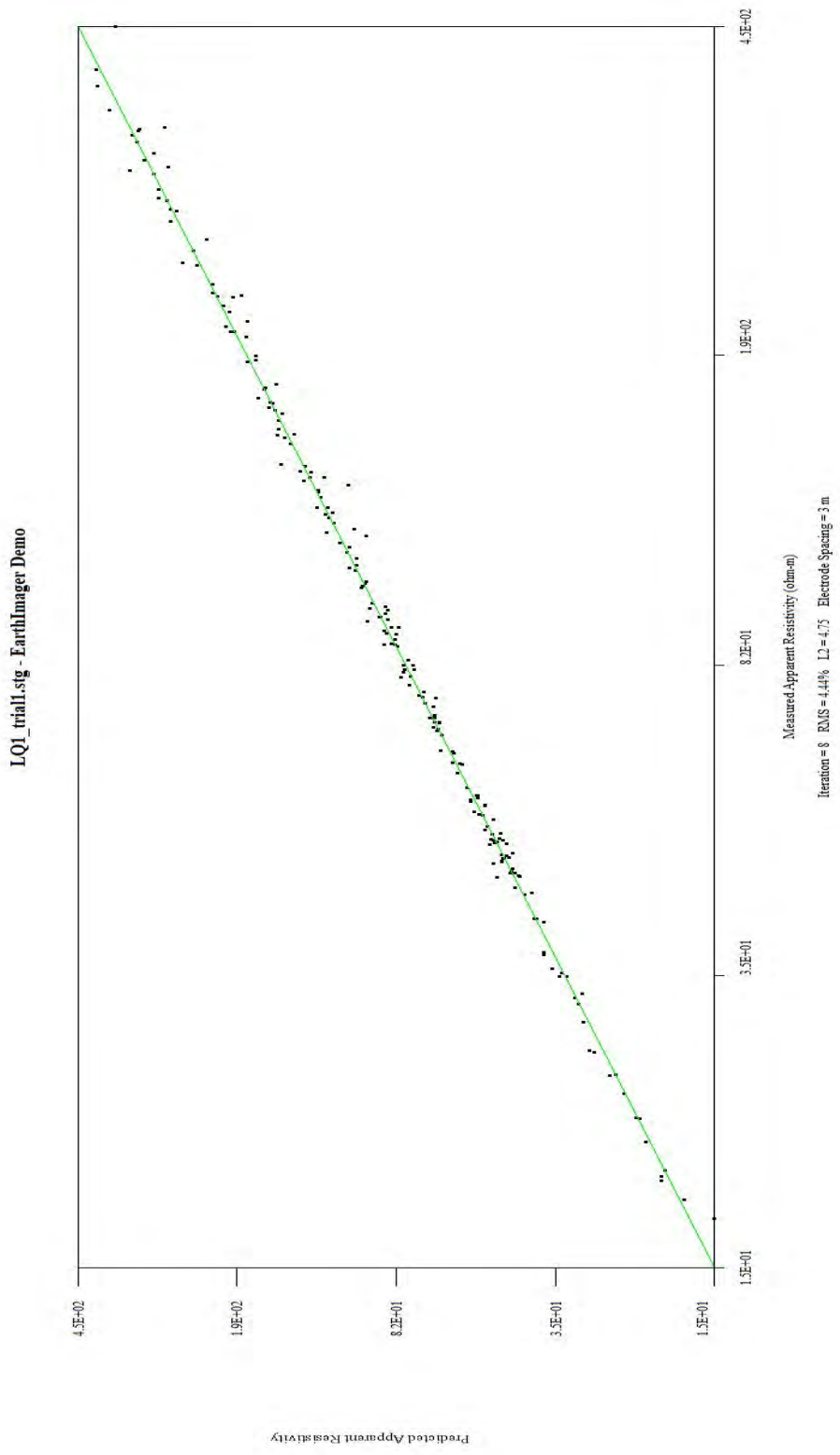

Figure 4.9. Data misfit cross-plot. The linear fit of the predicted versus measured apparent resistivity with few outliers means good data accuracy.

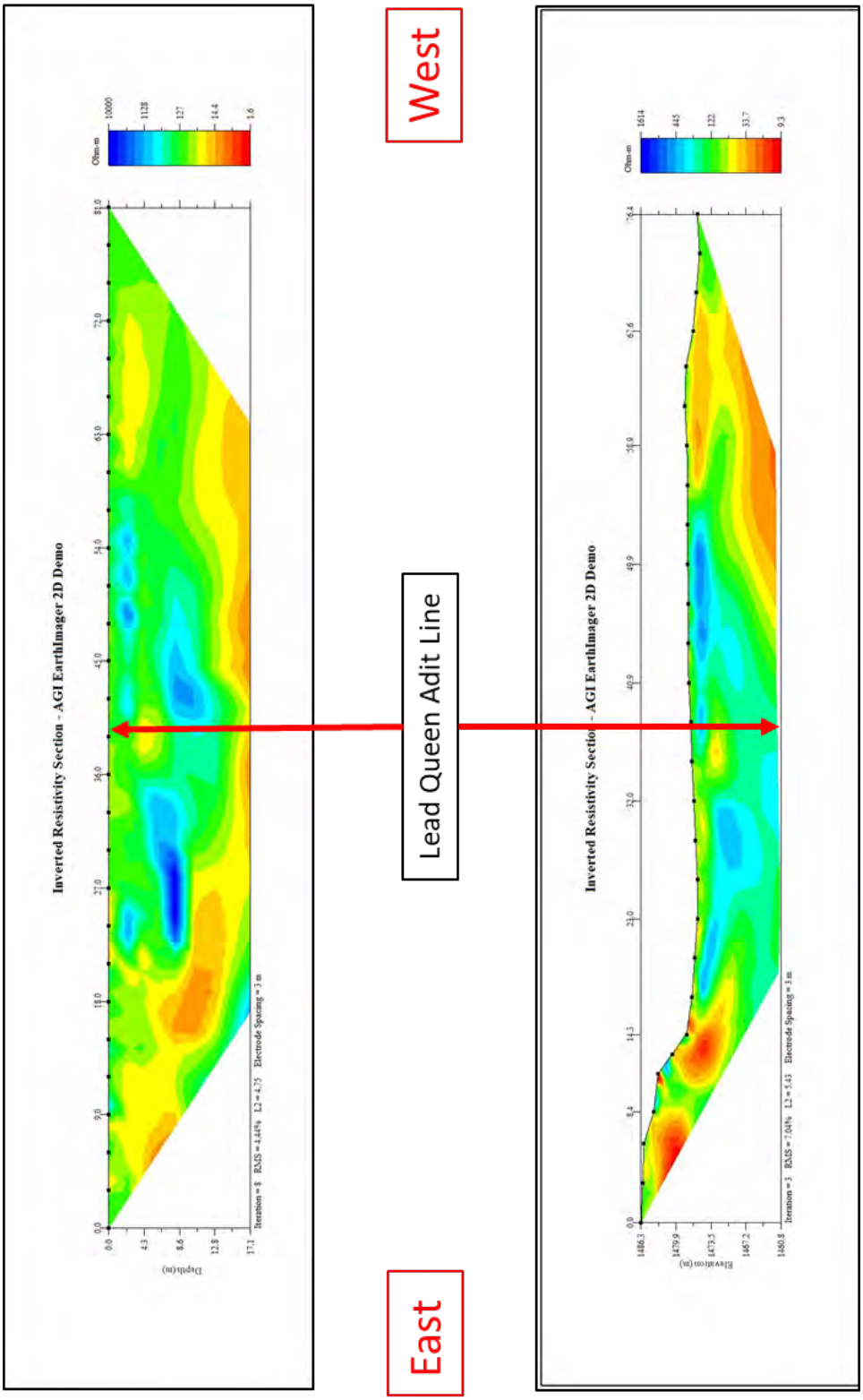

Figure 4.10. Side-by-side comparison of original model (left image) and elevation compensated model (right image). The linear distance across the cross-section has been reduced from 81 to 76 meters due to terrain changes in elevation. Note the conductive area at 1474 meters elevation (4 meter depth) is the location of the floor of the adit.

4.4 References:

Gasperikova, E., and Morrison, F., 2016. DC Electric Methods, *The Berkeley Course in Applied Geophysics,* http://appliedgeophysics.berkeley.edu/dc/index.html (April 16, 2017).

Kearey, P., Brooks, M., and Hill, I., 2002. *An Introduction to Geophysical Exploration, 3rd Edition*. Hoboken, New Jersey, 272p.

Parkhomenko, E. I., 1967. *Electrical Properties of Rocks*, G.V. Keller, transl. New York: Plenum.

Sharma, P. V., 1986. *Geophysical Methods in Geology.* New York: Elsevier.

Van Blaricom, R. & Northwest Mining Association, 1980, Practical Geophysics for the Exploration Geologist. Northwest Mining Association, Spokane, WA. pp. 40-150.

Van Nostrand, R. G., and Cook, K.L. 1984. *Interpretation of Resistivity Data.* U.S. Geological Survey, Geological Survey Professional Paper.

U.S. Army Corps of Engineers, 1995. *Geophysical Exploration for Engineering and Environmental Investigations.* 208p.

Zonge International. (2018). DC Resistivity & Electrical Resistivity Tomography (ERT). *Zonge.com.* Trusted Geophysics. Zonge International. http://zonge.com/geophysical-methods/electrical-em/dc-resistivity/ . Retrieved on 25 March 2018.

5. Electromagnetic Induction Survey (EM31)

5.1 Introduction

During the afternoon of March 3, 2018, an electromagnetic survey was conducted along the stream-bed, from 100 meters upstream and West of the Lead Queen Mine adit, and then 300 meters downstream and East of the adit; in order to understand how possible contaminants may have changed the conductivity of the water, after the water stream from the adit converged with a parallel stream from the West of the adit entrance. The mixing of these waters resulted in an orange precipitate and white precipitate downstream. The goal is to analyze how the conductivity may have changed from above stream before stream convergence, at the convergence, and downstream, till the precipitates dissipate.

5.2 Frequency-Domain EM methods at low induction numbers

Electromagnetic induction surveying techniques operate by running an alternating electric current through a wire loop or transmitting loop. This current creates a primary magnetic field that encompasses the coil and surrounding area. This primary field generates eddy currents in any surrounding conductors, which are in planes perpendicular to the magnetic field. A secondary magnetic field is produced by the eddy currents in the conductors. This magnetic field produced by the conductor is detected by a receiving loop (Figure 5.1). The proportion of the magnitude of the currents generated by the primary and secondary fields is related to the conductivity of the surrounding terrain or water (Subsurface Surveys Inc & Associates, 2007).

GROUND CONDUCTIVITY METERS

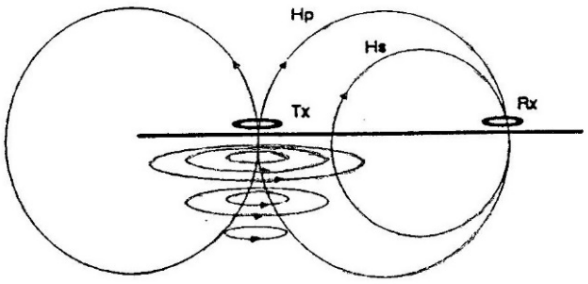

$$\frac{H_s}{H_p} = k\ f\ s^2\ \underline{\sigma}$$

Ratio of secondary/primary magnetic field is proportional to frequency, square of the intercoil spacing, and terrain conductivity.

RESPONSE AS A FUNCTION OF DEPTH

Vertical Dipole Mode (VDM)

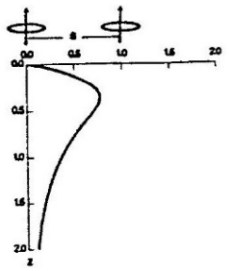

Horizontal Dipole Mode (HDM)

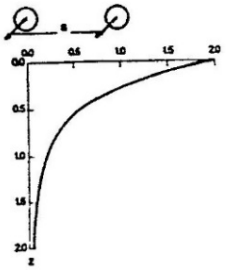

	s	Maximum depth ≅ 1.5 x s	Maximum depth ≅ 0.75 x s
EM38	1m	1.5m	0.75m
EM31	3.7m	6m	3.0m
EM34-3	10,20,40m	15,30,60m	7.5,15,30m

Figure 5.1. Ratio of primary and secondary magnetic field and depths of vertical and horizontal dipole measurements (Geonics Limited).

5.3 Instrumentation and Field Procedures

The survey was conducted with a Geonics Limited EM-31 electromagnetic surveying instrument. The model number is EM-31DL and the serial number is 8907006. The device had been recently calibrated and serviced by Geonics Limited. The magnitude of apparent conductivity is measured in milliSiemens per meter (mS/m). The intercoil spacing is 3.66 meters, while both the transmitting and receiving booms are 1.4 meters long (Figure 5.3). The EM-31 runs on 8 disposable alkaline C batteries and transmits at 9.8 kHz. The estimated operating time is 20 hours continuously. The accuracy of the measurements is +/- 5% at 20 mS/m. Accurate measurements can be taken by switching the millimhos/ meter knob depending on the magnitude of the measurement taken. The variations are 1000, 300, 100, 30, 10, and 3 (Figure 5.2). When using the ranges of 300, 30, and 3, take your measurement from the bottom of the meter labeled 0-30 and the top part of the meter labeled 0-10 when using ranges of 1000,100,10. During our profile, best accuracy was from the 30 and 10 range (Geonics Limited, 2013).

Measurements in the stream bed were taken every 5 meters a long a profile line starting 100 meters in the stream bed upstream from the adit. Another 300-meter-long set of measurements, taken every five meters were recorded downstream from the adit (Figure 5.5). Based on our visual observations during the survey, some contaminants from the adit water flow precipitated in the converged stream (Figure 5.4). At every measurement location, a reading was taken with the EM-31 held both vertical and horizontal. At areas where there was a dam consisting of cobble and metal cages, measurements were not taken, due to the influence of the metal cages. Measurements were halted at 300 meters downstream when there was no more presence of any precipitate (Table 1).

5.4 Analysis

From the data collected over the entire profile line, we conclude that there is no significant change in the earth resistivity or conductivity between the area up-stream from the adit and below-stream from the adit. The only significant observed changed in resistivity or conductivity is between the points -225 and -290 where most of the white precipitate is located (Figure 5.13). The largest jump in resistivity in this range of area is from 240-280 meters downstream past the adit, measuring at 200-833 Ohm/m, these measurements were take holding the EM-31 horizontally.

This is a big jump compared to the 100 Ohm/m average for the rest of the stream resistivity measurements taken horizontal.

5.5 Conclusions

Although the EM31 is a useful instrument for measuring subsurface and groundwater resistivity, our survey did not show much change in resistivity from non-adit water to the adit water near the entrance, where the water from the adit mixed with the fresh water from the surrounding stream. The only change in resistivity that was observed was related to when the white precipitate downstream was present and then quickly returned to normal once the precipitate was no longer visible.

5.6 Figures

Figure 5.2. Photo of the Geonics Limited EM-31 device control panel.

Figure 5.3. Geonics Limited EM instrument with booms attached (Brevik & Doolittle,2014).

Figure 5.4. EM-31 device with booms attached over areas downstream from the adit where the white precipitate was found. These areas were harder to get accurate distance readings due to difficult terrain and the size of the EM-31 device.

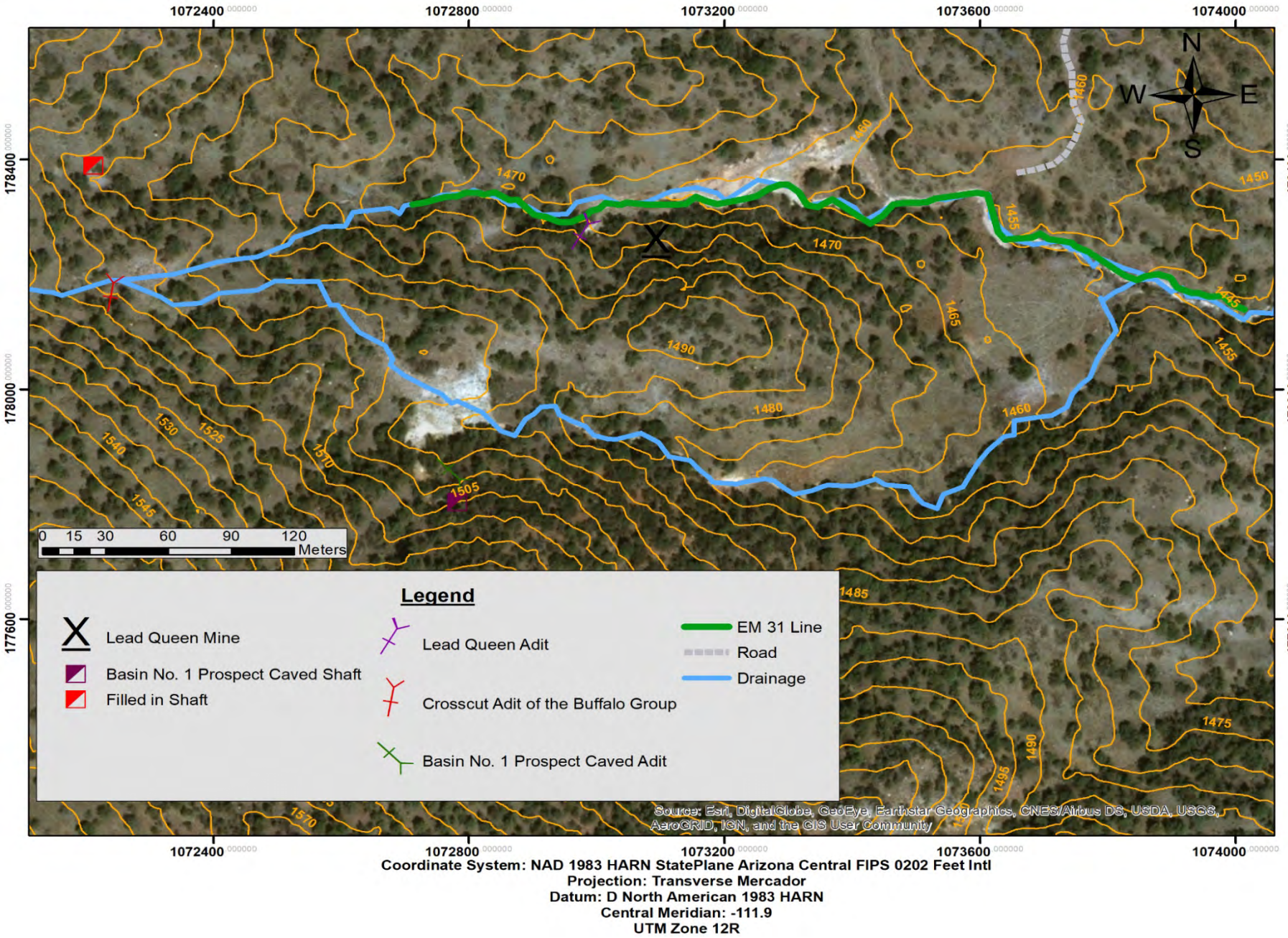

Figure 5.5. ArcGIS map portraying the EM-31 profile line on top of the steam path, upstream of the adit and downstream of the adit.

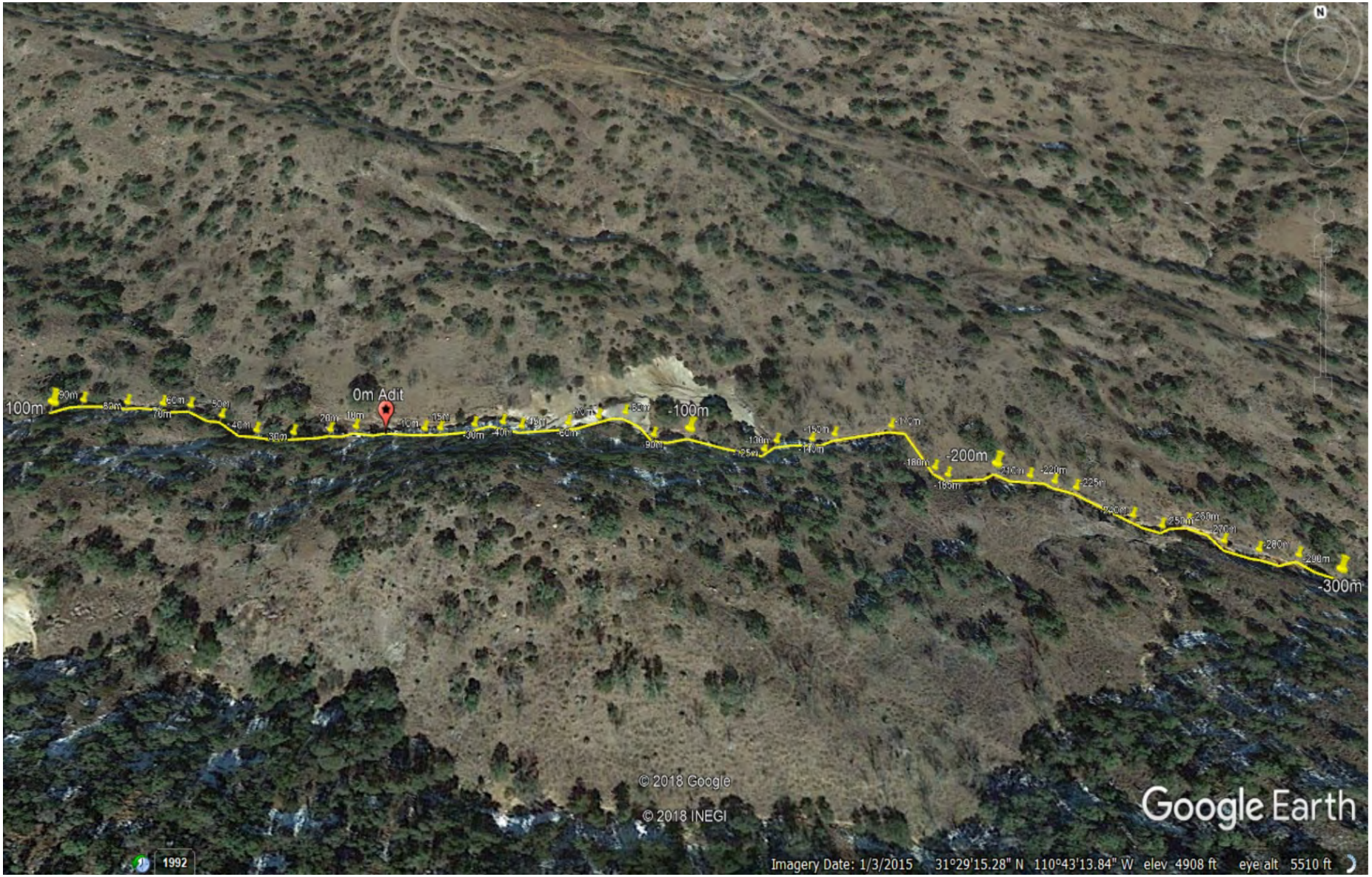

Figure 5.6. Google Earth Pro version of the EM-31 profile line 100 meters up stream before the adit and 300 meters downstream of the adit, with yellow pins marking some of the locations where measurements were taken.

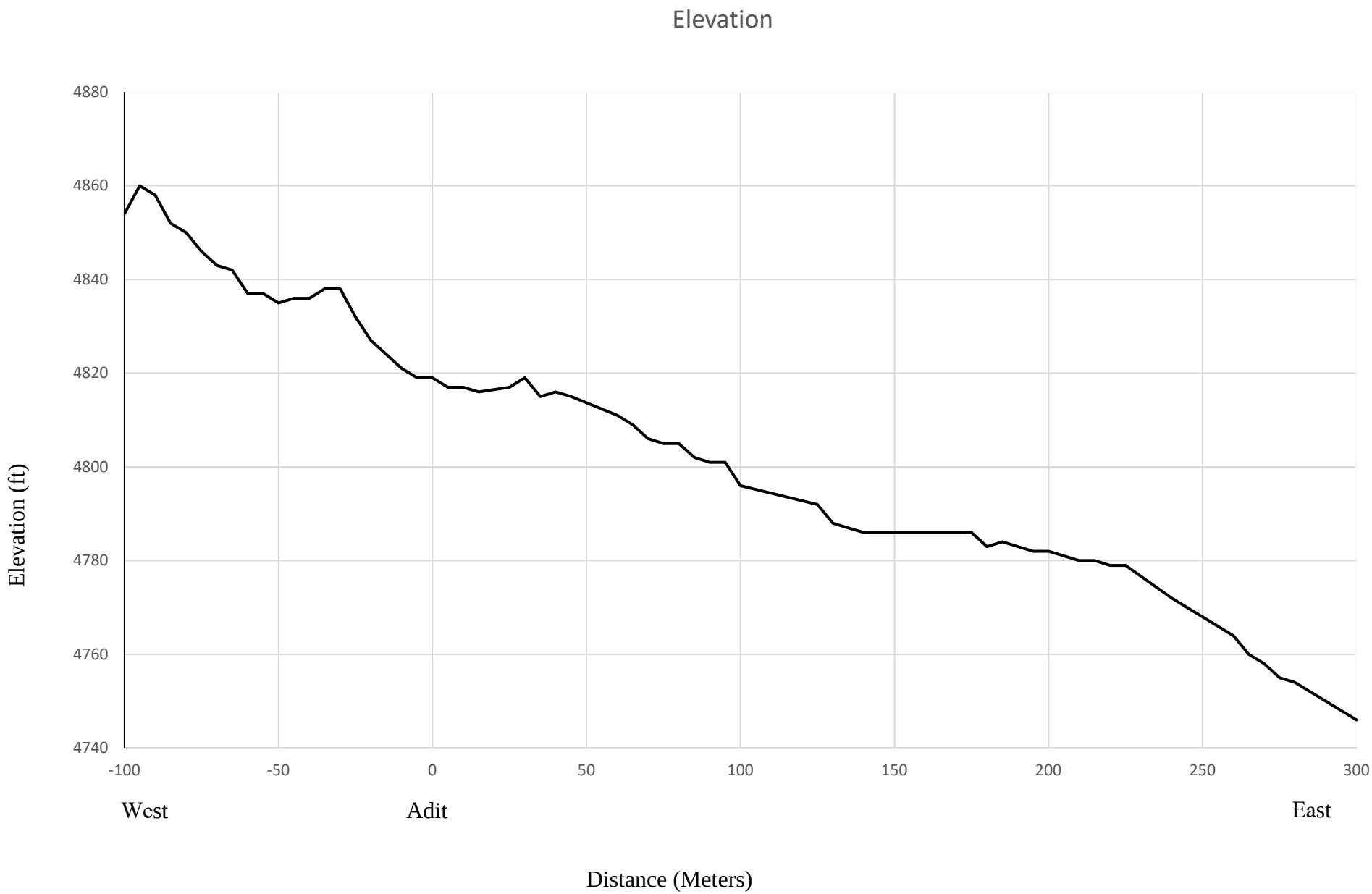

Figure 5.7. This figure represents the GPS elevation at each measurement taken for the EM-31 profile line from 100 meters upstream (West) of the adit and 300 meters downstream (East) of the adit.

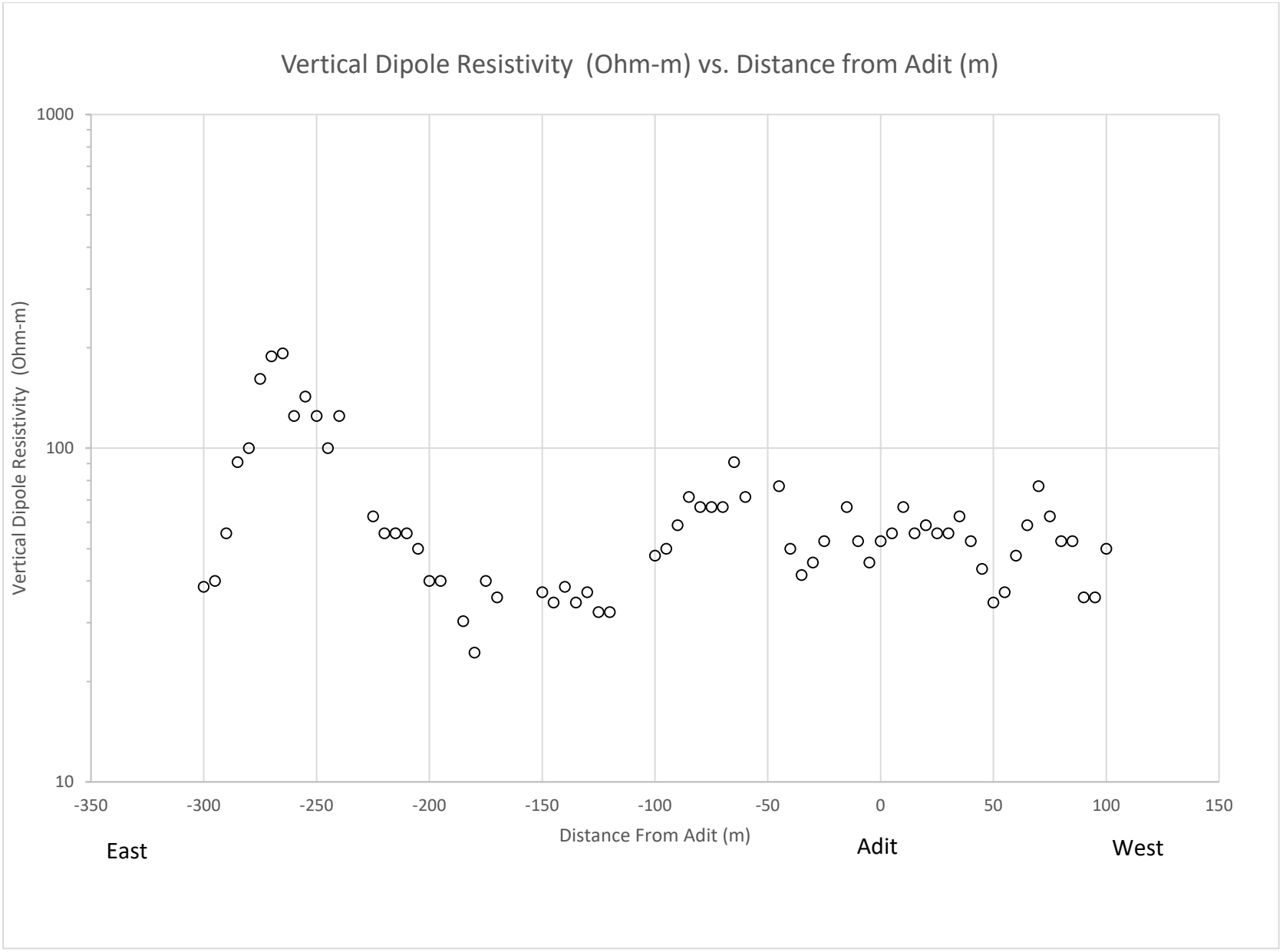

Figure 5.8. Plotted data results for vertical dipole resistivity collected with the EM-31 survey device.

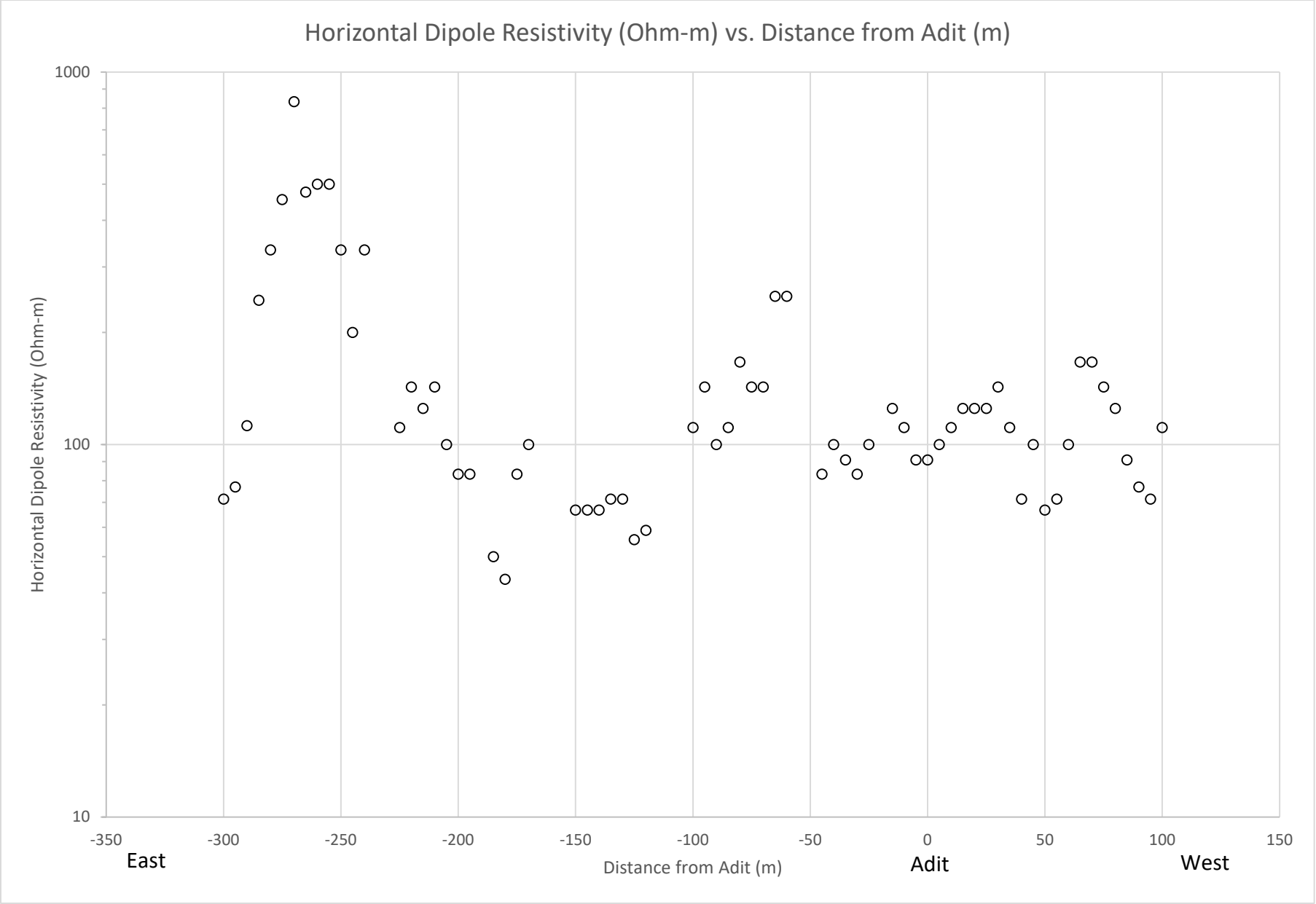

Figure 5.9. Plotted data results for horizontal dipole resistivity collected with the EM-31 instrument.

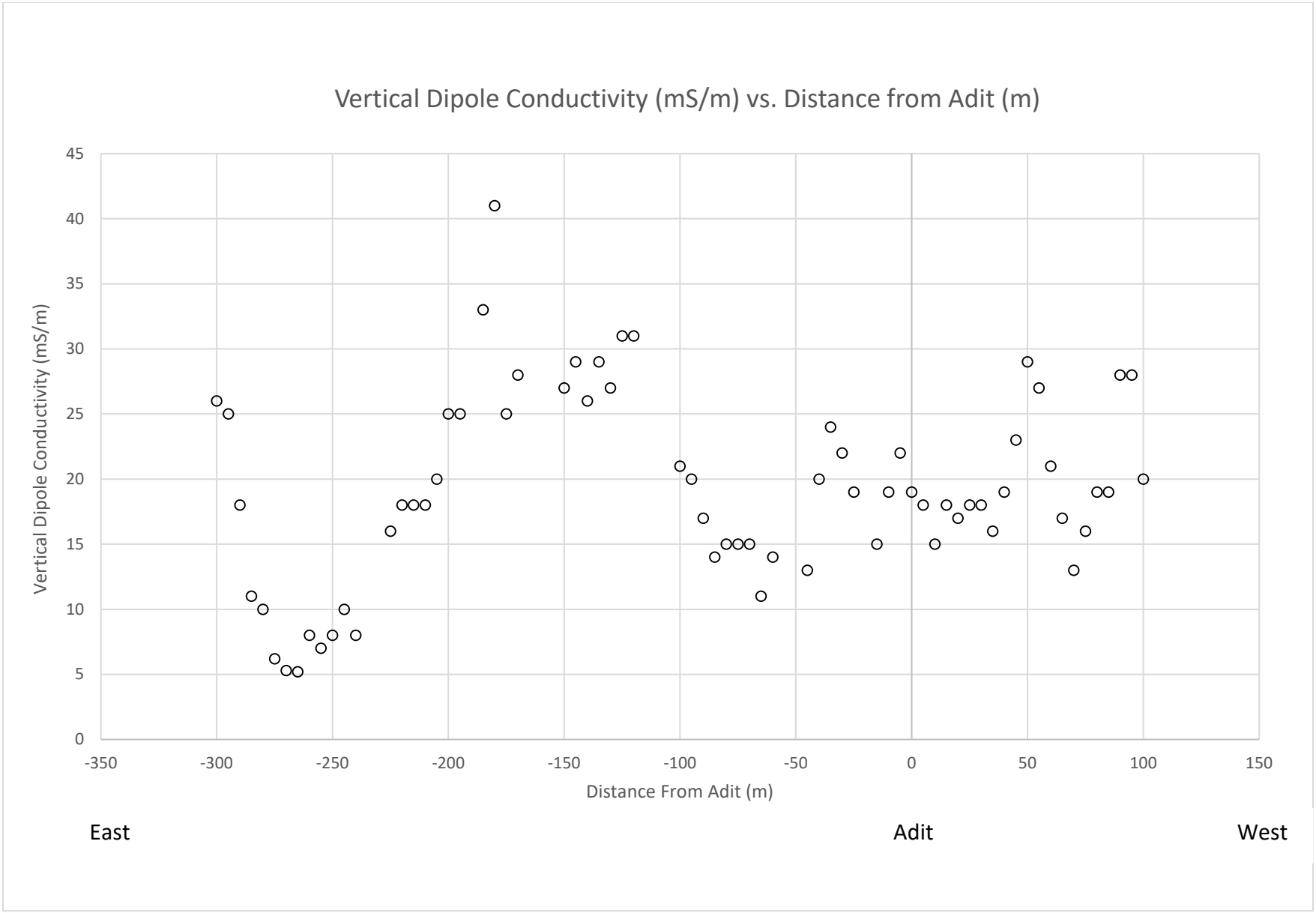

Figure 5.10. Plotted data results for vertical dipole conductivity collected with the EM-31 survey instrument.

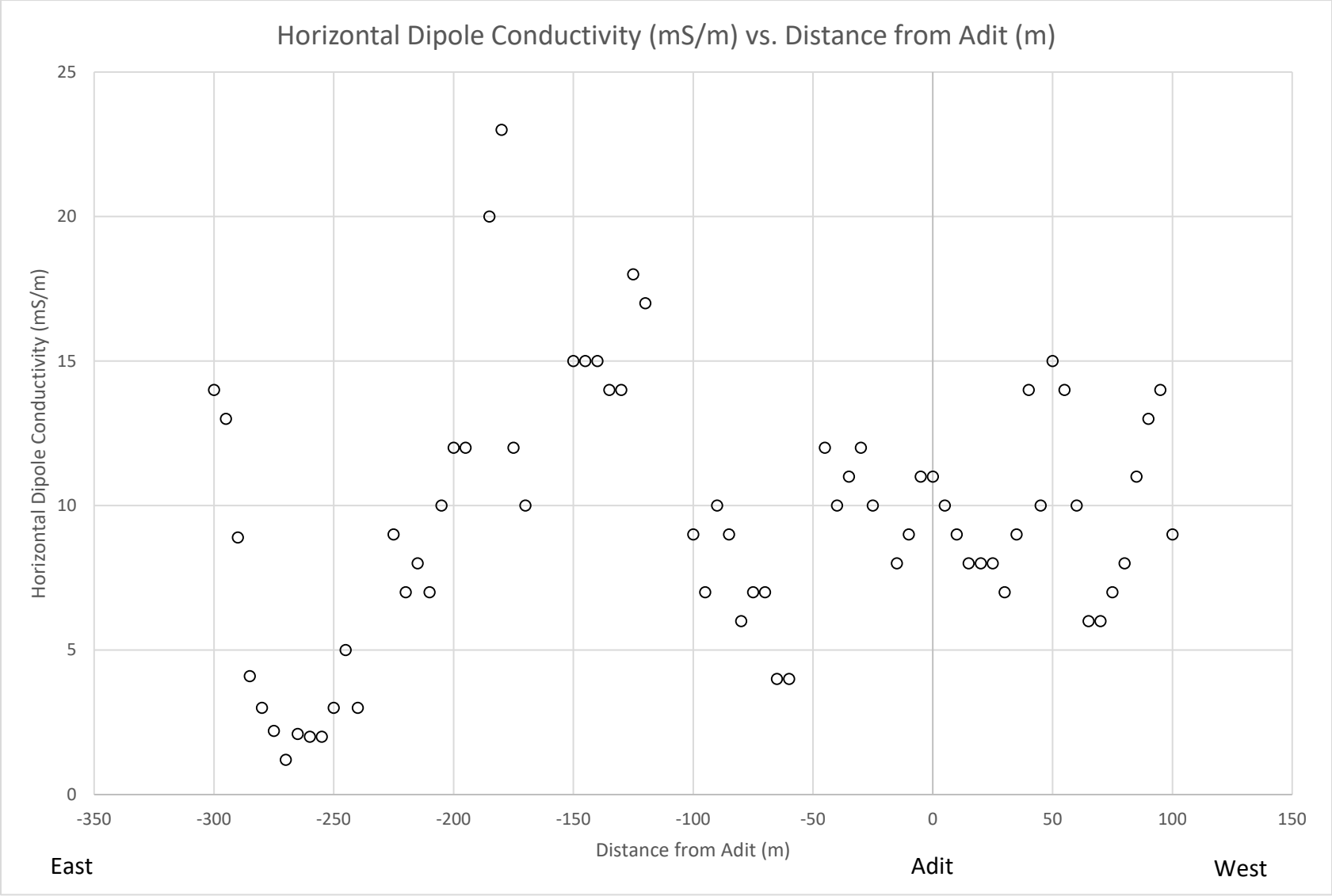

Figure 5.11. Plotted data results for horizontal dipole conductivity collected with the EM-31 survey instrument.

Figure 5.12. Orange precipitate found outside of Lead Queen Mine adit and was present in the wash for about 160 meters downstream.

Figure 5.13. White precipitate found from -225 meters to -290 meters downstream from the adit.

5.7 Data Table

Lead Queen Mine – EM31					
Distance (m)	Vertical (mS/m)	Horizontal (mS/m)	Notes	Vertical (Ohm-m)	Horizontal (Ohm-m)
100	20	9		50	111
95	28	14		36	71
90	28	13		36	77
85	19	11		53	91
80	19	8		53	125
75	16	7		63	143
70	13	6		77	167
65	17	6		59	167
60	21	10		48	100
55	27	14		37	71
50	29	15		34	67
45	23	10		43	100
40	19	14		53	71
35	16	9		63	111
30	18	7		56	143
25	18	8		56	125
20	17	8		59	125
15	18	8		56	125
10	15	9		67	111
5	18	10		56	100
0	19	11	Orange precipitate appears	53	91
-5	22	11		45	91
-10	19	9		53	111
-15	15	8		67	125
-20			Metal barrier		
-25	19	10		53	100
-30	22	12		45	83
-35	24	11		42	91
-40	20	10		50	100
-45	13	12		77	83
-50			Metal barrier		
-55			Metal barrier		
-60	14	4		71	250
-65	11	4		91	250
-70	15	7		67	143
-75	15	7		67	143
-80	15	6		67	167

-85	14	9		71	111
-90	17	10		59	100
-95	20	7		50	143
-100	21	9		48	111
-105			Metal barrier		
-110			Metal barrier		
-115			Metal barrier		
-120	31	17		32	59
-125	31	18		32	56
-130	27	14		37	71
-135	29	14		34	71
-140	26	15		38	67
-145	29	15		34	67
-150	27	15		37	67
-155			Metal barrier		
-160			Metal barrier		
-165			Metal barrier		
-170	28	10	Orange precipitate no longer present	36	100
-175	25	12		40	83
-180	41	23		24	43
-185	33	20		30	50
-190			Metal barrier		
-195	25	12		40	83
-200	25	12		40	83
-205	20	10		50	100
-210	18	7		56	143
-215	18	8		56	125
-220	18	7		56	143
-225	16	9		63	111
-230			Metal barrier		
-235			Metal barrier		
-240	8	3	More waterfalls	125	333
-245	10	5		100	200
-250	8	3		125	333
-255	7	2		143	500
-260	8	2	White precipitate appears	125	500
-265	5.2	2.1		192	476
-270	5.3	1.2		189	833
-275	6.2	2.2		161	455
-280	10	3	Abundance of white precipitate	100	333
-285	11	4.1	Less waterfalls and more pooling water	91	244

-290	18	8.9	Less waterfalls and more pooling water	56	112
-295	25	13	Less waterfalls and more pooling water	40	77
-300	26	14	Less waterfalls and more pooling water	38	71

Table 1. EM-31 data table showing vertical and horizontal orientation readings in mS/m and Ohm-m and notes on the surrounding area that could possibly affect the EM-31 readings. Distance from the Lead Queen Mine adit start at 100 meters West (upstream) and end 300 meters East (downstream).

5.8 References

Doolittle, James A., and Eric C. Brevik. "The Use of Electromagnetic Induction Techniques in Soils Studies." *Geoderma* 223-225 (January 26, 2014): 33-45. Accessed March 28, 2018. doi: 10.1016/j.geoderma.2014.01.027.

Geonics Limited - Geophysical Electromagnetic Instruments. "EM31-MK/ EM31-SH." Geonics EM31-MK2 Ground Conductivity Meter. 2013. Accessed March 28, 2018. http://www.geonics.com/html/em31-mk2.html.

Geonics Limited. “Theory and Case Histories,” Provided by Rob Harris, Geonics Limited. (April, 1994). Accessed April 12, 2018.

GeoVision. "Electromagnetic Methods." GeoVision. Accessed March 28, 2018. http://www.geovision.com/PDF/M_EM.pdf.

Subsurface Surveys. "Geophysical Methods: Electromagnetic (EM) Surveys." Electromagnetic (EM) Surveys. 2007. Accessed March 28, 2018. http://www.subsurfacesurveys.com/em.htm.

6. Ground Penetrating Radar (GPR)

6.1 Introduction

Ground-Penetrating Radar (GPR) is a nondestructive geophysical survey method that uses radio waves to detect subsurface structures. GPR has been used to detect underground voids, objects and archaeological artifacts for decades.

GPR sends high frequency radio waves into the ground. When the energy encounters an object with distinctly different electrical properties (conductivity and permittivity) than the surrounding soil or rock, the signal is reflected. A receiving antenna then records the returning reflections, which are displayed as hyperbolic arcs along a profile line (Figure 6.1). These reflections indicate the change in electrical properties compared to the surrounding medium (Daniels, 2004).

The depths at which GPR can penetrate is dependent on the medium and the radio wave frequency. Higher frequency electromagnetic waves do not attenuate as quickly as lower frequency waves; meaning deeper penetration. However, shorter wavelength waves allow for smaller objects to be more easily identified. Dry sandy soils and dry solid bedrock like granite and limestone are ideal for GPR applications, while saturated soils and highly conductive clay layers are not.

6.2 Instrumentation and Field Procedures

GPR data were collected over the course of two weekends: February 11th, 2018 and March 3rd 2018 on the same profile line. This 18-meter-long profile traversed the Lead Queen adit, roughly perpendicular to the adit bearing of 210 degrees. The adit itself was located below the 10 meter mark to ensure a large enough buffer was in place to differentiate it from the surrounding rocks. The depth of the transect to the roof of the adit was measured to be between 2.3 and 1.8 meters from the surface. This depth was measured using a tape measure from the top of the support cribbage used to shore up the Lead Queen adit roof to the 10m mark on the transect. The exact depth of the roof of the adit could not be narrowed to a smaller error considering the variation in roof height and the slope the transect was on. Due to safety concerns, there was also no access allowed into the adit for verification. The estimated width of the adit below the transect was 2 meters.

Equipment:

The equipment used was the same for both surveys. A GSSI SIR System-3000, a XII-15309 datalogger was used to record data and the antenna used was a GSSI 200 MHz. See Figure 6.2 for specific configuration details of both deployments.

Site Description:

The site itself required improvement in order for the GPR unit to be effectively used. The hill over the Lead Queen mine dipped between 10-45 degrees towards the adit, which would have

caused the antennae and its receiver to not be level, reducing any chance of getting a reflection from the adit. This was improved with trail work but the trail itself was still dipping 10-20 degrees (Figure 6.2b). Additionally, subsurface conditions for GPR work were less than ideal. The trachyandesite comprising the hillside was highly fractured and weathered. Because of the weathering process of mafic rocks it is possible that clays may be filling these fractures, which can be conductive (D.M Hendericks, 1968). Several outcrops were encountered while attempting to level the trail that had to be removed or covered with surrounding dirt using shovel and pickaxe. Finally, soil conditions also varied between collection periods. The nearest pubic rain gauge nearby in Barrel Canyon, Sonoita, recorded 4.7 cm (1.85 inches) of precipitation between February 11th (1st survey) and March 3rd, 2018 (2nd survey). Unsurprisingly, the moisture content for the 2nd survey was notably higher, and water flowing from springs near the Lead Queen adit was observed. Higher moisture content generally increases conductivity, which can significantly reduce the depths that GPR can reliably reach.

In total, 8 person-hours were spent on creating a trail for the 200 MHz antennae to travel over (Figure 6.2). To ensure NEPA compliance and minimize impact the trail was removed and covered with dirt and grass after data collection was complete.

Data Collection:

The trail was too primitive for the antennae to be wheeled along the transect. Instead, the antennae was dragged and pushed by two people. A third was positioned on the downhill side of the antenna, to stop it from sliding down the hillside, keeping it in line with the trail. A tape measure was laid out along the transect and every meter was manually marked as the antennae passed it.

6.3 Analysis of the Data

Data collected by the GSSI SIR System 3000 was processed using GSSI's RADAN 7 (Radar Data Analyzer for Windows) version 7.5.18.01190. Scan stacking, noise reduction, and manual gain processing adjustments were used in an attempt to improve visibility of any subsurface reflectors while reducing the return on the highly conductive layers near the surface (Figure 6.3a and b). Despite these improvements and a fairly good estimation of the location of the adit (10-meter mark of the line, around 2-m depth), no clear reflections from the adit were seen in the two surveys, post processing. Any possible signal from the adit, is obscured by the numerous times the contact between the antennae and the ground was lost. The air gap between the soil and the antennae creates a high intensity "ringing" effect that overpowers other reflections coming from deeper anomalies. This ringing can be clearly seen in both data sets (Figure 6.3a/b). In addition, the transect trail was also not level. Radio waves that are reflected off a subsurface object at an oblique angle will not be directed back to the receiver, resulting in under representation to no representation in the data.

For header information and specific step by step processing details please refer to Figure 6.3 c through f.

6.4 Conclusion:

Due to site conditions, a reflection of the adit is not obvious in either deployment period. If GPR will be used on this site in the future, additional people for trail cutting (4) and tools (2 buckets to carry dirt and rocks, more pickaxes, leveler, and a 5lb sledgehammer) are recommended. Levelling the trail will also be an issue due to the steep grade of the slope. Soil berms were ineffective at preventing loose material from falling down the hill. To maintain stability, the downhill part of the trail should be shored up with wooden stakes. It is unfortunate that the soil was saturated on the 2nd survey. To mitigate soil conditions in the future a lower frequency antennae might be better suited.

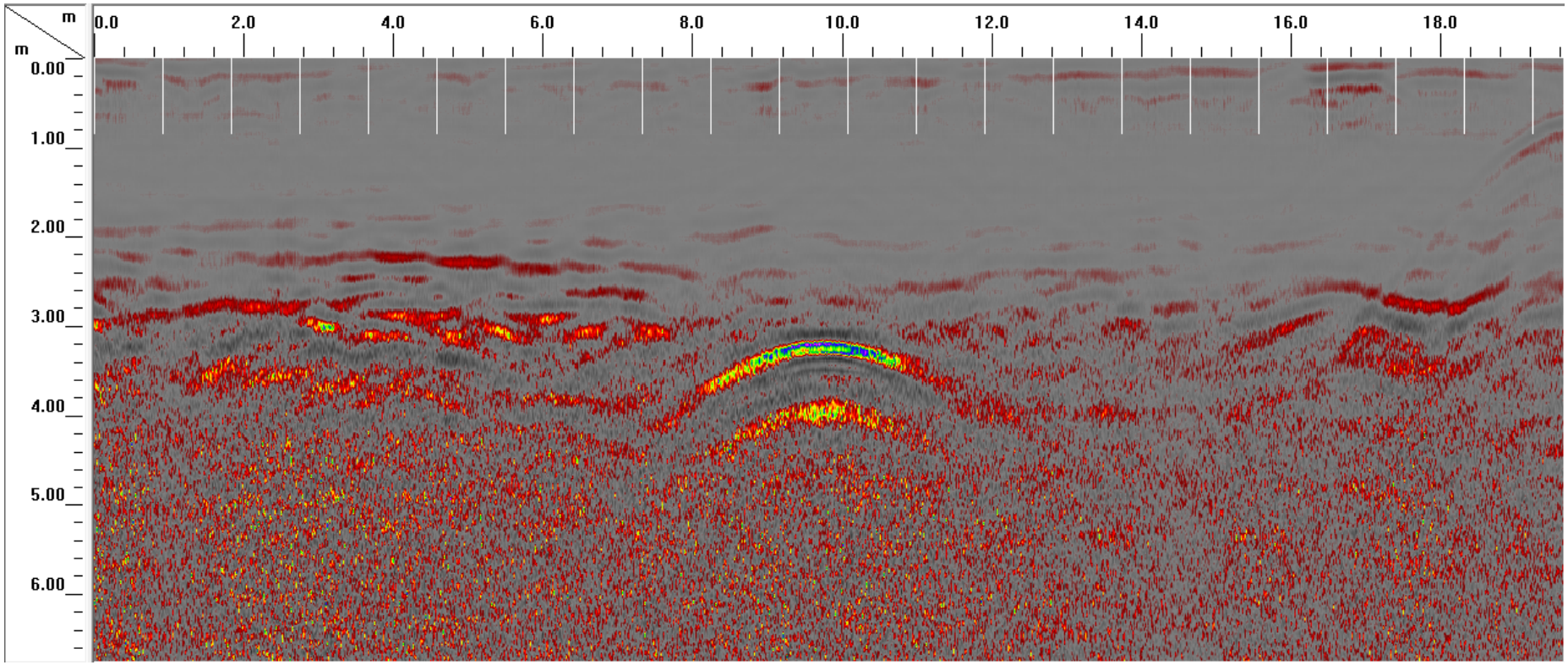

Figure 6.1. Example GPR transect from a student project in the Tucson basin showing the location of an aluminum sheet in conditions that are relatively amicable to GPR. The change in electrical properties can be seen as a change in color. The apex of the arch indicates the location of the sheet. The dielectric constant used for this plot was 4, which is an effective dielectric constant that produces the known target depth. The true dielectric constant would be higher than 4 in this moderately wet and lossy soil**.**

Figure 6.2a. Cutting trail for the GPR transect. Notice the angle of the hillside and trail. There were also several large rocks that needed to be removed to ensure a smooth and flat transect. After 8 hours of work, the slope over most of the 18 meter long transect was reduced to 10-20 degrees.

Figure 6.2b. Photograph of GPR transect looking North with the GSSI 200 MHz antennae in foreground. The Lead Queen adit is out of view on the right. Due to limited personnel, equipment and NEPA site guidelines, the trail was built around large obstructions, like trees. This resulted in a transect that was not perfectly straight.

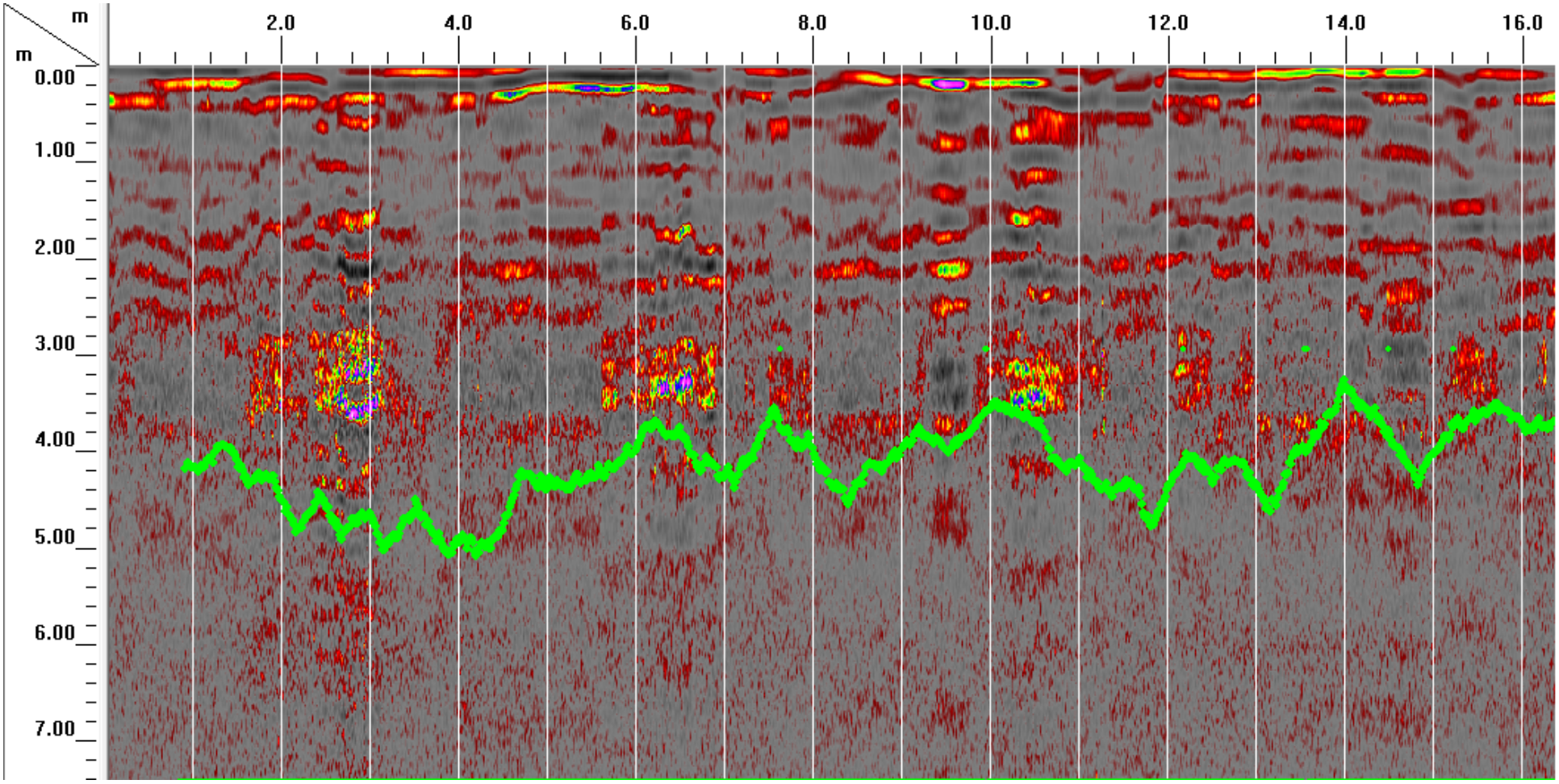

Figure 6.3a. GPR transect taken on 2/11/18 over the Lead Queen adit. The known location of the adit is near the 10m mark. Manual meter markings delineate every meter travelled. Areas where the antennae lifted off the ground can be seen just before meter mark 3, 6 and just after 10. The jagged green line delineates the signal floor. A highly reflective clay layer can be seen just below 0 meter depth.

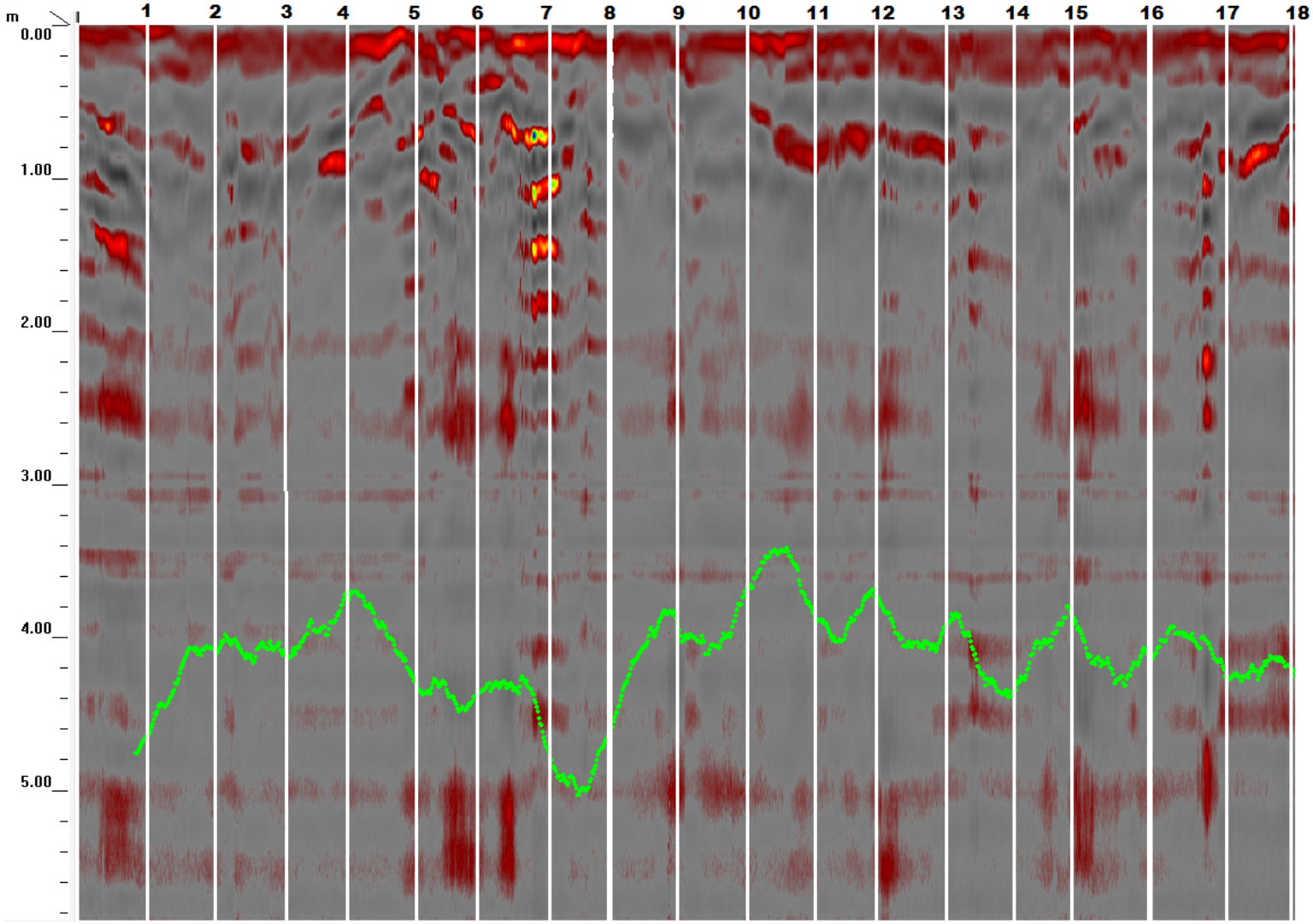

Figure 6.3b. GPR data from 3/3/18 taken from the 18meter transect over the Lead Queen adit. The known location of the adit is near the 10m mark. Manual markings every meter are highlighted in white. The characteristic ringing effect that occurs when the antennae loses contact with the ground can be clearly seen at 7m and 17m. Due to filesize constraints this dataset is actually 3 appended recordings. Each recording is separated by a bold white line. The jagged green line delineates the signal floor.

Header File Parameters	
Original File Name	FILE___014
Created	Feb, 11 2018, 23:22:30
Modified	Feb, 16 2018, 18:22:14
GPR System	SIR-3000
Number of Channels	1
Horizontal Parameters	
Scans / Sec	120.00
Scans / Unit (m)	75.000
Units / Mark (m)	1.000
Vertical Parameters	
Samps / Scan	512
Bits / Sample	16
Dielectric Constant	4.00
Channel Information	
Channel	1
Antenna Type	200MHz
Antenna Serial #	0
Position (ns)	-30.00
Range (ns)	176.37
Top Surface (m)	-1.500
Depth (m)	8.818
# Sample Stacks	Unavailable
# Scan Stacks	Unavailable

Figure 6.3c. Header information for first GPR recording (2/11/18, Figure 6.3a). Data was processed using GSSI's RADAN 7.

Processing History	
Range Gain	
# Of Points	5
Gain 1	-20.00
Gain 2	23.00
Gain 3	57.00
Gain 4	59.00
Gain 5	61.00
Position Correction	
Shift (nS)	-24.13
IIR Filters	
Vertical (MHz)	
Low Pass	1020
High Pass	85
Position Correction	
Shift (nS)	0.00
Horizontal Scaling	
Operation	Stacking
# of Scans	15
Distance Normalization	
Horz Norm: Scans/Mark	75.000000
Range Gain	
# Of Points	8
Gain 1	-84.00
Gain 2	10.00
Gain 3	34.00
Gain 4	18.00
Gain 5	12.00
Gain 6	13.00
Gain 7	15.00
Gain 8	16.00
Position Correction	
Shift (nS)	-14.06
Range Gain	
# Of Points	8
Gain 1	-29.00
Gain 2	15.00
Gain 3	0.00
Gain 4	0.00
Gain 5	0.00
Gain 6	0.00
Gain 7	0.00
Gain 8	0.00
FIR Filters	
Design	BOXCAR
Vertical (MHz)	
Low Pass	465
Background Removal	
Edit Data Block	

Figure 6.3d. Processing history for first GPR recording (2/11/18, Figure 6.3a). Data was processed using GSSI's RADAN 7.

Header File Parameters	
Original File Name	FILE___019
Created	Mar, 03 2018, 20:42:14
Modified	Apr, 11 2018, 20:34:48
GPR System	SIR-3000
Number of Channels	1
Horizontal Parameters	
Scans / Sec	64.00
Scans / Unit (m)	120.000
Units / Mark (m)	1.000
Vertical Parameters	
Samps / Scan	1024
Bits / Sample	16
Dielectric Constant	4.00
Channel Information	
Channel	1
Antenna Type	200MHz
Antenna Serial #	0
Position (ns)	-13.00
Range (ns)	130.00
Top Surface (m)	-0.650
Depth (m)	6.500
# Sample Stacks	Unavailable
# Scan Stacks	Unavailable

Figure 6.3e. Header information for second GPR recording (3/3/18, Figure 6.3b). Data was processed using GSSI's RADAN 7.

Processing History	
Range Gain	
# Of Points	5
Gain 1	-20.00
Gain 2	37.00
Gain 3	49.00
Gain 4	55.00
Gain 5	59.00
Position Correction	
Shift (nS)	0.28
IIR Filters	
Vertical (MHz)	
Low Pass	600
High Pass	50
Position Correction	
Shift (nS)	-5.46
Horizontal Scaling	
Operation	Stacking
# of Scans	30
Noise Band Removal	
Algorithm	Full Scan Band
Range Gain	
# Of Points	11
Gain 1	-17.00
Gain 2	-4.00
Gain 3	12.00
Gain 4	12.00
Gain 5	12.00
Gain 6	12.00
Gain 7	10.00
Gain 8	10.00
Gain 9	7.00
Gain 10	5.00
Gain 11	2.00
Horizontal Scaling	
Operation	Stacking
# of Scans	2
Position Correction	
Shift (nS)	10.28
Range Gain	
# Of Points	5
Gain 1	20.00
Gain 2	0.00
Gain 3	0.00
Gain 4	0.00
Gain 5	0.00

Figure 6.3f. Processing history for second GPR recording (3/3/18, Figure 6.3b). Data was processed using GSSI's RADAN 7.

6.4 References

Daniels DJ (ed.) (2004). *Ground Penetrating Radar* (2nd ed.). Knoval (Institution of Engineering and Technology). pp. 1–4. ISBN 978-0-86341-360-5.

D.M Hendricks (1968) *Andesite Weathering, Mineralogical transformations from Andesite to Saprolite.* Journal of Soil Science, Vol 19, No. 1 pp. 144

7. Conclusions

Our study included Transient Electromagnetics (NanoTEM), DC resistivity, EM-31 and Ground Penetrating Radar (GPR) surveys around the Lead Queen Mine for the United States Geological Survey. Data collected around Lead Queen Mine show a large highly conductive layer within the immediate area of the mine. Data from the NanoTEM and DC resistivity surveys show an anomaly with resistivities less than 6 ohm-m at depths varying from 20 to 60 meters. This anomaly is present in all TEM transects and the DC resistivity line. The DC resistivity line also shows a high-resistivity area near where the adit has been predicted to be. Further west, near another adit, a low-resistivity layer does not appear until beyond 60 meters depth. Data collected using the EM-31 shows no change in resistivity or conductivity along the streambed near Lead Queen Mine. GPR data also did not effectively show a response to the adit, even with extensive manipulation using the RADAN software.

8. Acknowledgements

The University of Arizona Field Geophysics class (GEN/GEOS 416/516), would like to thank the United States Geological Survey (USGS) for providing funding and support for this project. We would like to thank Jamie Macy, Bruce Gungle and Chris Magirl, from the USGS, for their assistance in the field. Jamie Macy has played a vital role in our Geophysics Field classes for many years, providing the required equipment, teaching us how to operate the equipment, and processing the data. We would like to thank Floyd Gray from the USGS for giving us a detailed introduction to the area and the project before our first weekend in the field. We would like to thank James Callegary from the USGS for providing a high-quality DEM of the area for use in our final report and presentation. Without the assistance of the USGS this project would not have been possible.

This class would also like to thank Thomas Tuten for his assistance in teaching the class how to use the Radan software and for helping us interpret and manipulate the data gathered at Lead Queen Mine. We would also like to thank Brian Jones for providing the class with access to the Radan software used to interpret and analyze the GPR data.

Finally, we would like to thank Zonge International for their 32 years of support of this class as well as providing relevant information for the report and presentation.